CRANFIELD UNIVERSITY

ARGYRO ZOUMPROULI

WIND FARM AND ENVIRONMENTAL AERODYNAMICS ASSESSMENT USING COMPUTATIONAL ENGINEERING

SCHOOL OF ENGINEERING
Department of Fluid Mechanics and Computational Science

MSc by Research Academic Year: 2009 - 2011

Supervisors: Dr N. Asproulis

August 2011

CRANFIELD UNIVERSITY

SCHOOL OF ENGINEERING
Department of Fluid Mechanics and Computational Science
MSc by Research

Academic Year 2009 - 2011

ARGYRO ZOUMPROULI

WIND FARM AND ENVIRONMENTAL AERODYNAMICS ASSESSMENT USING COMPUTATIONAL ENGINEERING

Supervisors: Dr N. Asproulis

August 2011
This thesis is submitted in partial fulfillment of the requirements for the degree of Master of Science

Abstract

The aim of this thesis is the application of computational engineering software for the study of wind resource assessment of a wind farm as well as for establishing the range of influence of different numerical and physical parameters, including turbulence modeling , surface roughness and wakes.

Simulations were performed for a wind farm which is in operation since 2006, called Panachaiko, located at the west part of Greece and encompassing an energy capacity of 34.85 MW. Simulations were performed using three variants of the k-ε model. Moreover, the effects of surface roughness and wake on the efficiency of wind farm operation were investigated. Comparisons were performed between linear and non-linear computational fluid dynamics (CFD) modeling, in the framework of the available engineering (commercial) software. Both qualitative and quantitative assessment of the results is presented.

The study revealed the dependence of the results on the CFD (linear vs non-linear) model employed. The results of the present study provide useful guidance regarding the applicability of CFD models for wing resource assessment.

Acknowledgments

The work on this thesis was performed in the context of my work engagement. Therefore, I would like to thank very much my directors for their comprehension.

I am most grateful to my supervisor Dr. Nikolaos Asproulis who supported me, whenever I needed his help and patience to answer all my questions throughout the course of this thesis. I would also like to thank Dr. Evgeniy Shapiro, Dr. Sanjay Patel and Prof. Dimitris Drikakis for further advice, as and when required. Last but not least, I would like to express my gratitude to my parents for their continuous support and encouragement.

Table of Contents

List of Figures

List of Equations

List of Tables

List of key symbols

ρ	Air density
E_k (KE)	Kinetic energy
U	Wind speed
$U_m, \bar{\mathrm{u}}$	Mean wind speed
k	Weibull shape coefficient
A	Weibull scale coefficient
$u(z)$	Air velocity at a desired height z
u_*	Air friction velocity
κ	Von Karman constant
z_0	Roughness length of surface$L$
L	Monin-Obukhov length
u, v, w *or* U1, V1, W1	Wind velocities
V	Volume
C_p	Thermal heat capacity
p	Pressure
k	Weibull scale coefficient
k	Thermal conductivity
$\mathcal{V}_t$	Turbulent viscosity
G	Turbulent generation rate
ϵ(EP)	Turbulent dissipation rate
u	Turbulent fluctuation velocity
F_T	Thrust force

C_t	Thrust coefficient
F_T	Thrust force
dt_f	Local time step

1 INTRODUCTION

1.1 Background and literature

The development of alternatively energy sources such as wind and solar energy has intensively been pursued worldwide since the 80's aiming to address the continuously increased energy requirements of the future. The oil crisis, the increasing environmental pollution, and the global warming due to the greenhouse effect are some of the main reasons towards the establishment of a worldwide independent energy policy that led to development and helped the growth of alternative energy sources. Wind turbines are one of the main strategies pursued by many countries as an alternative energy strategy encompassing very low CO_2 emissions.

Renewable energy comes from natural resources such as, wind, sunlight, rain, geothermal heat, tides, which are naturally replenished. According to energy studies (Tony Burton et al, 2001), the utilization of wind power covers the 43% of the energy supply of the European total. Wind energy is an attractive source of energy because it can be converted to electricity through the use of wind turbines (Bianchi et al, 2007), pumping water or drainage using wind pumps, generating mechanical power through wind mills and propelling ships through sails. The conversion of energy into usable energy depends upon the particular turbine design.

1.1.1 Wind Energy

The development of wind mills has begun since the ancient years in connection with agricultural activities. Technological advancements have led to the construction of new types of wind turbines with significantly improved characteristics compared to the traditional wind mills. Several wind turbine designs have been proposed with the most common ones comprising a rotor with two or three blades, which is placed at the tower's top and is oriented towards the

wind direction. Depending on the rotor's axis position, the wind turbines are classified into horizontal and vertical-axis turbines as shown in Figure 1-1.

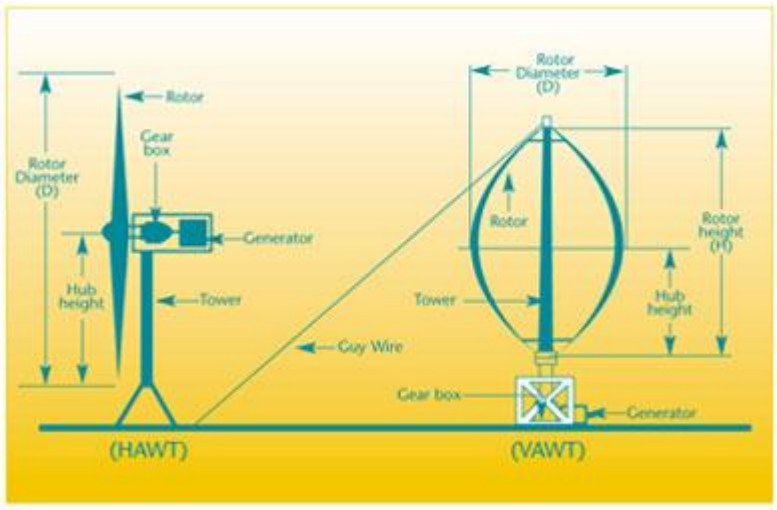

Figure 1-1 Wind turbines of horizontal and vertical axis

Source: www.therenewableenergycentre.co.uk

As regards the wind turbines of horizontal axis, the electrical generator is located at the tower's top while the main rotor of the vertical wind turbines runs vertically. Although the wind turbines of vertical axis are most advantageous since the tower doesn't need to support the generator or gearbox, the horizontal-axis turbines are most commonly used due to their increasing energy efficiency and reduced maintenance requirement compared to the vertical-axis turbines which are based on guy-ropes undertaking large land loads, thus their maintenance usually requires the removal of the rotor.

The kinetic energy of the air motion through an imaginary area *A* during the time *t* is given by Equation 1-1 as follows,

$$E_k = \frac{1}{2}mU^2 = \frac{1}{2}(AUt)U^2 = \frac{1}{2}At\rho U^3 \qquad \textbf{(1-1)}$$

where U is the wind speed, ρ the air density and AUt the volume of air passing through the imaginary area A. In similar fashion the power P_v obtained is calculated as follows

$$P_V = \frac{1}{2}\rho A U^3 \qquad \textbf{(1-2)}$$

where again U is the wind speed and ρ the air density.

The main wind features is its speed and direction. These parameters are dependent on several factors, including surface topography; climate characteristics; geographic location and height above ground. Furthermore, the wind turbines performance is significantly influenced by the geography, e.g. sea's vs. land's proportion, the existence of mountains or plain fields as well as the size of land masses. In addition to the geographic parameters, the surface topography with respect to the type of vegetation also has great influence in the atmospheric humidity and the temperature of the surface. Since the present study concerns a wind park in Greece, it should be noted that the country is characterized mostly by high hill mountains leading to high wind speeds (Schaffner et al, 2003).

The reason of increasing wind speed appearing frequently at hills and mountains is due to the fact that the wind speed increases with the height above the terrain. In general, mountain peaks and hill tops exist at places with high altitude. Furthermore, flow acceleration occurs around mountains and hill tops. The topography may also lead to wind speed reduction, when the flow passes over valleys or areas at high levels of a mountain ridge. Another reason for the wind velocity reduction is the appearance of obstacles like trees or buildings. Therefore, the development of wind farms on top of hills and mountains is preferred although the terrain becomes more complicated with slopes and steep hills appearing more frequently. A complicated terrain also leads to turbulence that in turn is responsible for wind speed fluctuations. Therefore, the wind assessment of an area should take into account the mean wind speed and the turbulence intensity.

The economic feasibility of the construction of a wind farm requires the knowledge of the potential expected mean wind speed. The most usual way of measuring the wind is to install a mast with appropriate instruments and collect data for an average period of 10 to 20 min during several years. Afterwards we take the probability distribution of the mean wind speed presented in a histogram. The wind speed distribution that required for the computational modelling is usually approximated through a Weibull probability density function with the probability for an annual mean velocity U_m being:

$$f\left(\mathrm{U_m}\right) = \frac{\mathrm{k}}{\mathrm{C}}\left(\frac{\mathrm{U_m}}{\mathrm{C}}\right)^{\mathrm{k-1}} \mathrm{e}^{-\left(\frac{\mathrm{U_m}}{\mathrm{C}}\right)^{\mathrm{k}}} \qquad \textbf{(1-3)}$$

where k is the shape factor selected by the user with $k > 1$, and C is the scale factor calculated from the following equation:

$$C = \frac{U_m}{\Gamma\left(1 + \frac{1}{1+k}\right)} \qquad \textbf{(1-4)}$$

where Γ correspond to the Gamma function.

The Weibull probability function shows that the frequency of moderate winds speed occurs more often in connection with the appearance of large mean wind speeds. Since the mean wind speed depends on the height, it is easy to understand that the ground produces friction even without the existence of obstacles around, thereby causing wind delays at the lower layers as shown in Figure 1-3.

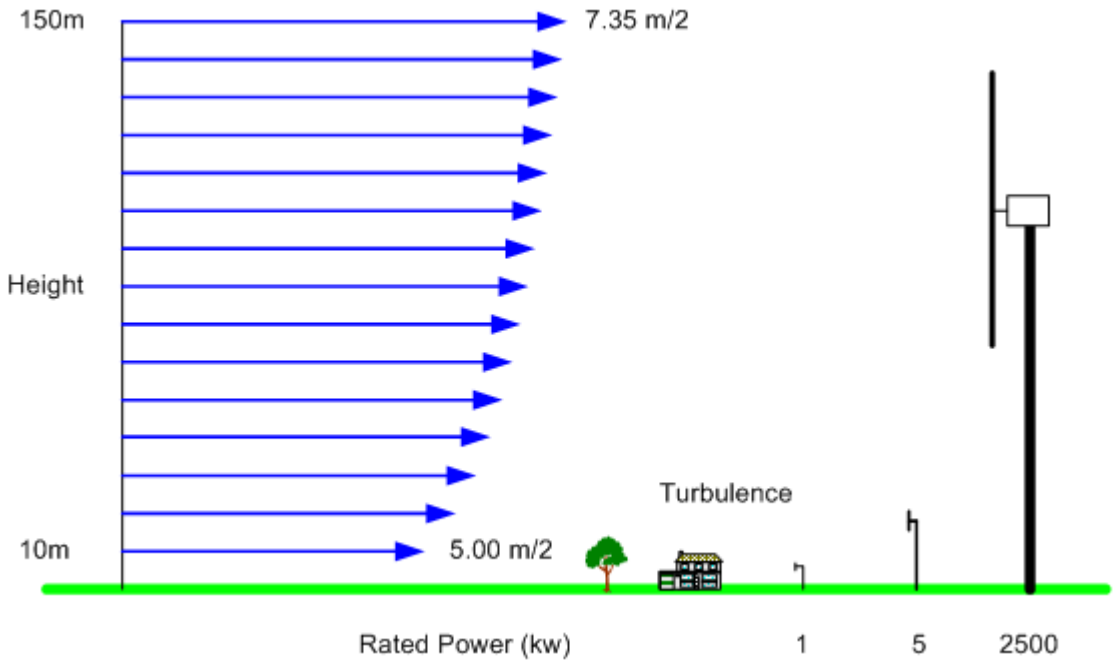

Figure 1-2 Wind turbine performance height

Source**:** www.brighton-webs.co.uk

This phenomenon is known as wind shear and is increasing when the height decreases. Wind shear has significant influence to wind turbine's operation. At height of 30m or less the wind velocity profile can be approximated by ignoring any order higher than second in the expression of the full atmospheric boundary layer an expressed by the Prandtl's logarithmic law (Afzal, 2001) as follows

$$\frac{U_m(\mathrm{z})}{U_m(z_{ref})} = \frac{\ln\left(\frac{\mathrm{z}}{z_0}\right)}{\ln\left(\frac{z_{ref}}{z_0}\right)} \qquad \textbf{(1-5)}$$

where U_m is the wind speed, z is the height above ground level, z_{ref} is the reference height usually selected as 10m and z_0 is the surface roughness parameter.

Another empirical formula (Troen & Petersen, 1989), which is often applied to describe the influence of wind speed due to the terrain, is given by Equation 1-5,

$$U_m(\mathrm{z}) = U_m(z_{ref})\left(\frac{z}{z_{ref}}\right)^{\alpha} \qquad \textbf{(1-6)}$$

where the surface roughness exponent α is also a parameter which depends on the terrain. Typical values of roughness length with respect to classified surface-roughness types, which are associated with the terrain but cannot measured directly, are presented in Table 1-1

Type of surface	**Roughness type**	**Roughness length (m)**	**Relative Energy (%)**
Water areas	0	0.0002	100
Mixed water and land area or very smooth land	0.5	0.0024	73
Open farmland-Only smooth hills	1	0.03	52
Farmland with some buildings & crossing hedges of 8m height and about 1250m apart	1.5	0.055	45
Farmland with some buildings & crossing hedges of 8m height and about 800m apart	2	0.10	39
Farmland with dense vegetation- crossing hedges of 8m height and about 250m apart	2.5	0.20	31
Villages, small towns, very close farmland with many or heigh hedges, forests	3	0.40	24
Large towns, cities with extended build-up areas	3.5	0.80	18
Large cities with build-up areas and high buildings	4	1.6	13

Table 1-1 Typical surface roughness lengths & roughness classes

The wind assessment in a complex terrain is a more demanding and complex task than in a flat terrain due to the turbulence generation. The wind speed in a turbulent flow can be decomposed according to Reynolds' formula, into a mean value and the turbulent fluctuation as shown at Figure 1-4 and :

Figure 1-3 Typical turbulent wind variation with turbulence

(WindSim,2008)

$$u(t) = \bar{u} + u'(t) \qquad \textbf{(1-7)}$$

where $u(t)$ corresponds to the instantaneous wind speed, $\bar{u}$ is the mean wind speed within a time interval and $u'(t)$ is the instantaneous turbulent fluctuation velocity. The turbulence intensity depends on the friction velocity and the wind shear produced by the surface topology. These parameters vary with the height from the surface with wind shear and friction velocity holding greater values near the surface. The energy produced depends on the wind speed, thus turbulence has important effects both on the aerodynamic loads and energy output. Specifically, turbulent fluctuations induce mechanical and vibration loads on the blades of a wind turbine, thereby leading to energy decrease.

Turbulence can be described by its power spectrum. Two well known models are the von Karman spectrum and the Kaimal spectrum (Burton et al, 2001). Both models are parameterized by constants relate to the frequency bandwidth of turbulence, and turbulence power, respectively depended on the mean wind speed and the topography of the terrain. Studies have shown that Karman spectrum gives a good estimation of turbulence in wind tunnels although the Kaimal spectrum may give a better fit to empirical observations of atmospheric

turbulence. Of course, one has to bear in mind that turbulence is a complicated process, which cannot be described through deterministic equations. However, for engineering purposes the above described models are used to provide an idea of the turbulent characteristics of a flow field.

Furthermore, the energy production is affected by wind wakes interacting with wind turbines. The wind carries less energy behind the wind turbine than in front of it. Wake effects are usually minimized by proper placement (known as *micro-sitting)* of the wind turbines in the terrain according to the dominant wind direction (Troen, 1990).

1.1.2 Engineering Software for wind energy studies

The assessment of wind resource can be made using established engineering software. The wind is measured by the installation of a wind mast with the appropriate instruments and the wind data are collected directly from a data logger and then imported to a database remotely. Depending on the calculations needed to be performed, different engineering software is used issuing wind energy results.

The aim of wind data engineering software is to help the user through a variety of tools to analyze and validate the wind data, which can then be exported for use in wind flow and wind farm modeling software.

For wind data analysis, Windographer and WindRose are commonly used to remove any errors arising from the measured data and perform specialized statistical analysis.

Wind flow modeling software is used for calculating special characteristics of the wind resource at areas where the measuring procedure cannot be achieved. The most prevalent application, which gives fast and reliable results, is Wasp, created at Risø National Laboratory in Denmark (http://www.risoe.dtu.dk/). WAsP applies a flow model for the prediction of wind flows over the terrain at a site. Meteodyn

WT, WindieTMandWindSim (http://en.wikipedia.org/wiki/Wind_energy_software), are commercial software that use CFD (Computational Fluid Dynamics) methods, which are potentially more accurate but also more complex, and their use is preferred for complex terrains (Mortensen et al, 2004).

Wind farm modeling software is used for simulating the behavior of a wind farm with respect to the energy production. Wind data, elevationand roughness contour lines, background maps are used for input, while wind turbine specifications are available in the software too. Collecting this information and taking into account environmental restrictions (e.g. protection from trees from taking them down, avoidance of crossing birds path, etc) and construction limitations (e.g. steep edges asking for expensive site works) and social impacts (e.g. aesthetic impact on existing villages or households), the energy production in the design of a wind farm can be potentially maximized. Wind farm modelling software commonly used include : Meteodyn WT, openWind, WindFarm, WindFarmer, WindPRO, and WindSim (http://en.wikipedia.org/wiki/Wind_energy_software)

In this study, the WindPro and WindSim commercial software have been employed to study the annual energy production of a wind farm, which is located in a complex terrain and is currently in operation.

WindPro

WindPro is commercial engineering software used for the design, development and assessment of wind energy regime and calculation of the annual energy production (AEP) of a wind farm. WindPro calculates the energy production using the **Basis** and **Energy** modules, which will be described in detail later on.

WindSim

Since wind farm owners frequently experience that AEP from their wind farms is lower than the estimated production, especially in areas with relatively complex terrain, the use of Computational Fluid Dynamics is employed to optimize wind turbine micro-sitting in order to minimize the energy losses (Ott et al, 2008).

The Windsim engineering software is a commercial package that calculates the wind fields over a discredited terrain, while keeping the turbine loads within acceptable limits. The loads on a wind turbine are influenced by wind field characteristics such as wind shear, inflow angle and turbulence. Since the wind field modeling is 3D all of these characteristics are calculated and checked to be within acceptable limits for the given turbine type.

Micro-sitting is an iterative process where various turbine locations and types have to be inspected for the investigation of the location yielding maximum energy for a wind turbine. For that reason the software offers the following six (6) modules covering the steps within micro-sitting:

- Terrain
- Wind Fields
- Objects
- Results
- Wind Resource
- Energy

1.1.3 Past Studies

Past computational studies have been performed to investigate the effects of terrain topology and wind resource.

Wessel (2006) calculated the turbulence intensity generated inside offshore wind farms produced by the sea roughness and by the wind turbine wakes. The calculations accomplished by the mean of a semi-empirical model based on the

wind speed profile in the wake and developed by Magnusson. Discrepancies between the measurements and the model were observed, which could be attributed to model inaccuracies associated with the calculation of multiple wakes, and the measurement uncertainties.

Center of Renewable Energy Sources (Prospathopoulos et al, 2008) simulated the wind turbine wakes using a Navier–Stokes solver along with the k – ω turbulence model. The numerical predictions for the hill configurations are compared with those in a flat terrain. It was shown that an increase in the inlet turbulence produces higher accelerations at the hill top and higher decelerations at the lee side of the hill, implying a weaker velocity deficit.

Pinard (Pinard, 1999) applied microscale and mesoscale models, which are considered to be one of the most suitable modeling techniques for the simulation of 3D wind flow over rough terrain. The microscale model is geographically referred to an area in the vicinity of the site whereas the mesoscale model to an area extended some tenths of kilometers around the site. In the RAMS model simulations performed to date it is not yet clear if this particular package is appropriate for modeling the present scale of interest. RAMS model which means Region Atmospheric Modelling System is a mesoscale model, which is presently installed at the Northern Forestry Centre1 in Edmonton. The RAMS model is being used to simulate a wind flow over real complex terrain on a domain size of 25 by 25-km. The lateral boundary conditions don't seem to provide constant inflow conditions. Finer grid spacing less than 1 km causes instability in the model and time step has to be increased to the point where the model runs are in the order of hours.

Petersen (Petersen, 1991) examined the application of mesoscale and microscale modeling procedure for short-term prediction with respect to the effect of surface roughness, where obstacles are and topographical features are present. The output from the comparison of the predicted yearly power production at 18 sites in Ireland and the power production estimated by the vertical

extrapolation of wind measurements agreed. However for very low productions the differences are high due to stability effects from the simplified modeling.

Mortensen and Petersen (Petersen et al, 1997) examined the accuracy of WAsP predictions in rough and mountainous terrain using data from northern Portugal and France (Berge et al , 2010). They concluded that WAsP provides accurate results outside its operation limits, assuming that the difference in ruggedness values between the reference and predicted site is small and the topographical input data is adequate as well as reliable (Rathmann et al, 1996).

A comparison of WAsP and CFD models with respect to the mean absolute error, the vertical variation of wind speed and turbulence with height and mesoscale wind variations across the wind farm has performed at a complex terrain which located at West Norway where measurements of one year by one 50m mast and one 10m mast were available. Although WAsP's weaknesses in complex terrain, CFD models shown no improvements of the average wind speed calculations. (Berge et al)

The accuracy of WAsP predictions in rough and mountainous terrain was explored using data from Northern Portugal and France giving accurate results outside WASp's operation limits provided small differences between the reference and predicted site when the topographical input data are reliable (Petersen et al, 1997).

1.2 Aim & Objectives

The aim of the present study is to assess by computational means the effects of topological and wind parameters on the energy characteristics of a (real) wind farm as well as to investigate computational uncertainties arising from grid resolution and turbulence models.
The objectives of the study are to:

- Assess the effects of surface roughness of the topology on the energy results.
- Perform simulations using different turbulence and wake models with respect to turbulence intensity.
- Investigate the effects of different grid resolutions on the simulation results.
- Assess the 3D nonlinear flow model (CFD) vs the linear flow model WAsP to predict the wind in a highly mountainous terrain in North - West Greece using field data of an operating wind farm.
- Baring in mind the associated numerical uncertainties, to provide some further insight with respect to the accuracy of the state of the art software and methods for complex terrain calculations.

2 THEORITICAL BACKROUND

In this chapter, the key components of the engineering software WindSim and WindPro, as well as the methodology used for the performing the engineering simulations over the wind farm terrain, are presented.

2.1 Description of the models & basic comparisons

In the course of this study linear and non-linear CFD model, called WindSim and WindPro, respectively, have been employed. These are described in detail below.

Linear Model - WindPro/WAsP

The linear model is based on the WAsP software (Wind Atlas Analysis and Application Program) developed in Riso National Laboratory in Roskilde in Denmark, which later merged with Technical University of Denmark and is known as Riso DTU National Laboratory.WAsP is based on the Wind Atlas model which was originally designed by Troen and Petersen (WINDPRO SOFTWARE) and is composed by a physical model (stability submodel, roughness change submodel, orographic submodel) and statistical model which are described below .

Non Linear Model - WindSim

WindSim which is a non linear software based on the Computational Fluid Dynamics (CFD) code PHOENICS is usually preferred for simulations
(Castellani, 2011) over rough terrain used in order to compare the results taken from WindPro (Watson, 2004), (Cabezon, 2005).

2.1.1 Equations

Physical Model

The **physical model** is comprised of the *Stability model*, the *Roughness change model*, the *shelter submodel* and the *orographic submodel*.

The physical flow model analyses the wind profile of the surface layer which is needed for the vertical and horizontal extrapolation of the wind climate results from one height to another as described by the logarithmic law in Equation 2-1

$$u(z) = \frac{u_*}{\kappa} ln \frac{z}{z_0} \quad \textbf{(2-1)}$$

The logarithmic law is referred only to homogenous terrain where the roughness is stable. In case the roughness changes the *roughness change submodel* is applied which described in section 1.1.1 (Equation 1-4) by taking into account a well-known velocity U_m at a reference height z_{ref}

$$\frac{U_m(\mathrm{z})}{U_m(z_{ref})} = \frac{\ln\left(\frac{\mathrm{z}}{z_0}\right)}{\ln\left(\frac{z_{ref}}{z_0}\right)} \quad \textbf{(2-2)}$$

The *stability submodel* examines the atmosphere's stability with respect to the surface's heat flux variations which have a real effect in the wind profile.

Therefore the stability model is described by the following Equations 2-2 and 2-3 for stable or unstable conditions (Petersen et al, 1989). In this study the calculations are performed for stable conditions.

$$\psi\left(\frac{z}{L}\right) = -4.7\frac{z}{L} \qquad for\ stable\ conditions \tag{2-3}$$

$$\psi\left(\frac{z}{L}\right) = \left(1 - 16_{\frac{z}{L}}\right)^{1/4} - 1 \quad for\ unstable\ conditions \tag{2-4}$$

The *shelter submodel* corrects the deviations of the wind profile which are responsible for the decrease of the wind velocity. These deviations arise from the wind wakes due to the existence of several kinds of obstacles.

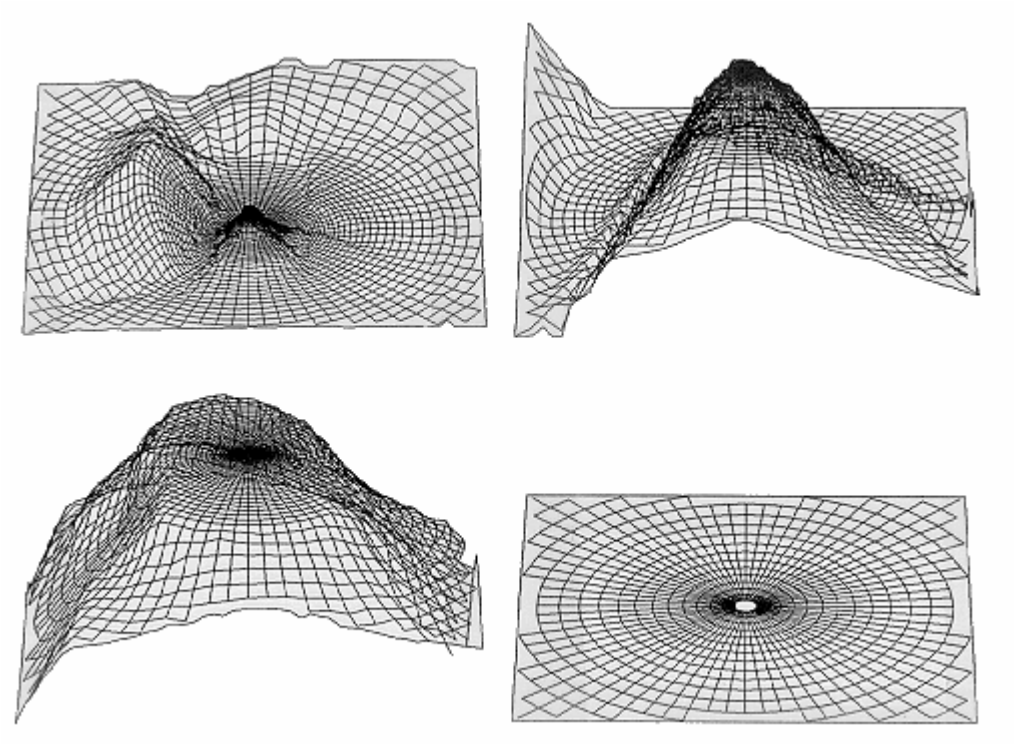

Figure 2-1 WAsP mesh calculation of and expansion of terrain information zooming at the central point of interest

(Wallbank, 2008)

According to the *Orographic submodel*, the terrain information from the height contours are calculated and expanded on a polar grid at the central point of interest only, as shown in Figure 2-1. This is achieved by the use of Fourier-Bessel equations (Nielsen et al, 2007).

Statistical model

Through the statistical model a frequency distribution from the wind speed as well as the wind direction is supplied from the area of interest which has been separated at twelve sectors. The statistical model is described by Equation 1-3-section 1.1.1 known as Weibull distribution.

WINDSIM

WindSim is based on the Computational Fluid Dynamics (CFD) code PHOENICS (Gravdahl, 1998). PHOEINICS is a code that allows users to add their own subroutines, a useful feature when simulating the atmospheric boundary layer.

The CFD code solves the incompressible flow equations that correspond to the conservation of mass, conservation of momentum and heat transfer equation (Tu et al, 2008), (Wallbank, 2008), (Anderson, 1995):

$$\frac{\partial u}{\partial x}+\frac{\partial v}{\partial y}+\frac{\partial w}{\partial z}=0 \qquad \textbf{(2-5)}$$

$$\rho\left(\frac{\partial u}{\partial t}+u\frac{\partial u}{\partial x}+v\frac{\partial u}{\partial y}+w\frac{\partial u}{\partial z}\right)=-\frac{\partial p}{\partial x}+\mu\left(\frac{\partial^2 u}{\partial x^2}+\frac{\partial^2 u}{\partial y^2}+\frac{\partial^2 u}{\partial z^2}\right) \qquad \textbf{(2-6)}$$

$$\rho\left(\frac{\partial v}{\partial t}+u\frac{\partial v}{\partial x}+v\frac{\partial v}{\partial y}+w\frac{\partial v}{\partial z}\right)=-\frac{\partial p}{\partial y}+\mu\left(\frac{\partial^2 v}{\partial x^2}+\frac{\partial^2 v}{\partial y^2}+\frac{\partial^2 v}{\partial z^2}\right)+\rho g_y \qquad \textbf{(2-7)}$$

$$\rho\left(\frac{\partial w}{\partial t}+u\frac{\partial w}{\partial x}+v\frac{\partial w}{\partial y}+w\frac{\partial w}{\partial z}\right)=-\frac{\partial p}{\partial z}+\mu\left(\frac{\partial^2 w}{\partial x^2}+\frac{\partial^2 w}{\partial y^2}+\frac{\partial^2 w}{\partial z^2}\right) \qquad \textbf{(2-8)}$$

$$\frac{\partial T}{\partial t}+u\frac{\partial T}{\partial x}+v\frac{\partial T}{\partial y}+w\frac{\partial T}{\partial z}=\frac{k}{\rho C_p}\frac{\partial^2 T}{\partial x^2}+\frac{k}{\rho C_p}\frac{\partial^2 T}{\partial y^2}+\frac{k}{\rho C_p}\frac{\partial^2 T}{\partial z^2} \qquad \textbf{(2-9)}$$

where ρ is the density, u the x velocity component, v the y velocity component, w the z velocity component, p the pressure, g corresponds to the gravity components and T to the temperature. For the present study the pressure variations within the computational domains are between 1^o to 2^o and therefore any temperature analysis is not of interest since the simulations can be considered as isothermal.

2.1.2 Numerical Methods

The WindSim software solves the RANS equations (Reynolds Averaged Navier Stokes), using the finite volume method through a graphical interface and the CFD solver Phoenics. CFD is a numerical method for solving the fundamental

equations of fluid flow. The fundamental behavior of fluid flow is described by the Navier-Srokes equations which are non-linear partial differential equations with analytical solutions being available only for simple cases.

Difference between the WAsP and the CFD is noticed primarily in areas with flow separation and this can be illustrated by looking at speed-up over a ridge. The speed-up increases when the inclination angles increasing until the flow separates, as seen in Figure 2-2 (Gravdahl, 2007).

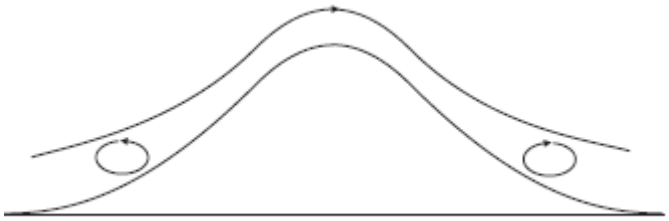

Figure 2-2 Flow separation over steep hill presenting the flow recirculation
(Wallbank, 2008)

For an inclination angle above 20 degrees the flow separates. The recirculation acts as an extension of the terrain, the ridge becomes more like a plateau and the acceleration is reduced, which is an effect impossible to be modelled WAsP due to its linear behavior.

The Navier-Stokes equations are solved in a time averaged fashion (Reynolds-Avegared Navier-Stokes or RANS equations) according to which the turbulent fluctuations appear in the right hand side of the equations. A turbulence model is required to close the equation set of the RANS equations. The RANS equations are discredited in a computational domain and integrated in time and space using a finite-volume method. The non-linear CFD model is expected to be more accurate even for smaller inclination angles when the flow does not separate.

WindPro Software

WindPro uses the *Basis* and *Energy* modules for the calculation of the energy production and the analysis of wind resource.

The *Basis* module is provides tools that can utilize scanned maps or maps which can be found through the internet or other digital sources. These maps can be further edited and used as input data (digital background maps). In addition, the software provides special tools for creating digitized height contour lines, maps of roughness data as well as visualization capabilities such as as photomontages or virtual reality presentations through Google Earth tools for presenting the terrain with the wind turbines.

The Energy module is used for the assessment of energy production of a wind turbine/wind farm in simple or complex terrain. The module utilizes different tool options, such as *Atlas, Meteo, WasP interface, Stagen, Resource* and *Park.*

The *Atlas* module calculates the energy production from a give terrain description (roughness, hills and obstacles) and wind statistics. Atlas is usually employed for non-complex terrains and is never used in conjunction with mountainous terrain since the hills and obstacles are calculated with less complex flow models.

The *Meteo* module calculates the energy production based on measured wind data measured at the future wind turbine location. If the measurements are taken at a height lower than the hub height of the selected wind turbine, the data can be extrapolated by giving in a wind gradient exponent.

The WindPro software uses the *WAsP interface* known as calculation "engine" to calculate the energy production through the wind speed distribution, which is obtained by wind statistics and terrain description. In contrast to the Atlas module, which is limited to calculations of simple terrain, WAsP allows the use of digitized height contour lines and a free definition of obstacles.

The *Stagen* tool works together with *Meteo* and WAsP interface modules by taking measured wind data and convert them into Wind Statistics. The measured wind data are “cleaned” from local terrain conditions, so a regional wind climate is established for use in calculations at alternative locations from those where the wind measurements were taken.

The *Park* module is used for the calculation of the energy production of one or more wind farms. The input for the *Park* calculation are the wind turbines positions, types and hub heights, plus the wind energy delivered from one of the previous mentioned modules (*Atlas, Meteo, WAsP interface*) or wind data, from the *Resource* module. This can be obtained by giving the thrust coefficient curve of the wind turbine(s) and the wind farm layout (H.Miller, 1978). The thrust coefficient (***Ct***) is an input parameter to estimate the characteristics of the wake effect of the wake producing turbine. In particular the added turbulence will be a function of the thrust coefficient (Frohboese & Schmuck, 2010).

For the calculating the energy production of a wind farm, the existence of wake(s) which generate(s) behind each wind turbine should be taken into account (R.J. Barthelmie University of Endiburgh (UK) and Riso National Laboratory/DTU, 2007). WAsP is able to estimate the total wake losses through the *Park* module for the entire wind farm and thereby the total annual energy production calculated for each wind turbine and for the whole wind farm. The *Par*k module makes advanced calculations regarding the turbulence intensity through many different array loss models. Although there are numerous of wake models available in WindPro for the calculation of wake loss in a wind farm, N.O. Jensen (Risø/EMD) wake model was only applied in this study by WindPro due to its old version whereat the beginning only Jensen model used for wake modeling. Therefore Jensen model has been chosen in this study because it is used both in WindPro and WindSim software. Jensen Wake model is a simple single wake model in terms of an initial velocity deficit and a wake decay constant and is based on the assumption that the wake behind the wind turbine has a starting diameter equal

to the rotor diameter which is expanding in linear way as a function of the downwind distance X.

The flow field which is used for wind turbine output is describing below two wind turbines A_o and A_1 where the wake of A_o overlaps with the downstream velocity of A_1 wind turbine as seen in Figure 2-3:

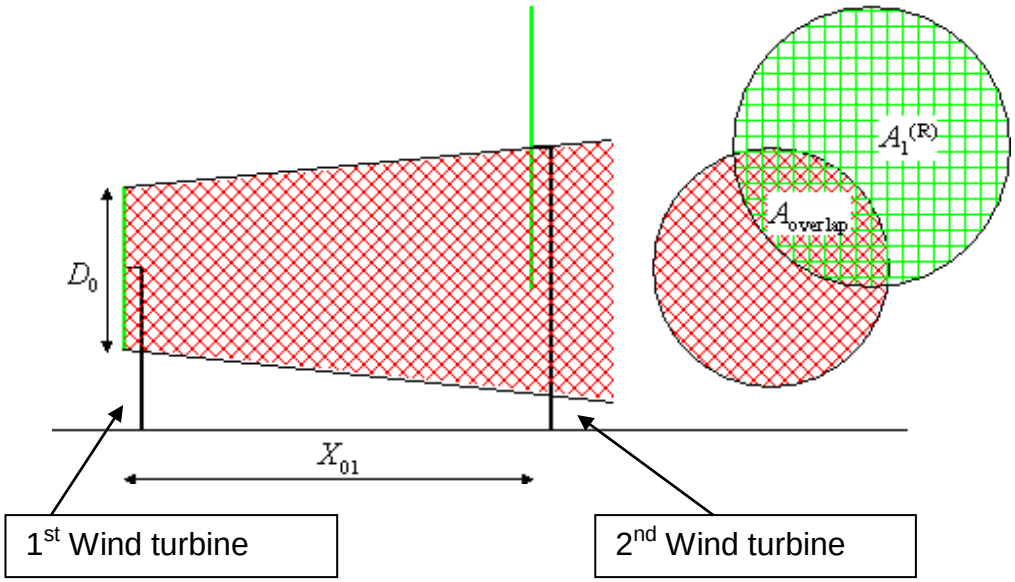

Figure 2-3 Wind speed deficit by the interaction of two wind turbines

The effective wind speed deficit at the down-wind wind turbine ("A1") is calculated using the following Equation 2-10,

$$\delta V_{01} = U_0 \left(1 - \sqrt{1 - C_t}\right) \left[\frac{D_0}{D_0 + 2kX_{01}}\right] \frac{A_{overlap}}{A_1{}^{(R)}} \qquad \textbf{(2-10)}$$

where δV_{01}expresses the wind speed deficit where "0" corresponds to the rotor diameter of first wind turbine and "1" to the rotor diameter of the second one, and where U_0(m/s) is the undisturbed wind speed at the up-wind turbine ("A0") with

rotor diameter D_0(m), C_t the thrust coefficient, X_{01}(m) the downwind horizontal distance between the wind turbines and *k* is the wake decay constant.

The thrust coefficient C_t is related to the thrust force F_T, the air density ρ and displayed at the following Equation 2-11,

$$C_t = \frac{2F_T}{\rho \frac{\pi}{4} D_0^2 U_0^2} \quad \textbf{(2-11)}$$

The initial wind speed reduction from U_0 to V, when passing the rotor plane, is related to C_t by: $(1\text{-}C_t) = (V/U_0)^2$. The wake effect decay constant has the default value k= 0.075, however in off-shore applications is recommended a lower limit of k = 0.04 and increases as ambient turbulence increases.

WINDSIM

The following modules displayed further down are applied for the calculation of energy production and the examination of wind assessment of an area of interest for the development of wind farm.

Terrain

The micro siting process which means the selection of the area for the establishment of wind turbines, begins with the *Terrain* module; this generates a 3D model area around the wind farm. The process involves choosing the horizontal and vertical extension of the volume to simulate. This volume is called the computational domain and is built based on roughness and elevation data from a specified grid. Either roughness values can be read by the specified grid or several values of roughness height can be selected by the values mentioned in Table1.1 according to the roughness class. The roughness height is described by log-law, see Section 2.1 – Eq. 2-1

The accuracy of the numerical calculations depends not only on the grid and roughness characteristics but also on the grid resolution. The most common resolution for meso scale modelling is 100x100m, however the desired resolution

cannot always be achieved due to limited computational means. There is availability to specify a finer grid, making the distribution of nodes denser in case of micro scale modeling, creating a resolution of 10x10m. In addition, forested areas and physical objects can be modeled, like buildings, in order to examine their influence to the wind flow.

Wind Fields

The *Wind Fields* module is used for the generation of wind database. Simulations are performed for the examination of the terrain's dependence on the wind conditions in case of wind acceleration or turbulence. The module includes several different numerical or physical models. The k-ε model is usually applied for turbulent flow simulations. The solution procedure is iterative and starts with the initial conditions and through iteration progress the converged solution is achieved. The convergence of the wind field simulations is evaluated by inspection of the spot and residual values for the velocity components (U1, V1, W1), the turbulent kinetic energy (KE) and its dissipation rate (EP). All variables are scaled according to the min and max values. VARMIN and VARMAX are used to specify the maximum permissible values of each variable. The default values effectively impose no constraints (VARMAX of 1e10, 1e6 or 1e4 and VARMIN = -VARMAX) but sometimes convergence can be improved by lower absolute values, usually to control excessive changes in the early stages of the simulation. In some cases these would otherwise prove fatal: extreme temperatures or pressures can have disastrous consequences because of their effect on density (Phoenics Encyclopedia)

It is also possible the evolution of convergence to be animated during the iterative progress. Maximum correction behavior is probably a reliable guide to convergence behavior. If the largest correction is zero, the solution will not change any more and iteration can stop. If the biggest correction settles to a non-zero value, or is diminishing very slowly, this may well be a sign of too-tight relaxation.

Objects

The *Object* module is used for the placement of turbines and climatology data. The domain can be visualized by the 3D tool, giving the option to be viewed by different angles and distances.

Results

When the wind field simulations have been completed and the climatology files has been defined the *Results* module is performed for the examination of flow variables, such as wind speed in 3D space, turbulence intensity, inflow angle or wind direction in horizontal plane.

Wind Resources

The *Wind Resource* module is crucial for the energy optimization because it contributes to the weighting of the wind database against the measurements (Rene Cattin, 2004). Wake effects can be calculated using the following wake models (Prospathopoulos et al, 2010):

- Jensen
- Larsen

which are all analytical models used for the calculation of velocity deficit. The Larsen wake model is a semi-analytical assuming that the wake area can be described by Prandtl's rotational symmetric turbulent boundary layer equations. (Larcen, 1998).

The mean wind velocity deficit is determined by the following Equation 2-12:

$$\delta V = \left(\frac{1}{9}\right)(C_t A_r x^{-2})^{\frac{1}{3}} \left[r^{\frac{3}{2}} \ (3C_1^2 C_t A_r x)^{-\frac{1}{2}} - \left(\frac{35}{2\pi}\right)^{\frac{3}{10}} \ (3C_1^2)^{-\frac{1}{5}}\right]^2 \qquad (2\text{-}12)$$

where:

C_t is the thrust coefficient

$A_r=\pi D^2/4$

D= rotor diameter

$C1 = (D/2)^{5/2}(C_t A_r x_0)^{-5/6}$

X_0= 9.5D/$\left(\frac{2R_{95}}{D}\right)^3 - 1$

R_{95}= 0.5 (R_{nb}+min($h_1 R_{nb}$))

R_{nb}= max (1.08D+21.7D(I_a-0.05))

Energy

The *Energy* module is used for the calculation of the energy production of individual wind turbines or the entire wind farm; the module takes into account wake losses in every calculation.

2.1.3 Grid Generation techniques

The grid generation is one of the most important procedures and sometimes a very demanding task, subject to the complexity of the examined case. Finer meshes, which correspond to increased spatial accuracy, are usually required for improving the numerical solution by allowing the employed numerical method to capture all the relevant scales.

In WAsP regarding the grid generation procedure, the model developed by Troen at 1990 for the calculation of wind's velocity perturbation which appears especially at hills or rough terrains, is employed. The BZ model is used for the optimization of wind turbines' micro-sitting. WAsP applies Fourier-Bessel equations by the expansion of a polar grid which zooms at the central point of interest. An orthogonal-curvilinear mesh is produced with increased density as the center is approached as shown in Figure 2-4.

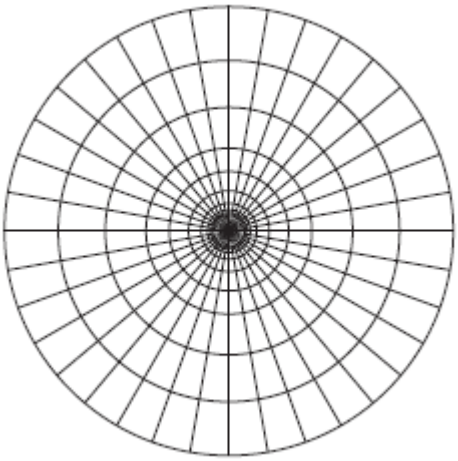

Figure 2-4The WAsP grid generation technique by the production of polar grid

(Wallbank, 2008)

In the framework of WindSim an embedded structured mesh generator is utilized through the terrain module. The computational domain contains information about elevation and roughness based on the digital terrain map.

WindSim has employed structured grid methods using 2D elements of quadrilateral form and elements of 3D of hexahedral form for the computation of a rectangular array. One of the features of this block is the ability to be twisted or stretched even when the topology is fixed.

Previously, the mesh of structured grid method existed only of one block while later the multiblock structured grid developed (Liseikin, 2009) where many blocks could be connected for the construction of the entire domain as seen in
Figure 2-5. The development of a good quality multi-block structured grid is a time consuming task that sometimes may takes several days.

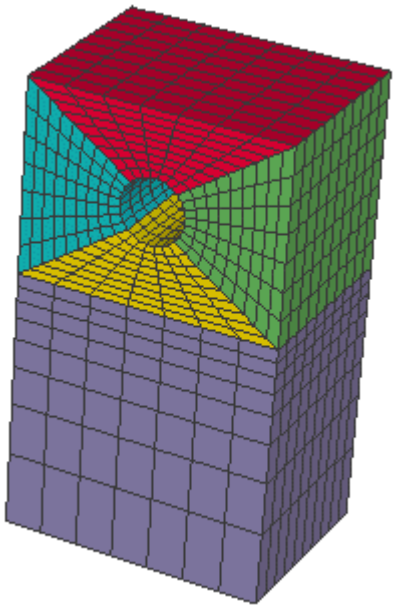

Figure 2-5 Structured multiblock grid consisting of elements of 3D hexahedral form

source: www.windsim.com/ModuleDescriptions

2.1.4 Turbulence Models

WindPro

WindPro has seven turbulence models available in combination with the N.O. Jensen (EMD) 2005, and Larsen wake models.

WindSim

The turbulence intensity is calculated by several turbulence models included in the WindSim package. Past research has shown (Nilsson, 2010) that the standard k-ε model behaves best under most conditions and gives the most reliable results. According to the type of surface, the choice of turbulence model has the largest impact on areas, especially where the flow is separated. Flow separation usually occurs behind hills (Mann et al, 2000).

The present simulations have been performed by the two equations k-ϵ model, where k stands for the Turbulent Kinetic Energy (TKE), and ϵ for the Turbulent Dissipation Rate (TDR). The equations are given below:

Turbulent kinetic energy

$$\frac{\partial k}{\partial t}(\rho k) + \frac{\partial}{\partial x_i}(\rho k u_i) = \frac{\partial}{\partial x_j}\left[\left(\mu + \frac{\mu_t}{\sigma_\kappa}\right)\frac{\partial k}{\partial x_j}\right] + G_k + G_b - \rho\varepsilon - Y_M - S_k \qquad \textbf{(2-13)}$$

Turbulent dissipation rate

$$\frac{\partial}{\partial t}(\rho\varepsilon) + \frac{\partial}{\partial x_i}(\rho\varepsilon u_i) = \frac{\partial}{\partial x_j}\left[\left(\mu + \frac{\mu_t}{\sigma_\kappa}\right)\frac{\partial \varepsilon}{\partial x_j}\right] + C_{1\varepsilon}\frac{\varepsilon}{k}(G_k + C_{3\varepsilon}G_b) - C_{2\epsilon}\rho\frac{\epsilon^2}{k} - R_\varepsilon - S_\varepsilon \qquad \textbf{(2-14)}$$

In these equations, G_k represents the generation of turbulence kinetic energy due to the mean velocity gradients, calculated as described in Modeling Turbulent Production in the k- ε Models. G_b is the generation of turbulence kinetic energy due to buoyancy, calculated as described in Effects of Buoyancy on Turbulence in the k- ε Models. Y_M represents the contribution of the fluctuating dilatation in compressible turbulence to the overall dissipation rate, calculated as described in Effects of Compressibility on Turbulence in the k- ε Models. S_k and S_ε are user-defined source terms.

$\boldsymbol{\mu_t}$ is the turbulent viscosity defined by as:

$$\mu_t = C_\mu \frac{k^2}{\epsilon} \qquad \textbf{(2-15)}$$

where: c_μ=0.09, σ_k=1.0, σ_ε=1.3, $C_{1\varepsilon}$=1.44 and $C_{2\varepsilon}$=1.92

Investigation into changing the model constants to achieve better results, has shown that for wind flows in a neutral atmospheric boundary layer, the constant do not have an important effect. Two variants of the model that are available in WindSim and are used in the present work are the Yap [Yap C. J. (1987)] correction and RNG (ReNormalization Group) version [Yakhot et al (1992)]

The YAP correction takes into account the variations of the turbulence length scale from its local equilibrium level.
The RNG version of the k-ε model is obtained by applying the Renormalized Group Theory (RNG) to obtain the coefficients of the model (Pironneau et al, 1994)

The main difference between the RNG and standard k-ε models lies in the additional term in the ε equation given by

$$R_\varepsilon = \frac{C_\mu \rho \eta^3 (1-\eta/\eta_0)}{1+\beta\eta^3}\frac{\varepsilon^2}{k} \qquad \textbf{(2-16)}$$

where $\eta = S_k\,/\boldsymbol{\varepsilon}$, $\eta_0 = 4.38$, $\beta = 0.012$

The effects of this term in the RNG **ε** equation can be seen more clearly by rearranging **Equation 2–14**. Using **Equation 2–16**, the third and fourth terms on the right-hand side of **Equation 2-14** can be merged, and the resulting ε equation can be rewritten as

$$\frac{\partial}{\partial t}(\rho\varepsilon) + \frac{\partial}{\partial x_i}(p\varepsilon u_i) = \frac{\partial}{\partial x_j}\left[\left(\mu + \frac{\mu_t}{\sigma_\kappa}\right)\frac{\partial \varepsilon}{\partial x_j}\right] + C_{1\varepsilon}\frac{\varepsilon}{k}(G_k + C_{3\varepsilon}G_b) - C^*_{2\varepsilon}\rho\frac{\epsilon^2}{k} \qquad \textbf{(2-17)}$$

where $\boldsymbol{C^*_{2\varepsilon}}$is given by

$$C^*_{2\varepsilon} \equiv C_{2\varepsilon} + \frac{C_\mu\,\eta^3(1-\eta/\eta_0)}{1+\beta\eta^3} \qquad \textbf{(2-18)}$$

In regions where, $\eta < \eta_0$ the R term makes a positive contribution, and $\boldsymbol{C^*_{2\varepsilon}}$ becomes larger than $\boldsymbol{C_{2\varepsilon}}$. In the logarithmic layer, for instance, it can be shown that $\eta \approx 3.0$, giving $\boldsymbol{C^*_{2\varepsilon} \approx 2.0}$, which is close in magnitude to the value of $\boldsymbol{C_{2\varepsilon}}$in the standard k- ε model. As a result, for weakly to moderately strained flows, the RNG model tends to give results largely comparable to the standard k- ε model.

In regions of large strain rate ($\eta > \eta_0$), however, the R term makes a negative contribution, making the value of $\boldsymbol{C^*_{2\varepsilon}}$ less than $\boldsymbol{C_{2\varepsilon}}$. In comparison with the standard k- ε model, the smaller destruction of **ε** augments **ε**, reducing k and, eventually, the effective viscosity. As a result, in rapidly strained flows, the RNG model yields a lower turbulent viscosity than the standard k- ε model.

Thus, the RNG model is more responsive to the effects of rapid strain and streamline curvature than the standard k- ε model, which explains the superior performance of the RNG model for certain classes of flows.

2.2 Methodology

2.2.1 Site Description

The wind assessment concerns the mountain called Panachaiko (Figures 2-6 & 2-7*)*. This wind park is in operation since 2005 in South - West Greece and consists of 41 850KW Acciona Enegia wind turbines with total power of 34.85 MW. It is located in the west part of Peloponnese in an altitude of approximately 1600m, while the highest peak extends 1928m. The southern and western part is forested, while the rest of it is mostly rocky and partly grassy. The park is constructed at a relatively flat plateau which extends for 2.5m before the terrain drops away steeply *(*Figure 2-8*)*. The height variation from the ground to the top of the mountain is approximately 600m. Therefore the reason of making interesting the research of wind resource behavior to this site is the effect of "speed-up" phenomenon as described in Figure 2-2. on the energy production.

Figure 2-6 Panachaiko Windfarm from SSE direction

Source: www.geosolutions.gr

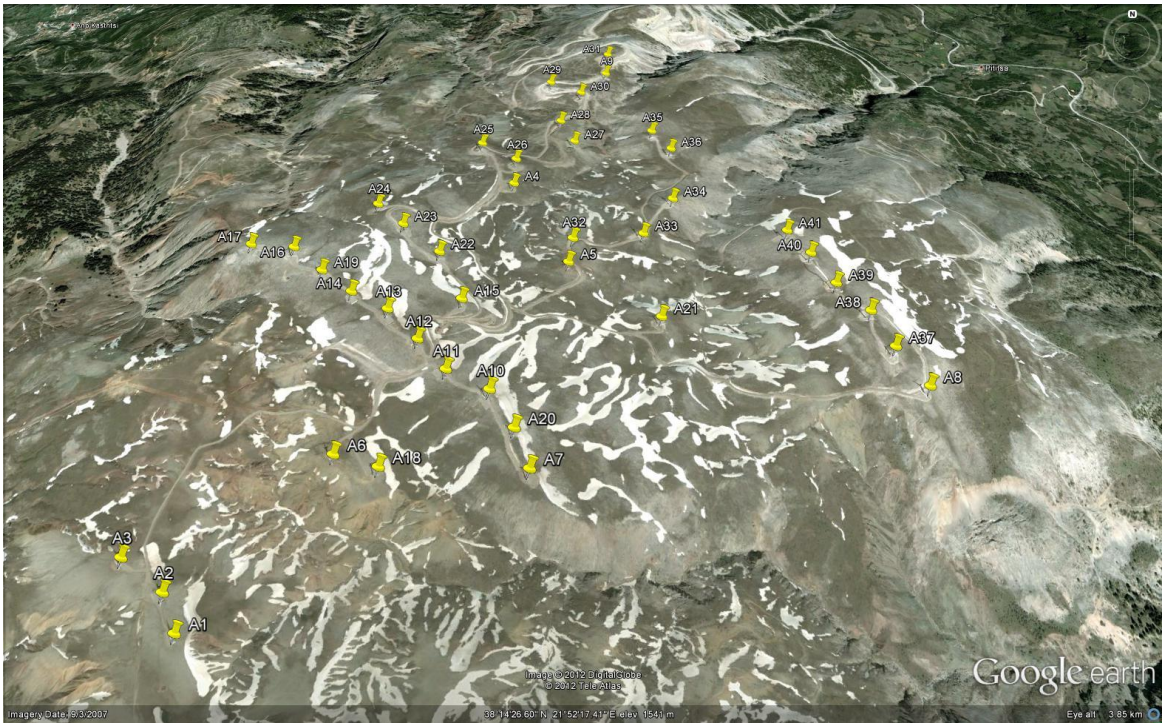

Figure 2-7 Panachaiko plan, with yellow pins showing the wind turbines places with their corresponding number.

Figure 2-8 Presentation of Steep Inclination at North direction (google earth)

2.2.2 Terrain

The maps are provided by the Military Geographical Service which is called GYS and is a public authority of the military in order to be inserted in both software.

The following maps in scale 1:50.000 used for the required simulations which have been merged and then converted to digitized maps containing information regarding elevation and roughness:

- Chalandritsa map
- Nafpaktos map

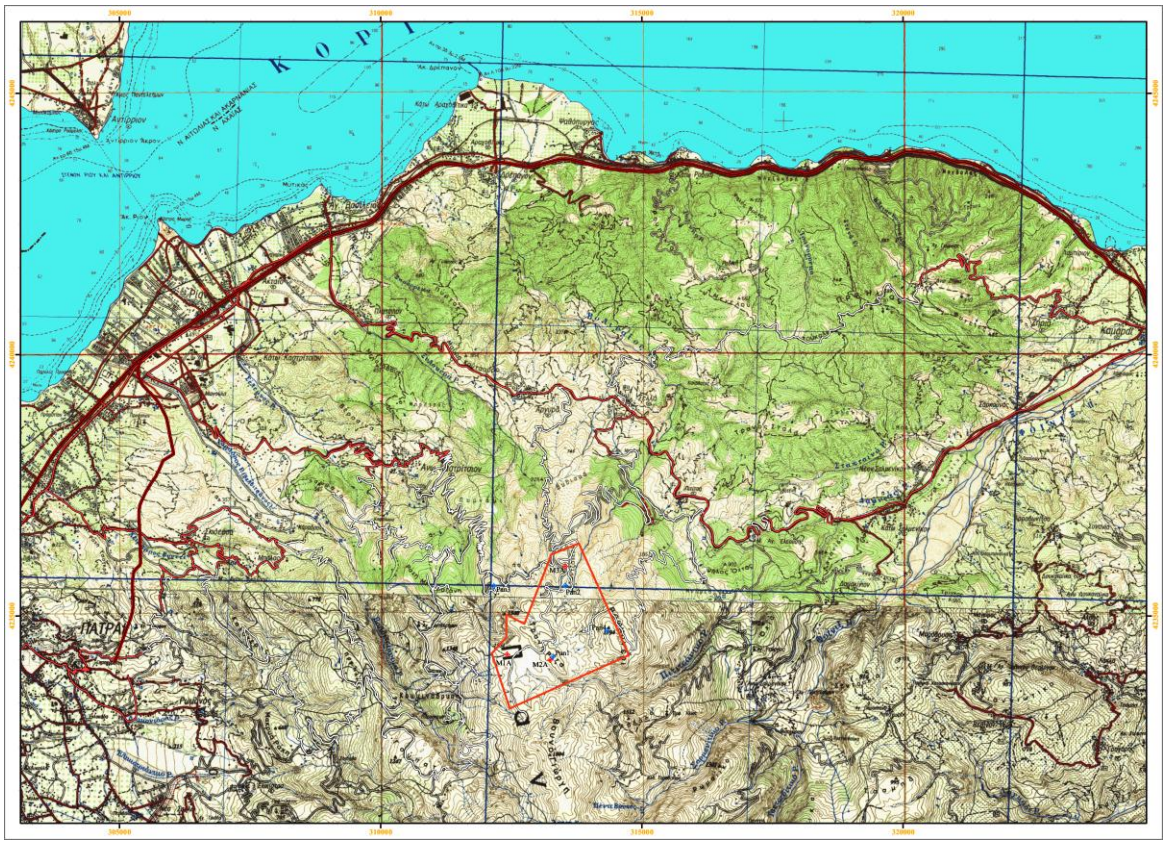

Figure 2-9 Panachaiko Windfarm layout presentation at merged Nafpaktos & Chalandritsa maps

2.2.3 Wind Data

Data from eight (8) different positions have been collected for the evaluation of wind speed. Out of the eight (8) measurement positions which are within the site borders, at three (3) masts there have been measurements at 10m height (code: Pan1, Pan2, Pan4) and at the other four (4) there have been measurements at 50m height (code: M1, M2, M3, Pan 5). One (1) 10m (code: Pan 3) mast installed at a nearby location at a distance of approximately 1,5 km for correlation reasons as seen in *Fig.14*. Masts' measuring period starting from year of 2003 until 2005.

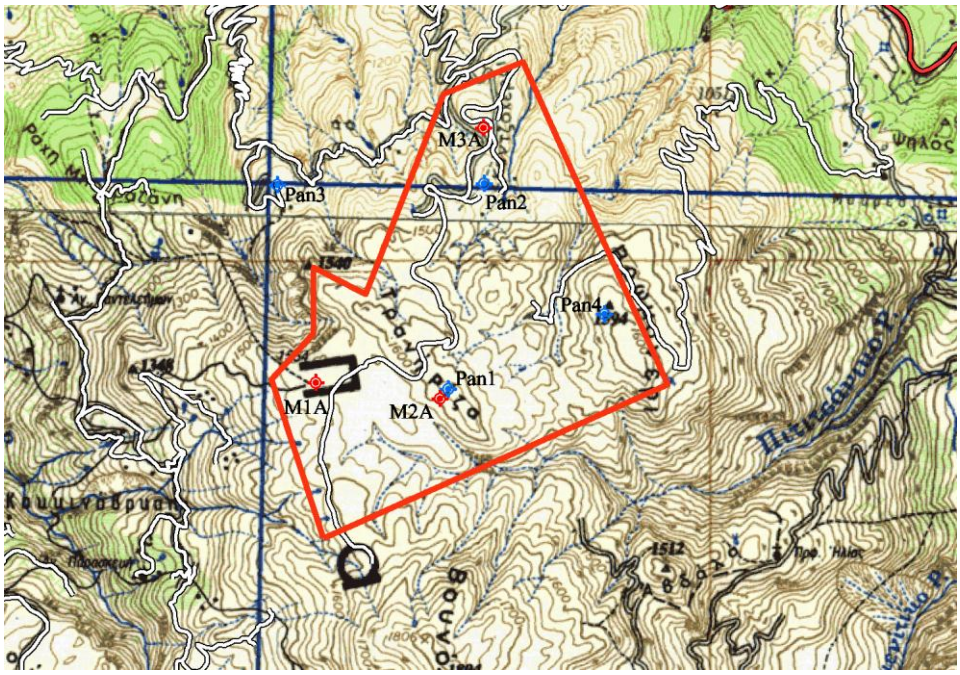

Figure 2-10 Plan of wind farm area including the mast location

Although there were eight (8) masts, only four (4) of them were used for wind resource simulation, since for the rests we did not have the required availability. For the evaluation of the wind potential of the project, long term on-site measurements have been available at four (4) different positions from two (2) 10m masts and two (2) 50m masts. The coordinates in local system EGSA '87, the height of each mast as well as the elevation of the area of mast installation and the measurement period are presented in Table 2-1 and Figure 2-10 and 2-11.

Local Coordinates EGSA '87					
Mast Name	Easting	Northing	Mast height (m)	Elevation	Measurement Period
PAN 5	313292	4234243	40	1600	04-01-04/31-12-04
M1	312417	4234260	49.1	1548	12-07-03/12-07-04
Pan 3	312040	4235419	10	1325	30-07-03/30-07-04
Pan 4	314330	4234715	10	1557	04-01-04/31-12-04

Table 2-1 Features of measurement masts

Figure 2-11 Presentation of Panachaiko site and masts location

The measured data have been manually inspected and filtered, identifying inconsistencies and missing data. In addition, masts which have common period have been correlated to each other. Therefore M1 and Pan3 are representative of July of 2003 to June of 2004, while Pan5 and Pan4 from January of 2004 to December 2004.

2.2.4 Remarks on existing experimental data

The wind farm investigated has been in operation since 2006. Detailed experimental results related to the energy yield and the corresponding wind speed time series have been available since then for each one of the 41 wind turbines.

However, due to the marketing policy of the company that owns the wind farm, such experimental data has been handed over to us for the turbines No1 and No39 corresponding only to the year 2010.

3 NUMERICAL AND GRID CONVERGENCE EFFECTS AND ENERGY ANALYSIS

3.1 Dependence of energy calculations on the CFD results

Calculation of the annual energy production requires the CFD results to be obtained as accurately as possible. Therefore, one has to ensure that

- the CFD results used to calculate the energy production are as much as possible independent of the grid resolution;
- and the computations have numerically converged by performing an adequate number of numerical iterations.

The above points should, however, be considered by bearing in mind a number of computational constraints as well as common engineering practices:

1) Turbulent flow simulations can never be fully grid-independent unless all scales of turbulence are captured. This would require extremely fine grids at the level of direct numerical simulation, where the equations are solved without any approximations such as the Reynolds averaging and without using any turbulence model.
2) Although the Reynolds-averaged Navier-Stokes formulation allows for computations to be performed on moderate grids in order to obtain predictions within an acceptable engineering threshold, fine grids may still be required to achieve a reasonable order of accuracy. This is not, however, always possible due to the lack of available computational resource. Note that most wind calculations within an engineering design environment are performed on very coarse grids due to the aforementioned reason.
3) Turbulence modeling usually leads to numerical stiffness, i.e. the numerical convergence is difficult to be achieved. This is due to the fact that turbulence models contain a number of source terms, which cannot be

expressed in a conservative form in the framework of the turbulence transport equations. As a result of this, the transport equations of the turbulence models converge slower than the fluid flow transport equations. Consequently, transport variables such as the turbulent kinetic energy and the turbulent dissipation rate may never converge at the same level as the flow variables.

Bearing in mind the above, the objectives of our grid and numerical convergence studies are to

- Investigate the effects of the grid resolution on the results, particularly on the annual energy predictions, within the limits of our available computational power. The present computations have been performed on a single processor of a Desktop PC with Intel Corei7, 2.93GHz and 6GB. This system is the commonly used platform within the environment of many wind engineering companies. 'A parallel cluster and the corresponding software licences were not available during the course of this study, thus the calculations were performed on a single processor machine.
- Examine the numerical convergence of the WindSim software.

The calculations of the annual energy production are made by the WaSP software, which uses as input the CFD results obtained by WindSim.

3.2 Numerical Convergence

The numerical convergence has been examined through residual criteria provided by WindSim. The program defines the numerical convergence applying the most widely-known technique for achieving convergence is the use of relaxation. This slows down (relaxes) the changes made to the variables from sweep to sweep. Relaxation does not alter the final solution, only the way in which it is achieved. Two types of relaxation are available: linear and local time step. In our case the false time step relaxation is selected since is usually applied to velocities.

Local time step *relaxation:*

Local time step relaxation modifies the finite-volume equations by adding an additional, pseudo-transient term:

$$(\text{mass in cell}) \times (\square^{old} - \square^{new}) / dt_f$$

where, dt_f is the local time step, mass in cell is the flow mass, local time step is variable that takes into account the grid spacing and cell velocity.

These squares “old” and “new” represent any of the variables listed below

- The residuals of five variables are monitored in each sector: The three velocity components (U1, V1, W1)
- The turbulent kinetic energy (KE), and
- The turbulent dissipation rate (EP)

The residual values are plotted in Figures 3-1 to 3-12 for a) 12 different wind direction sectors in which the wind rose is divided and b) different grids. Computations have been performed on five different grids with size ranging from 46,500 to 217,080 cells. The different grid sizes are shown in Table 3-1

Total Number of cells	X	y	Z
46500	31	25	60
85680	42	34	60
151200	56	45	60
217080	67	54	60

Table 3-1 Grid resolution with respect to number of cells in x, y, z direction

We should note that the calculations are considered as numerically converged when the residuals are stabilezed, i.e. they do not fluctuate. Therefore, although ideally we wish to achieve numerical convergence by approaching the *MIN* residual value as defined by WindSim, this may not be achieved in practice, as experience shows, especially for complex surface terrains.

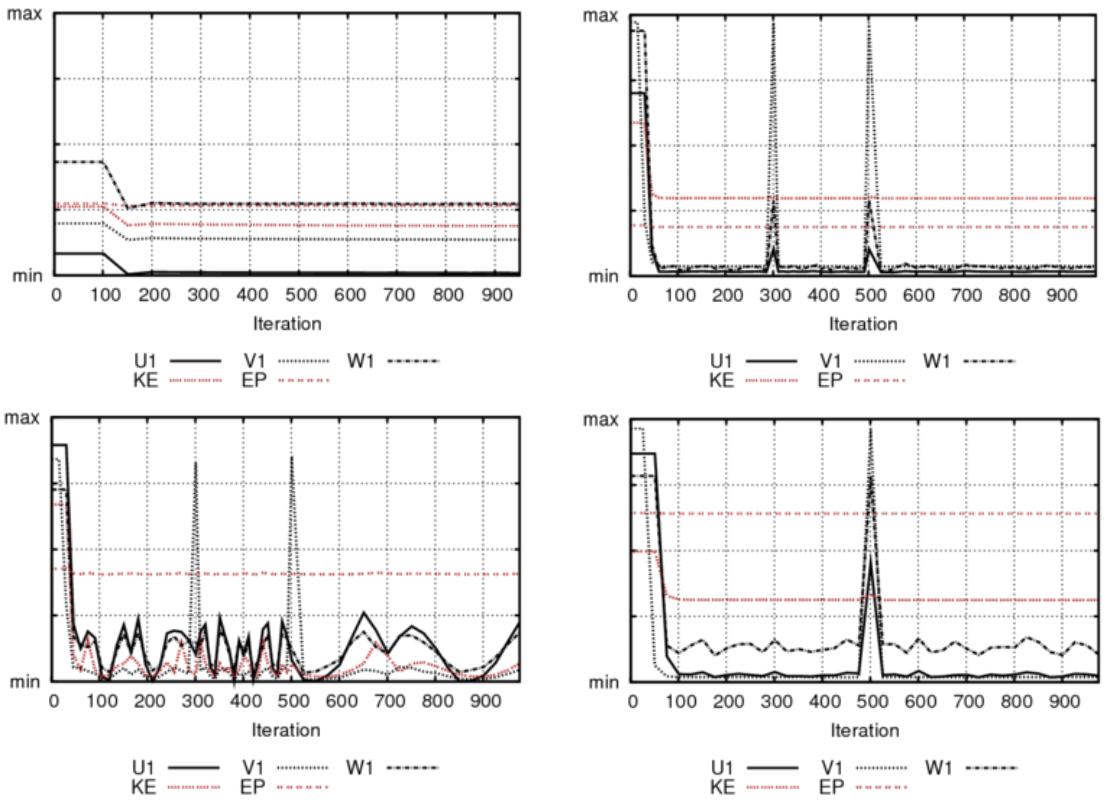

Figure 3-1 Residuals of flow and turbulence model variables in 0- sector for different grids with 46500, 85680, 151200 and 217080 cells, from top to bottom respectively

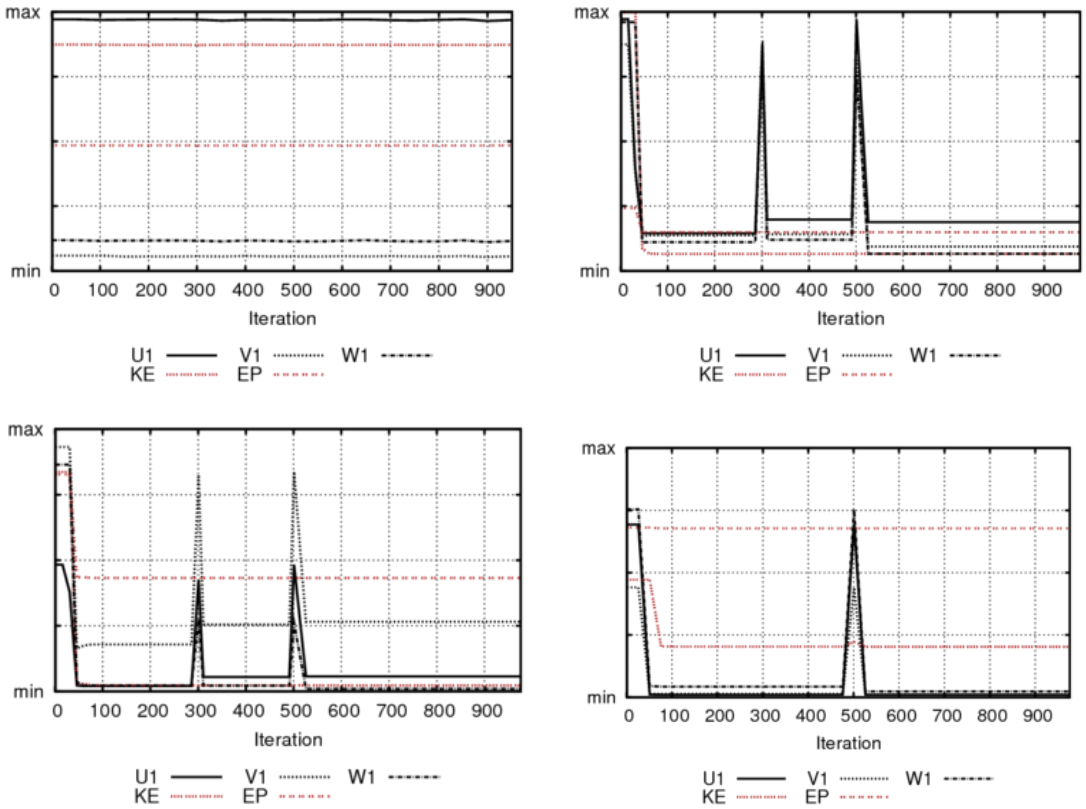

Figure 3-2 Residuals of flow and turbulence model variables in 30 sector for different grids with 46500, 85680, 151200 and 217080 cells, from top to bottom, respectively

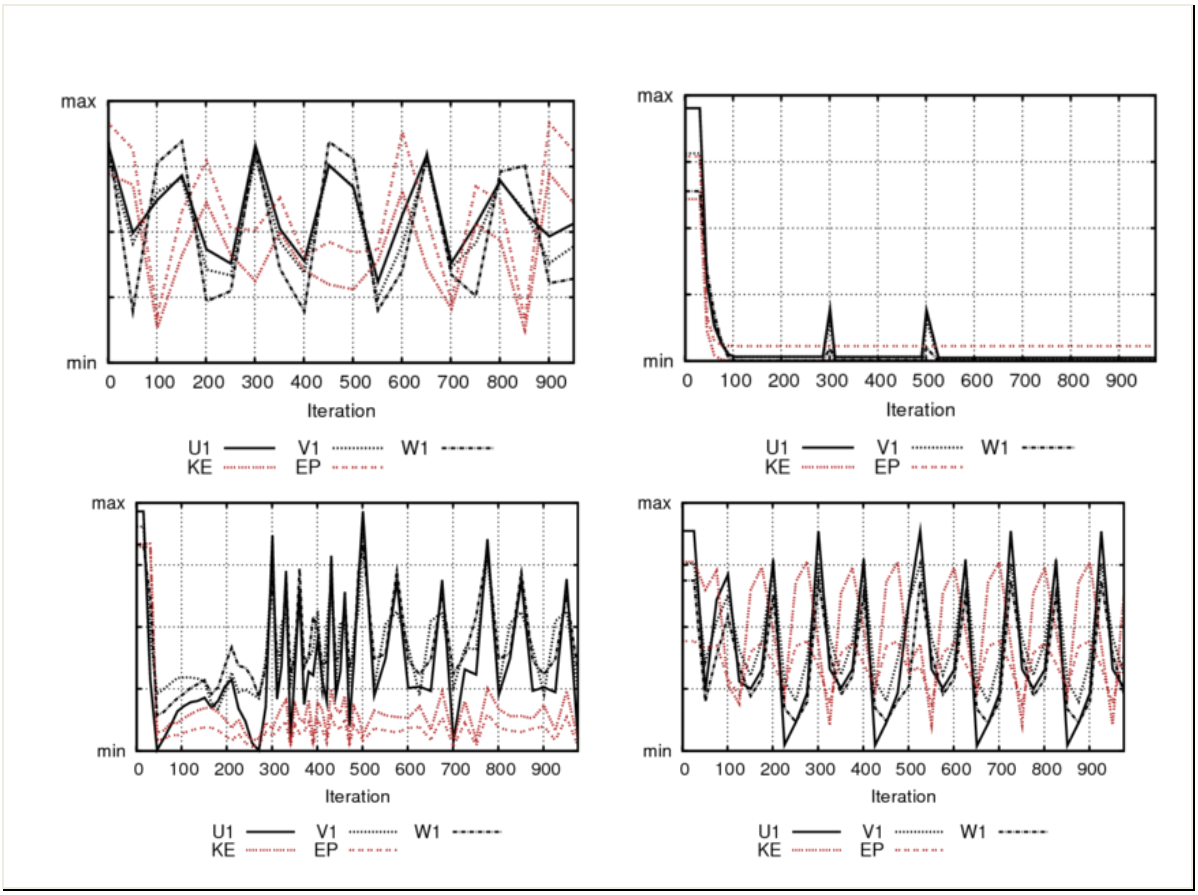

Figure 3-3 Residuals of flow and turbulence model variables in 60 sector for different grids with 46500, 85680, 151200 and 217080 cells, from top to bottom, respectively

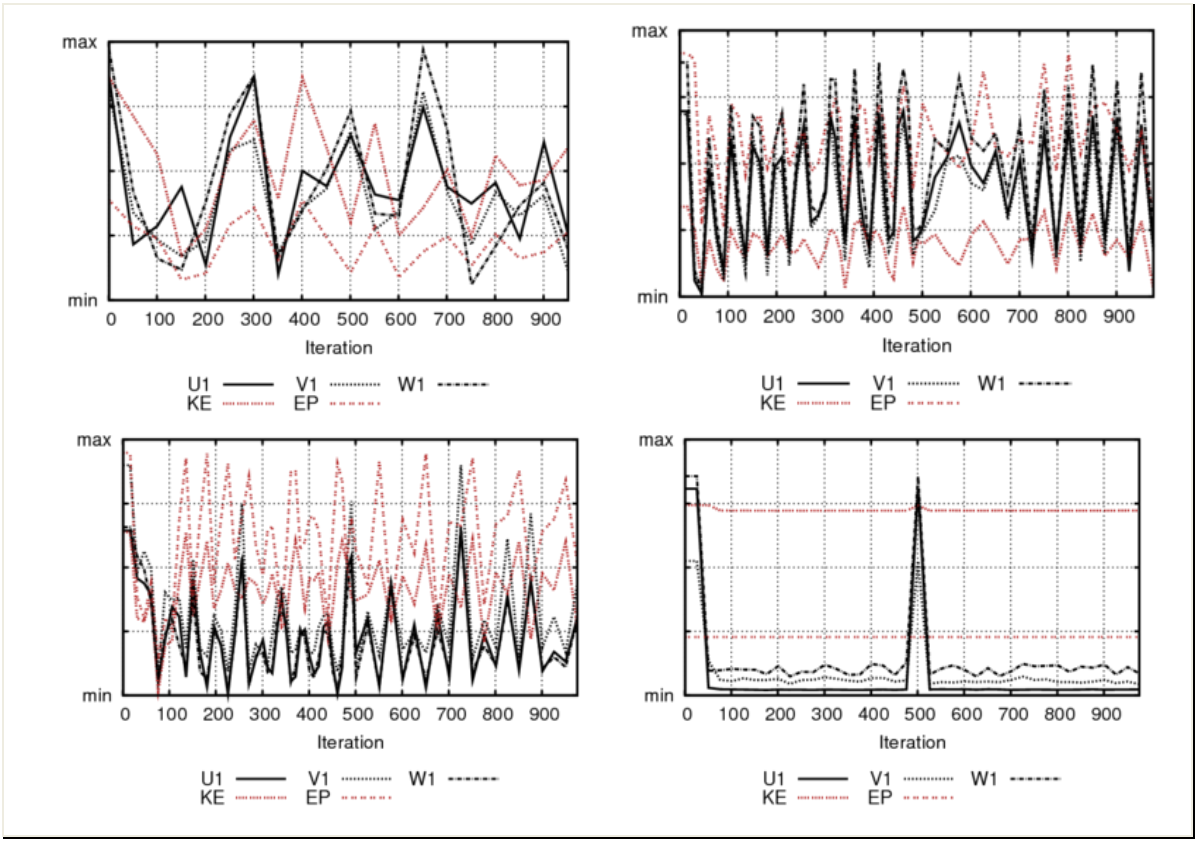

Figure 3-4 Residuals of flow and turbulence model variables in 90 sector for different grids with 46500, 85680, 151200 and 217080 cells, from top to bottom, respectively

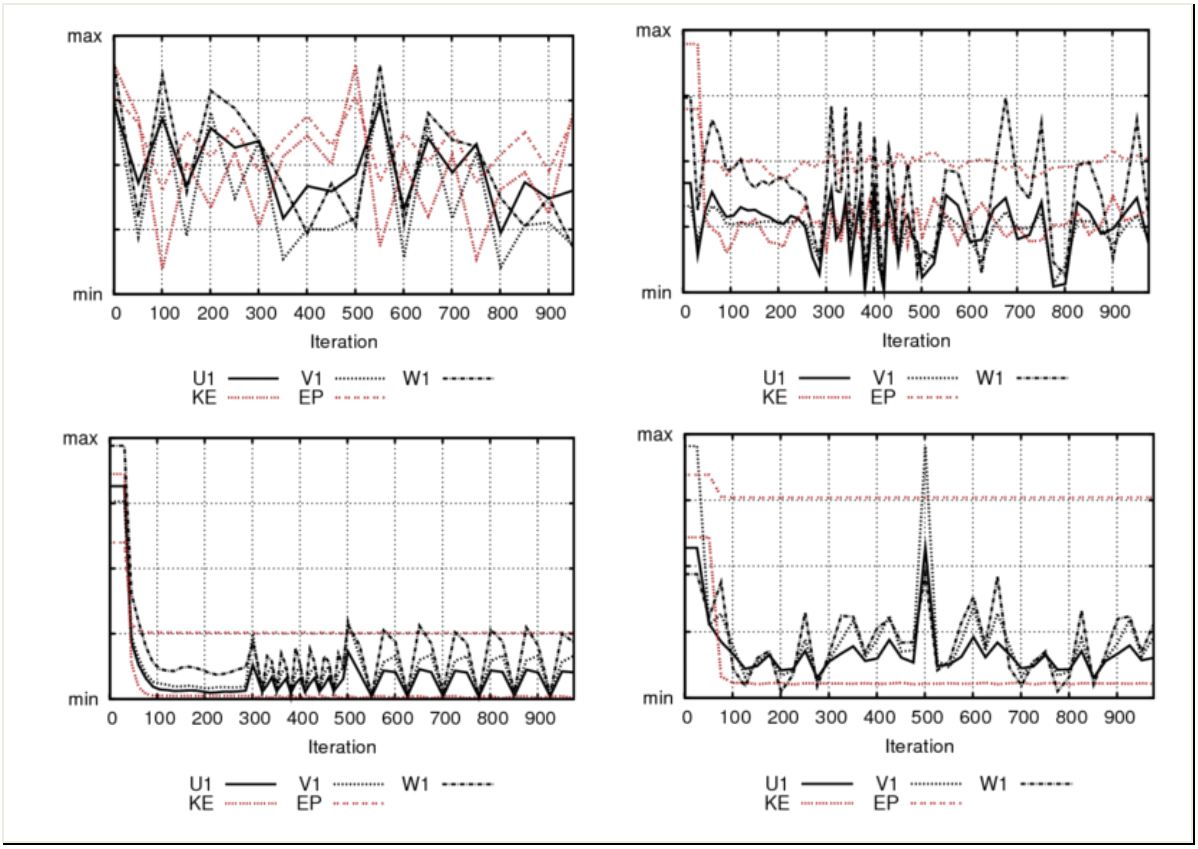

Figure 3-5 Residuals of flow and turbulence model variables in 120 sector for different grids with 46500, 85680, 151200 and 217080 cells, from top to bottom, respectively

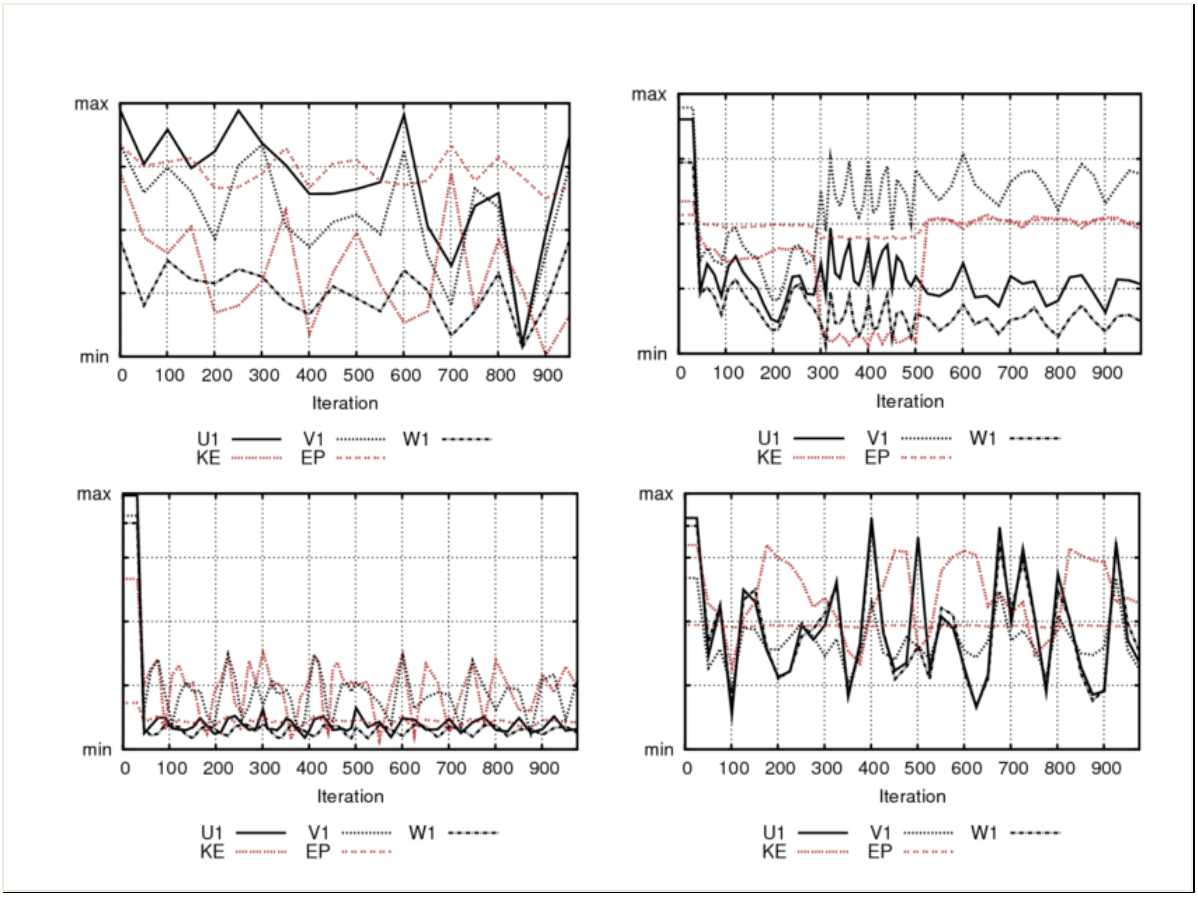

Figure 3-6 Residuals of flow and turbulence model variables in 150 sector for different grids with 46500, 85680, 151200 and 217080 cells, from top to bottom, respectively

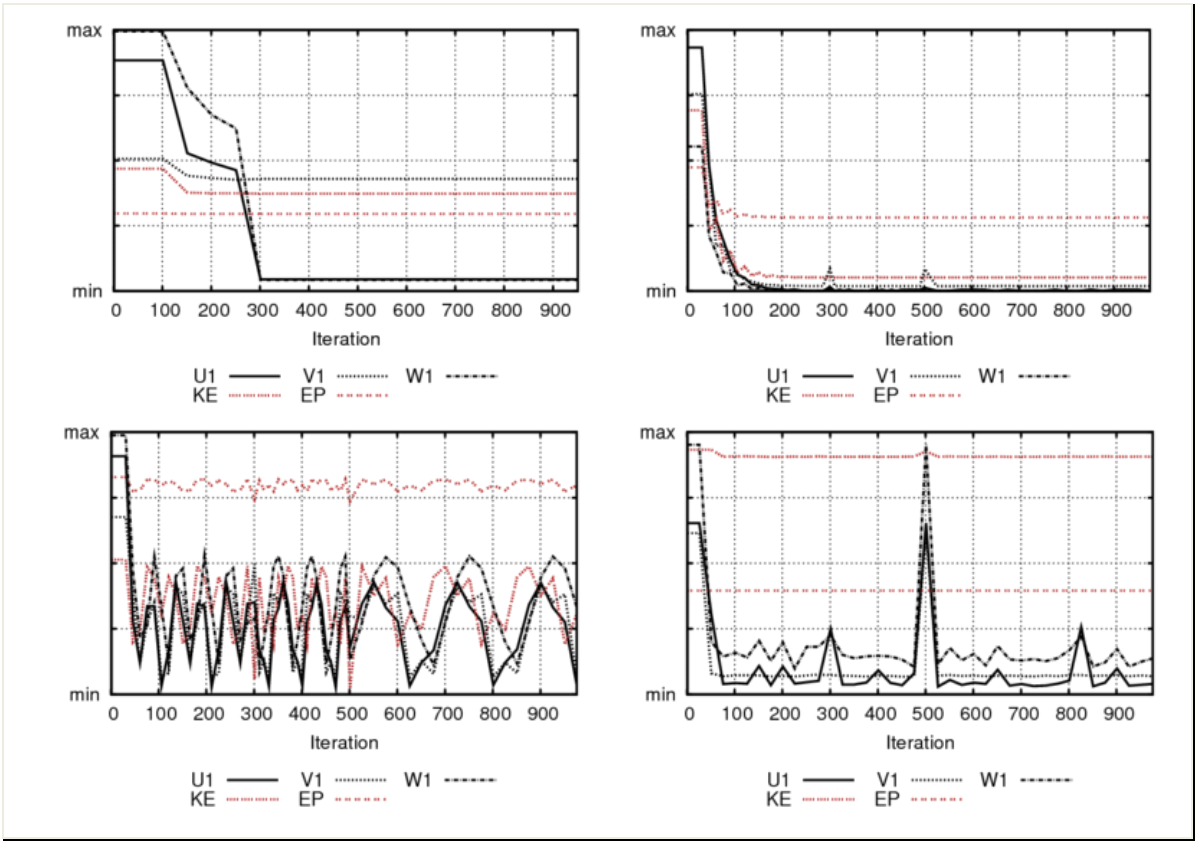

Figure 3-7 Residuals of flow and turbulence model variables in 180 sector for different grids with 46500, 85680, 151200 and 217080 cells, from top to bottom, respectively

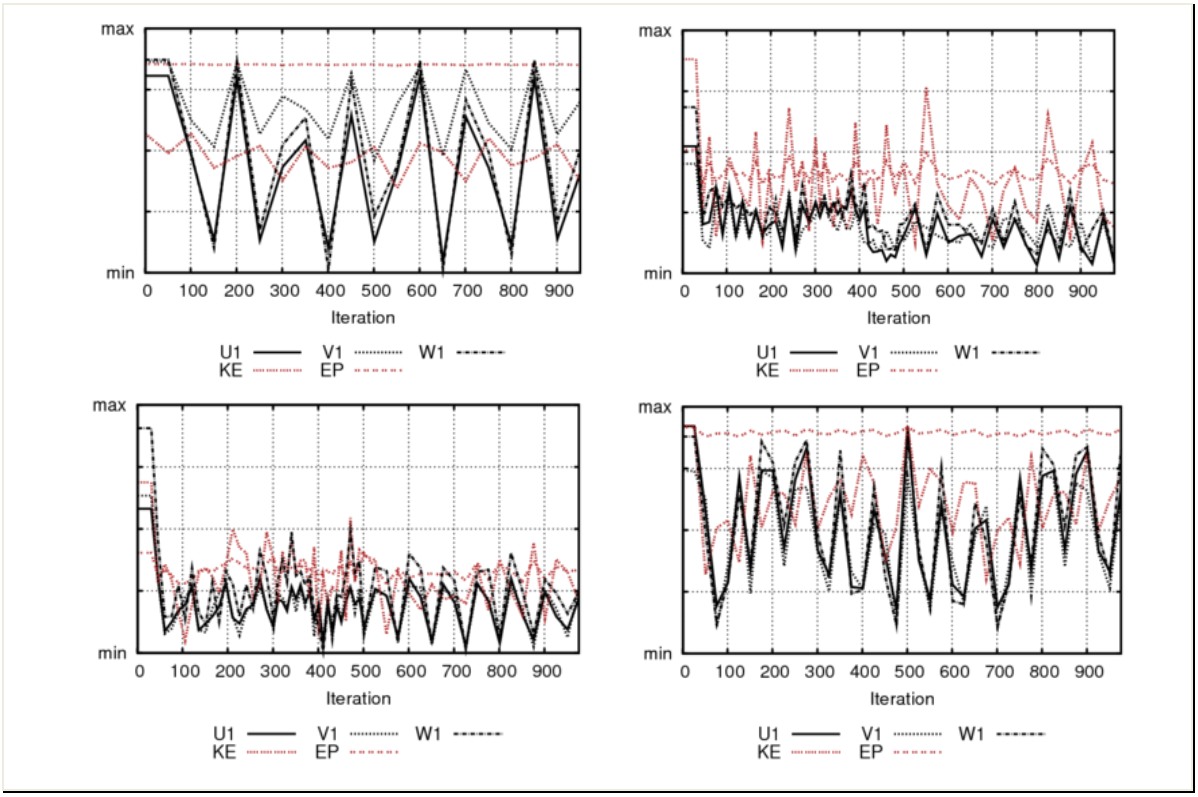

Figure 3-8 Residuals of flow and turbulence model variables in 210 sector for different grids with 46500, 85680, 151200 and 217080 cells, from top to bottom, respectively

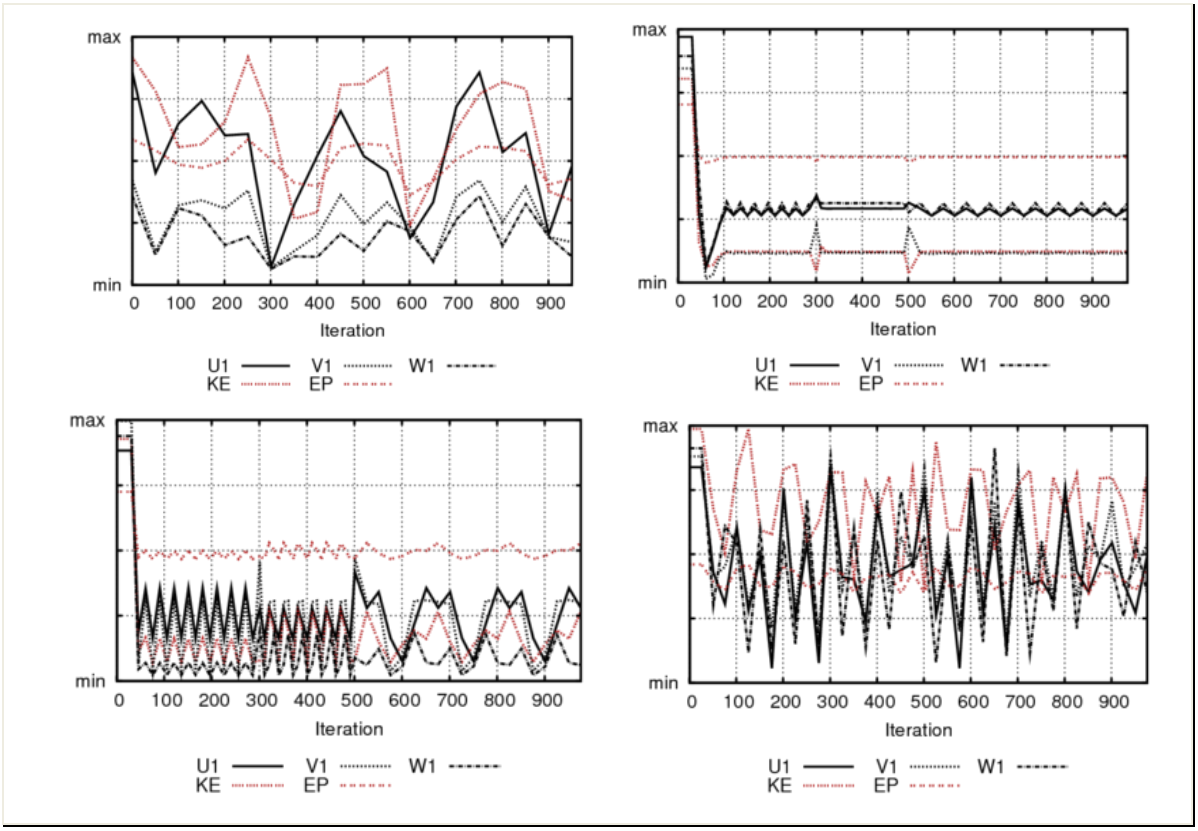

Figure 3-9 Residuals of flow and turbulence model variables in 240 sector for different grids with 46500, 85680, 151200 and 217080 cells, from top to bottom, respectively

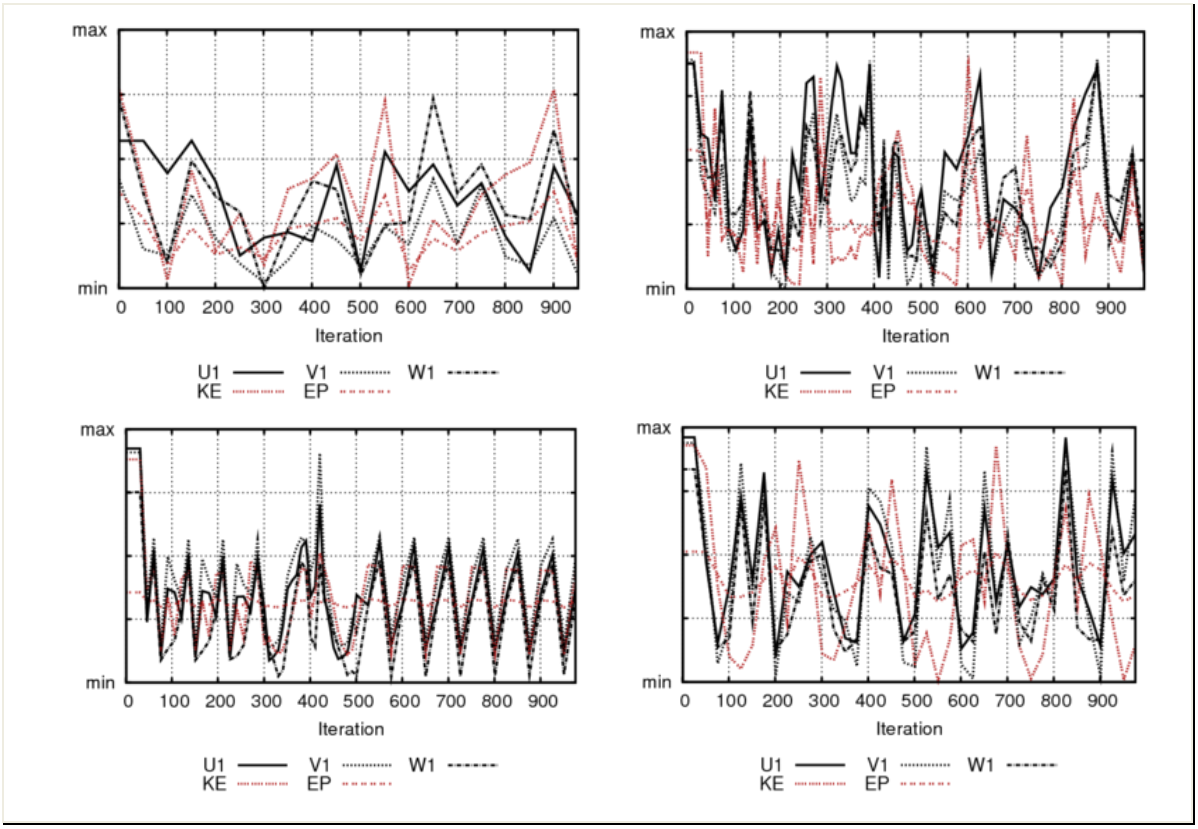

Figure 3-10 Residuals of flow and turbulence model variables in 270 sector for different grids with 46500, 85680, 151200 and 217080 cells, from top to bottom, respectively

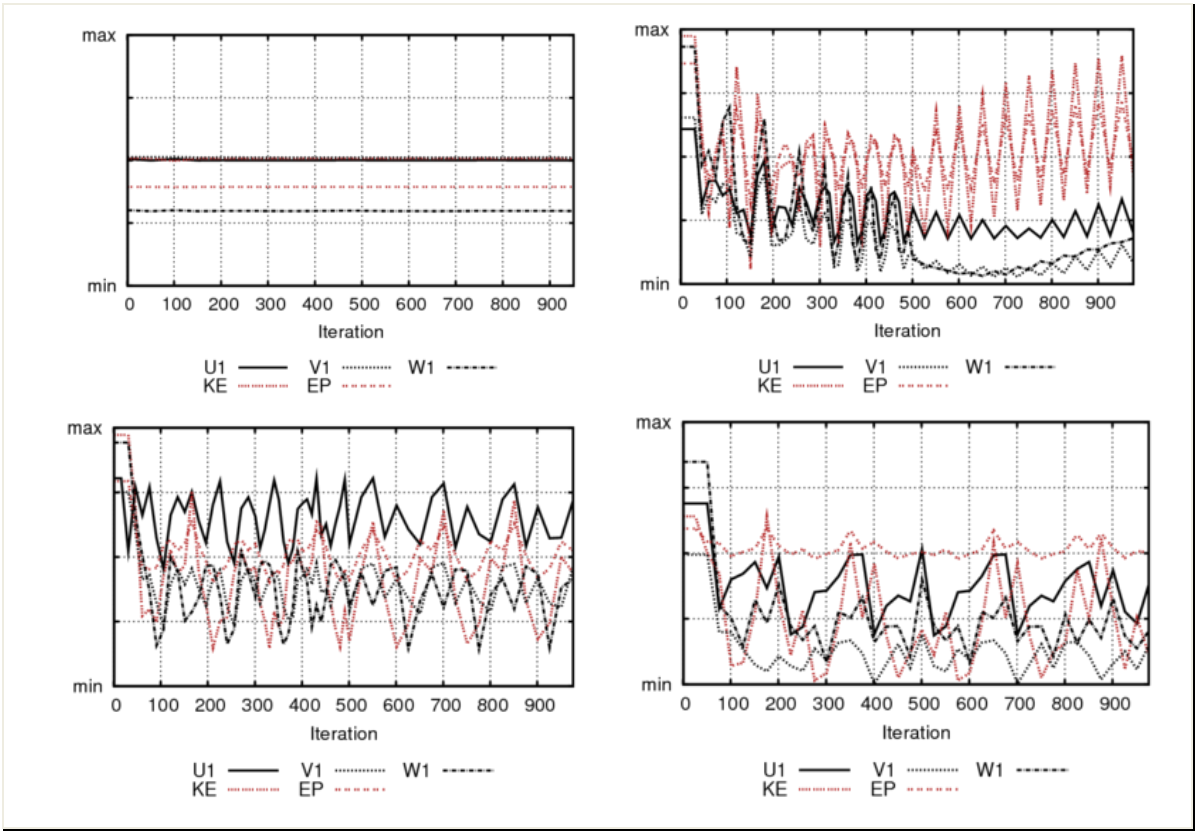

Figure 3-11 Residuals of flow and turbulence model variables in 300 sector for different grids with 46500, 85680, 151200 and 217080 cells, from top to bottom, respectively

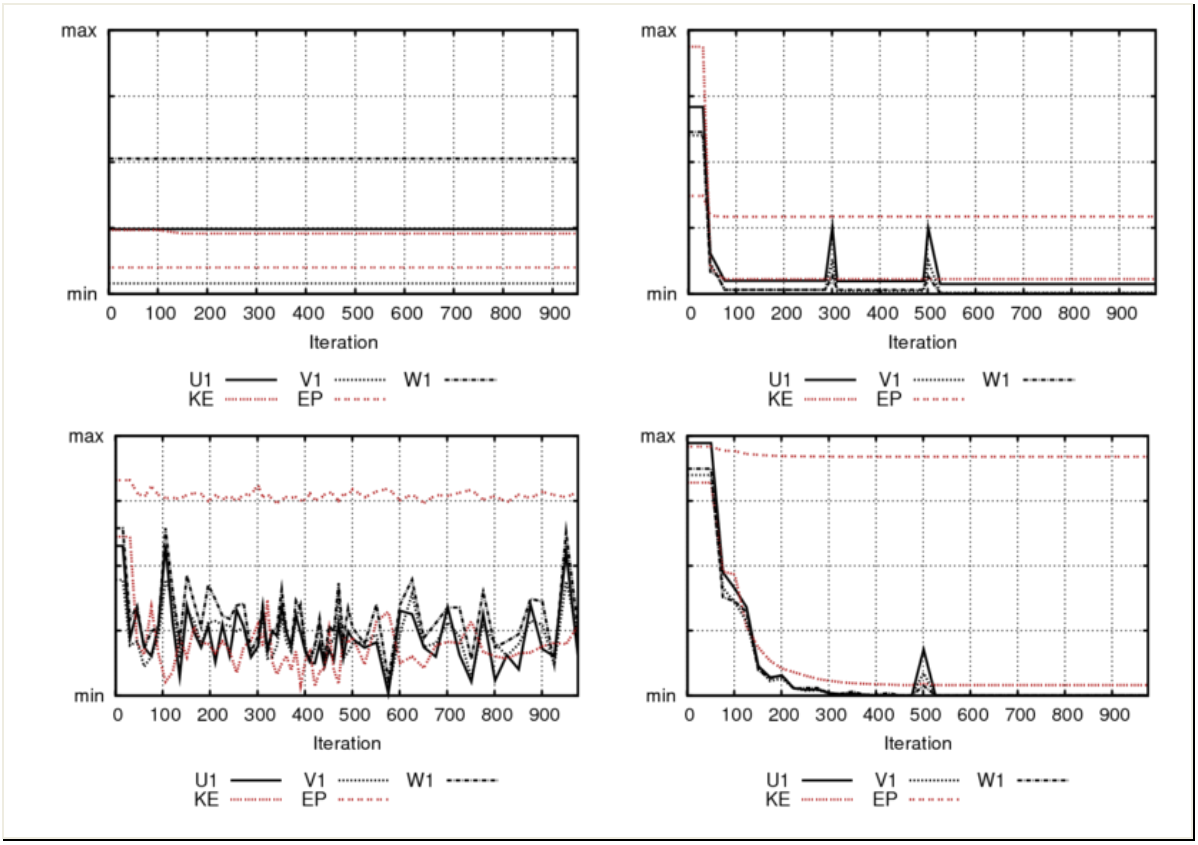

Figure 3-12 Residuals of flow and turbulence model variables in 330 sector for different grids with 46500, 85680, 151200 and 217080 cells, from top to bottom, respectively

According to the results of Figures 3-1 to -3-12 the following observations can be recorded:

- Additional iterations and further refinement are required for achieving improved convergence.
- The grid of 151,200 points exhibits convergence difficulties and in some cases the magnitude of the oscillating properties is comparable and even higher to the finer mesh of 217,800. This could be attributed to the way the grid cells have been distributed in the domain. In such complicated terrains for coarse grid, that are primarily applicable for industrial purposes, even the redistribution of few cells in the domain can affect the behavior of numerical convergence. This kind of numerical sensitivity has been observed by the author in different terrain calculations using WindSim.

- Sufficiently converged data have not been obtained in certain sectors. For example, sectors 60, 210, 240, and 270, exhibit slow convergence and/or fluctuations of the residual values. This effect is more severe on the grid of 151,200 points but also occurs in the case of the 217,080 grid points. These sectors contain either steep or rough areas which effect negatively to the convergence of the solution.
- In the majority of the sectors, the most difficult convergence is exhibited by the turbulent kinetic energy and turbulent dissipation rate. This is due to the aforementioned numerical stiffness encompassed by the turbulence transport equations.
- In some plots distinct peaks of the residual values occur. This is a numerical effect that is common in iterative calculations where the residuals may abruptly change as the flow develops. For example, the capturing of a separation region or a vortex as the iterations evolve can be the reason for a sudden change of the numerical convergence.

Although the numerical convergence results could be considered unsatisfactorily for some sectors, the reported numerical behavior is typical of WindSIM for complex terrains (Graeme Watson, Comparison of wind flow models in complex terrain). One may argue that by refining further the grid, the numerical convergence would be improved in certain sectors. The present results, however, do not show that there is a clear trend for this. For example, although the numerical convergence is improved in some sectors when increasing the grid resolution from 151,200 to 217,080 grid points, the solution still remains non-converged in certain sectors or for some solution variables. In the course of this study, it was also observed that by increasing the number of iterations when the residuals fluctuate, it does not necessarily improve the results or, significantly, affect the annual energy calculations.

Typical calculations times to obtain results range from about 8.24 hrs on the coarsest grid to 25.5 hrs on the finest grid.

3.3 Grid dependence studies

As it was already mentioned at the beginning of the present Chapter, the numerical results are grid dependent. The grid resolutions employed in this study are dictated by the availability of the modest computational resource. Therefore, we do not expect to obtain a well-established grid-independent solution for the flow in question. Nevertheless, it is important to ensure that our results for the annual energy production, the key parameter for the design of a wind farm, are computed within a minimum uncertainty threshold. Otherwise, the wind farm cannot be reliably designed and this may affect the decision of the investor as whether or not the project should go ahead, or the reputation of the engineering firm if the wind farm does not deliver in the end the predicted performance.

A qualitative way to show the effects of the grid on the numerical results is to plot the field values (iso-contours) of key variables such as pressure, wind speed etc In Figs. 3-13 to 3-14 the contour values of velocity have been used to show the variation of the flow field with the grid size. 'The colors in the contour plots represent the range of wind speed scaled between minimum and maximum speeds by a palette with eight different colors starting from white color indicating the lowest wind speed values up to the brown color where the highest values reach. Taking as an example the first field value with total 46500 grid cells presented at Figure 3-13, the wind speed starts from 1.34m/s to 4m/s with the white color and reaches 19.11m/s with the brown color. The plots show that as the grid is refines the flow field starts taking shape with the results on 151,200 cells start approaching the results on 217,080 cells. We should point out that most of the differences are observed in mountain peaks or abrupt slope areas.

The above qualitative assessment by no means implies a grid converged solution with respect to the annual energy production. Therefore, calculation of the energy

production was performed to examine in more details the effects of grid resolution on the results.

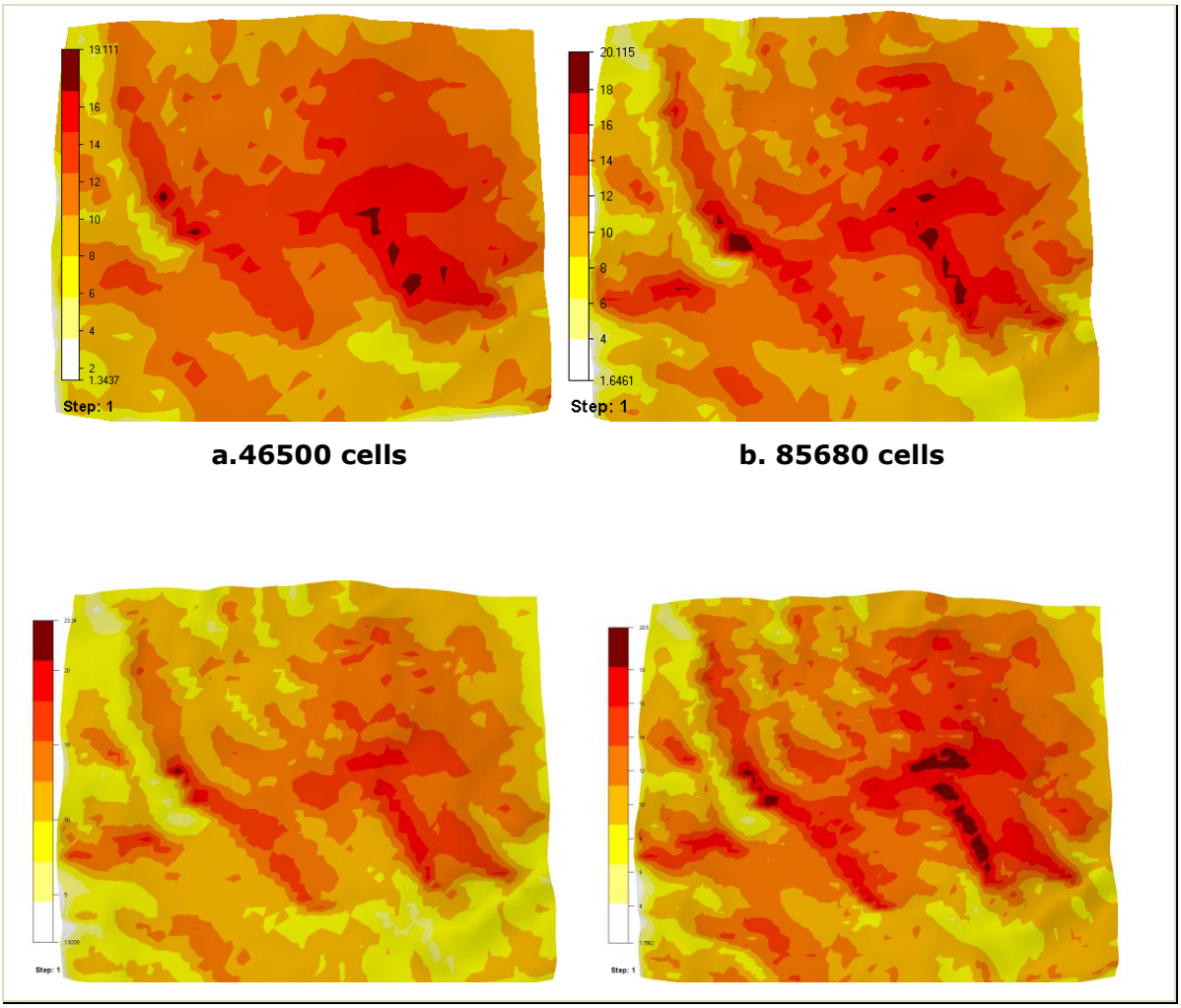

a.46500 cells **b. 85680 cells**

c. 151200 cells **d. 217080 cells**

Figure 3-13 Convergence of file values in 30 sector for grid cells spanning from 46500, 85680, 151200 and 217080

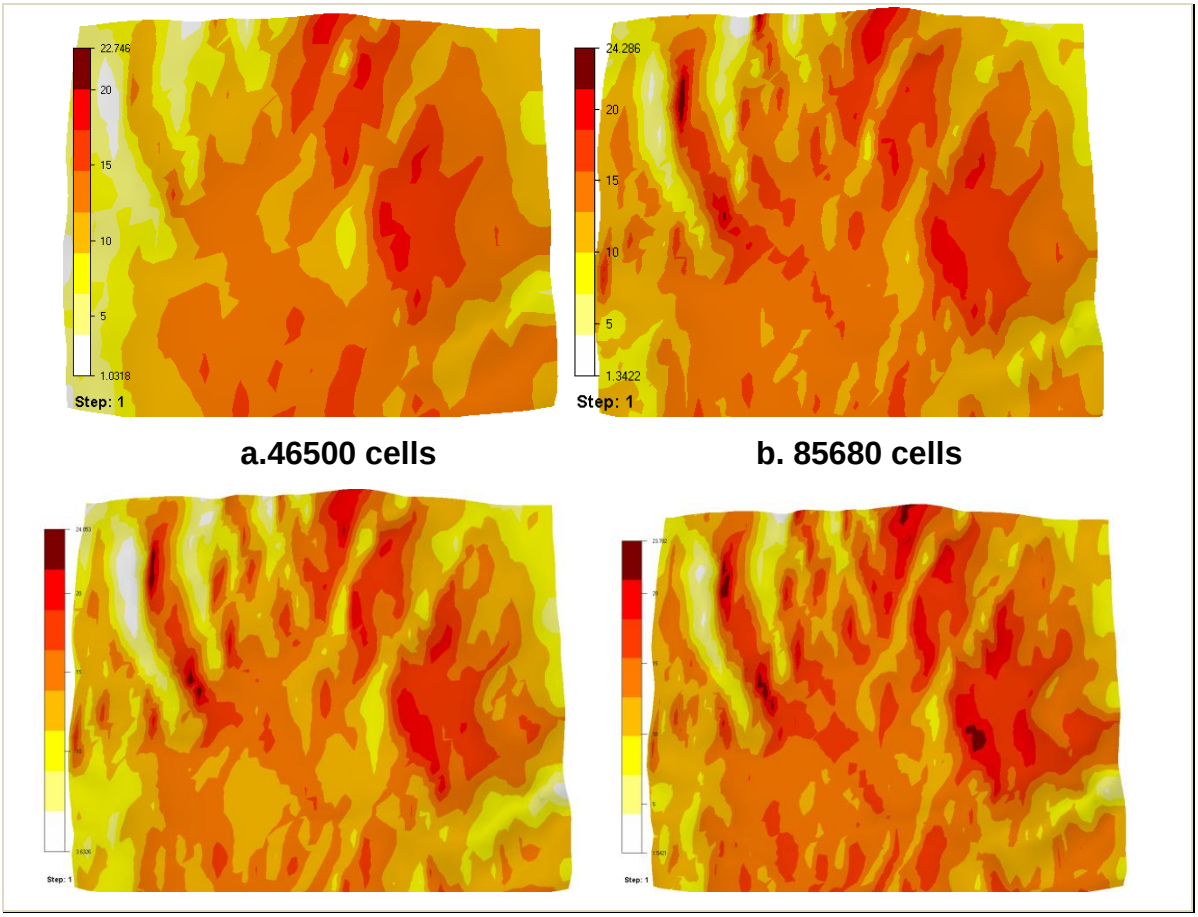

a.46500 cells **b. 85680 cells**

c.151200 cells **d. 217080 cells**

Figure 3-14 Convergence of file values in 90-120 sector for grid cells spanning from 46500, 85680, 151200 and 217080

The wind speed values have been calculated on different grid resolutions and are shown in Figure 3-15. The results on different grids show very good agreement. Specifically, the maximum difference of the results between the results on 200,000 and 300,000 grids is 2.13%.

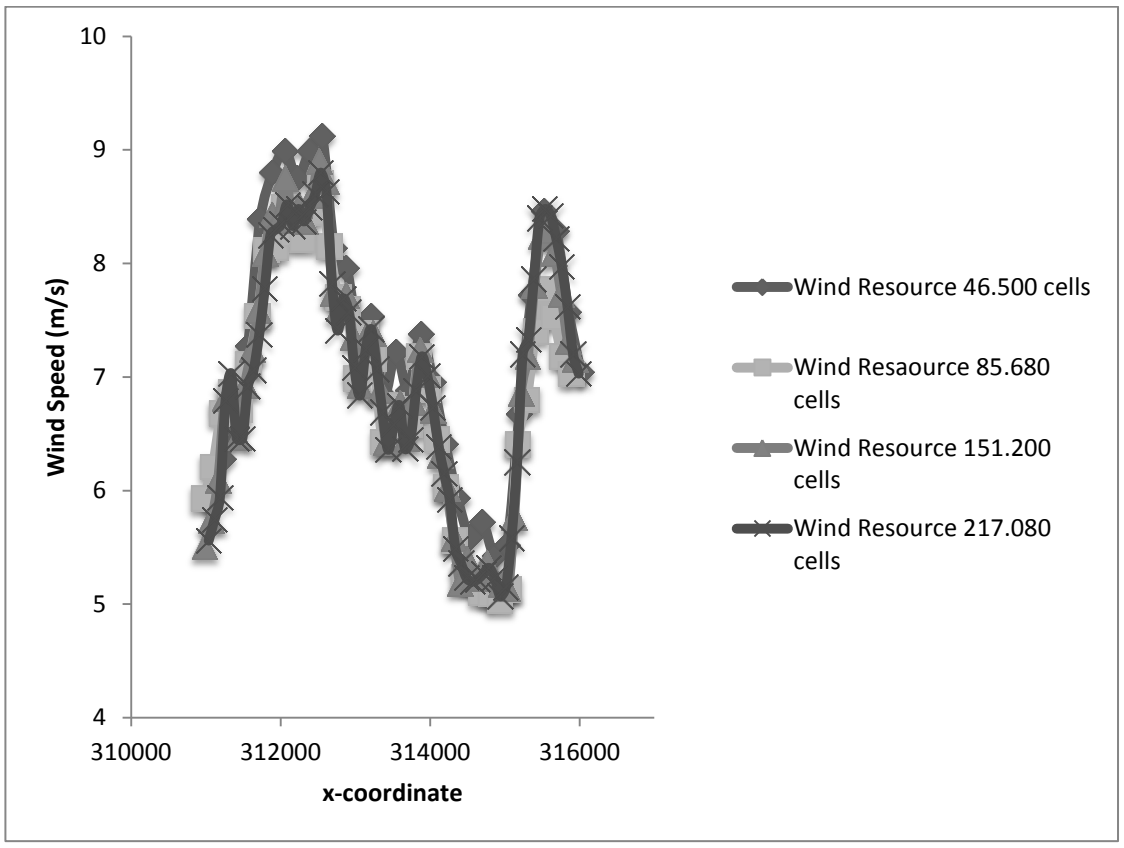

Figure 3-15 Wind resource for grid cells spanning from 46500, 85680, 151200 and 217080

These results have been obtained using Gamesa G52 wind turbine, which has a 65m hub height and a 52m rotor diameter, having the same technical characteristics as Acciona Enegia. The power curve of G52 is presented in Figure 3-16

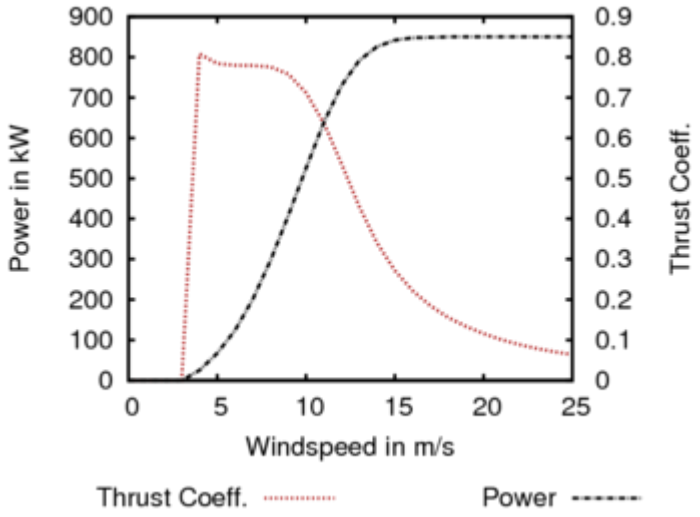

Figure 3-16 Gamesa G52 power curve

Source: Gamesa technical description

The calculation of Annual Energy Production (AEP) performed using the available data of the meteorological masts M1, PAN3, PAN4, PAN5 and is displayed in Tables 3-2 until 3-5. AEP has been calculated twice, one for frequency distribution and one for Weibull distribution.

Mast	Distribution	Energy
M1	Frequency table	140.6983
M1	Weibull distribution	140.4650
PAN3	Frequency table	121.5389
PAN3	Weibull distribution	122.8616
PAN4	Frequency table	125.1780
PAN4	Weibull distribution	128.2221
PAN5	Frequency table	107.2843
PAN5	Weibull distribution	109.2749
All	Frequency table	122.8343
All	Weibull distribution	124.4808

Table 3-2 Energy production in GWh/y based on mast represented by frequency table and Weibull distribution for 46500 cells

Masts	Distribution	Energy
M1	Frequency table	140.1850
M1	Weibull distribution	140.1263
PAN3	Frequency table	121.3509
PAN3	Weibull distribution	122.6029
PAN4	Frequency table	123.0961
PAN4	Weibull distribution	126.3379
PAN5	Frequency table	105.7042
PAN5	Weibull distribution	107.4816
All	Frequency table	121.5699
All	Weibull distribution	123.2252

Table 3-3 Energy production in GWh/y based on mast represented by frequency table and Weibull distribution for 85680 cells

Masts	Distribution	Energy
M1	Frequency table	141.8981
M1	Weibull distribution	141.9644
PAN3	Frequency table	123.4842
PAN3	Weibull distribution	124.7959
PAN4	Frequency table	124.0644
PAN4	Weibull distribution	127.4047
PAN5	Frequency table	104.1284
PAN5	Weibull distribution	105.8743
All	Frequency table	122.1303
All	Weibull distribution	123.8469

Table 3-4 Energy production in GWh/y based on mast represented by frequency table and Weibull distribution for 151200 cells

Masts	Distribution	Energy
M1	Frequency table	141.7503
M1	Weibull distribution	141.8722
PAN3	Frequency table	124.7652
PAN3	Weibull distribution	126.1155
PAN4	Frequency table	122.2202
PAN4	Weibull distribution	125.4251
PAN5	Frequency table	103.4726
PAN5	Weibull distribution	105.2202
All	Frequency table	121.6475
All	Weibull distribution	123.3274

Table 3-5 Energy production in GWh/y based on mast represented by frequency table and Weibull distribution for 217080 cells

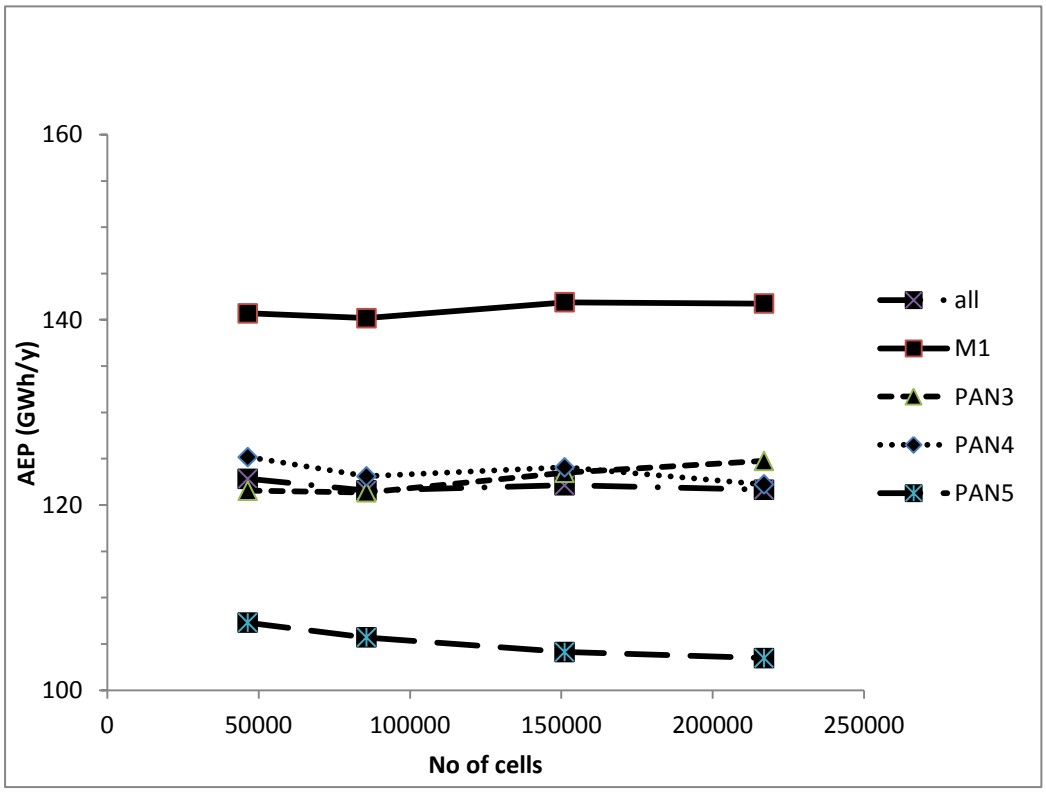

Figure 3-17 AEP for four measurement masts against grid resolution

The results of the annual energy production presented in the tables above as well as in Figure 3-17, show a fairly good convergence of the results, in terms of AEP,

with the grid size. The maximum difference of the predicted AEP between resolutions of 151,200 and 217,080 grid cells between the four measuring masts and M1 mast is 0,99 This difference is within the acceptable error of wind farm engineering calculations.

4 PARAMETRIC STUDEIS

4.1 Statistical Analysis of wind results obtained from WindPro & WindSim

The measuring campaign has been implemented through four (4) on-site installed, fully equipped, certified wind masts. Prior to the statistical analysis of the results, the quality of the obtained time series was examined in order to clean the data from various types of errors, e.g. reading errors etc. After the data cleaning the availability of the time series was found 88%, 95%, 85%, and 92% for each one of the wind masts, which is considered as high. In the following Figures 4-1 to 4-3 the results of the statistical elaboration are given.

Since the four wind masts are located at neighbor spots on the same hilly plateau, the statistical results show not only the same trends but in some cases identical behavior as well.

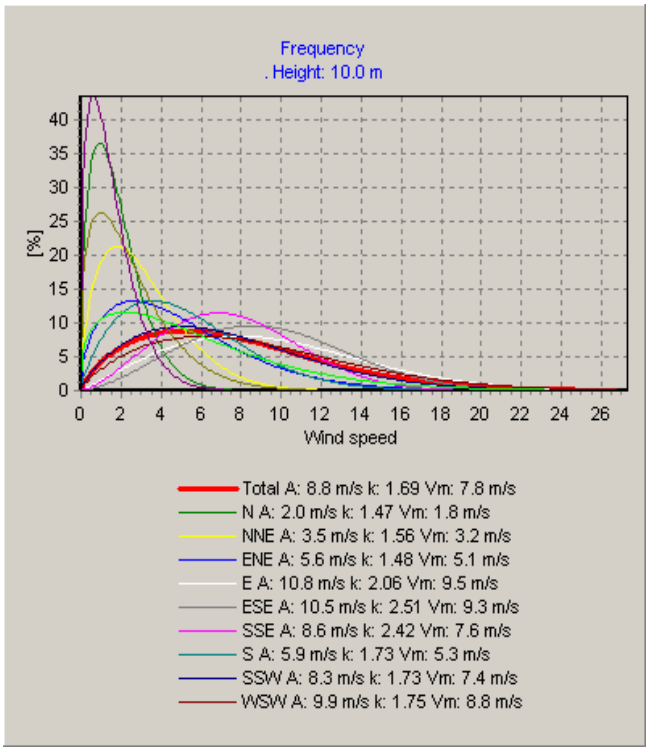

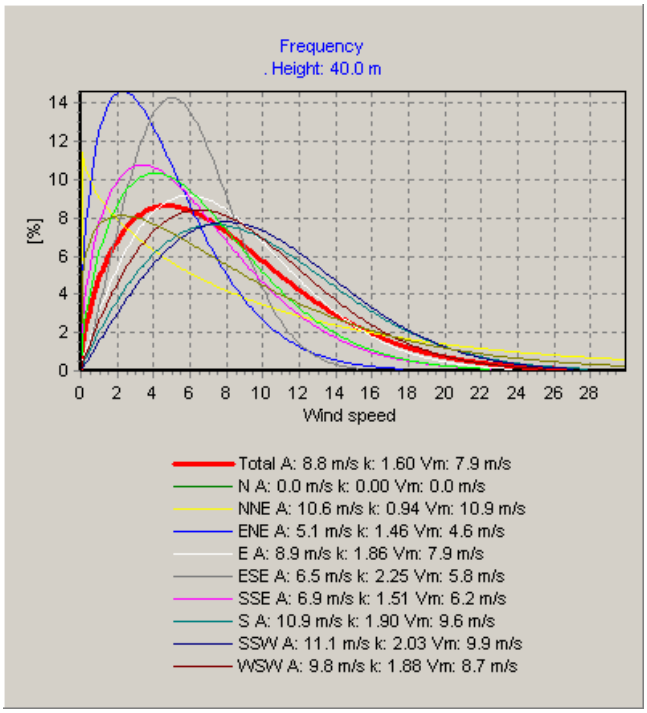
Frequency
. Height: 40.0 m
[%]
Wind speed
Total A: 8.8 m/s k: 1.60 Vm: 7.9 m/s
N A: 0.0 m/s k: 0.00 Vm: 0.0 m/s
NNE A: 10.6 m/s k: 0.94 Vm: 10.9 m/s
ENE A: 5.1 m/s k: 1.46 Vm: 4.6 m/s
E A: 8.9 m/s k: 1.86 Vm: 7.9 m/s
ESE A: 6.5 m/s k: 2.25 Vm: 5.8 m/s
SSE A: 6.9 m/s k: 1.51 Vm: 6.2 m/s
S A: 10.9 m/s k: 1.90 Vm: 9.6 m/s
SSW A: 11.1 m/s k: 2.03 Vm: 9.9 m/s
WSW A: 9.8 m/s k: 1.88 Vm: 8.7 m/s

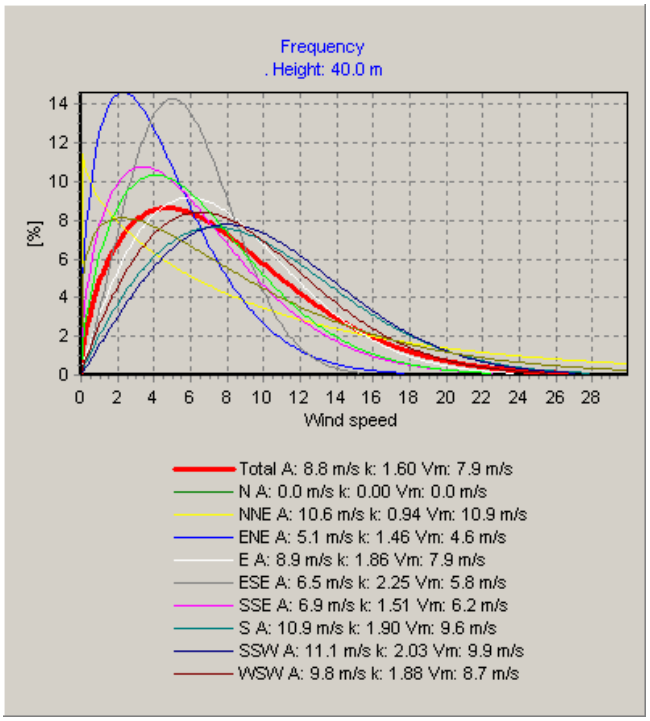

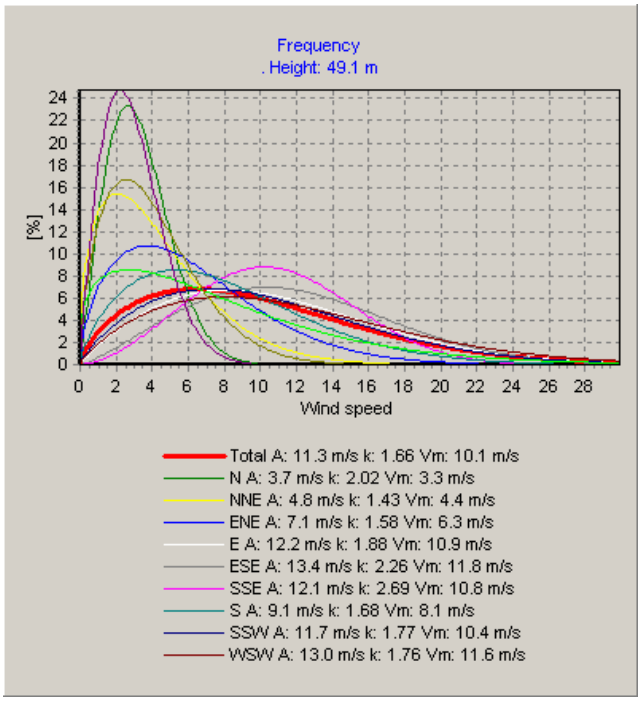

Figure 4-1 Weibull Distribution adjusted on 12 months of measured data for PAN3, PAN5, PAN4 & M1 masts respectively

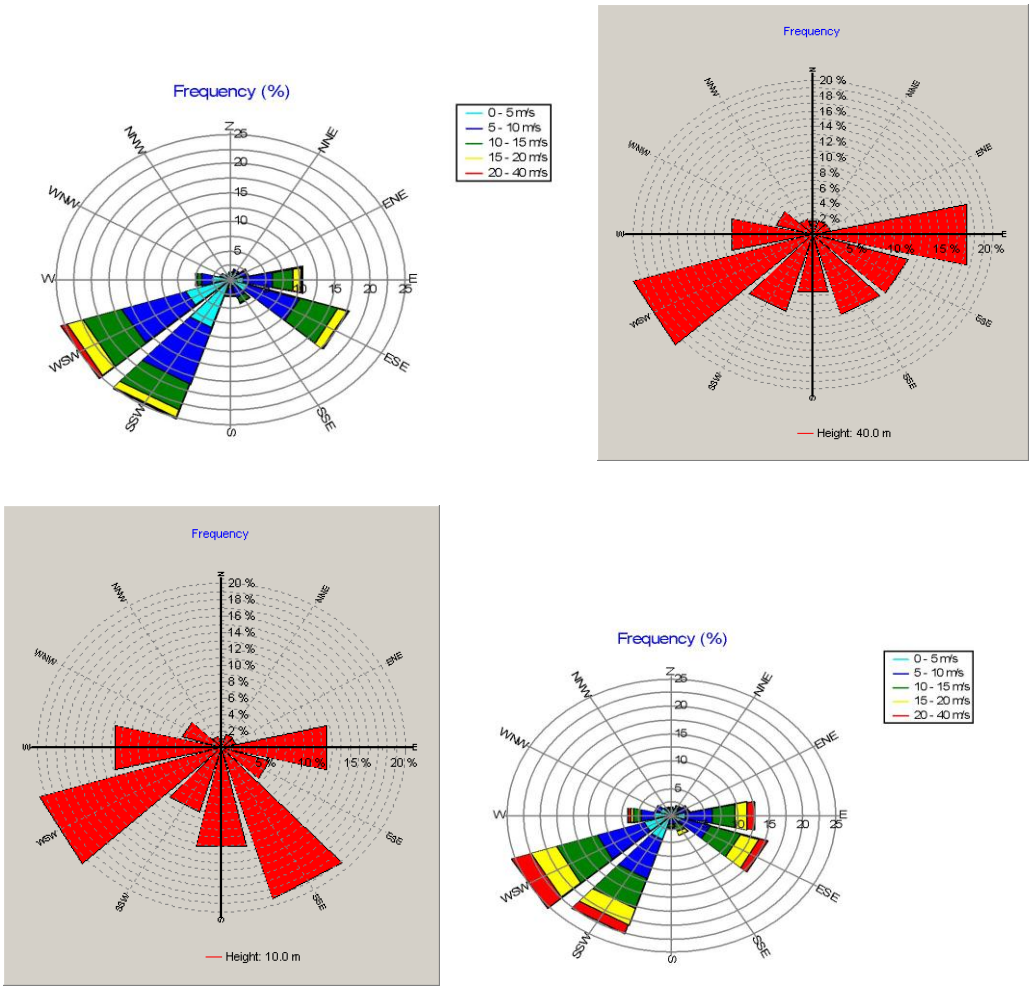

Figure 4-2 Frequency Rose from measurements from PAN3, PAN5, PAN4 & M1 masts respectively

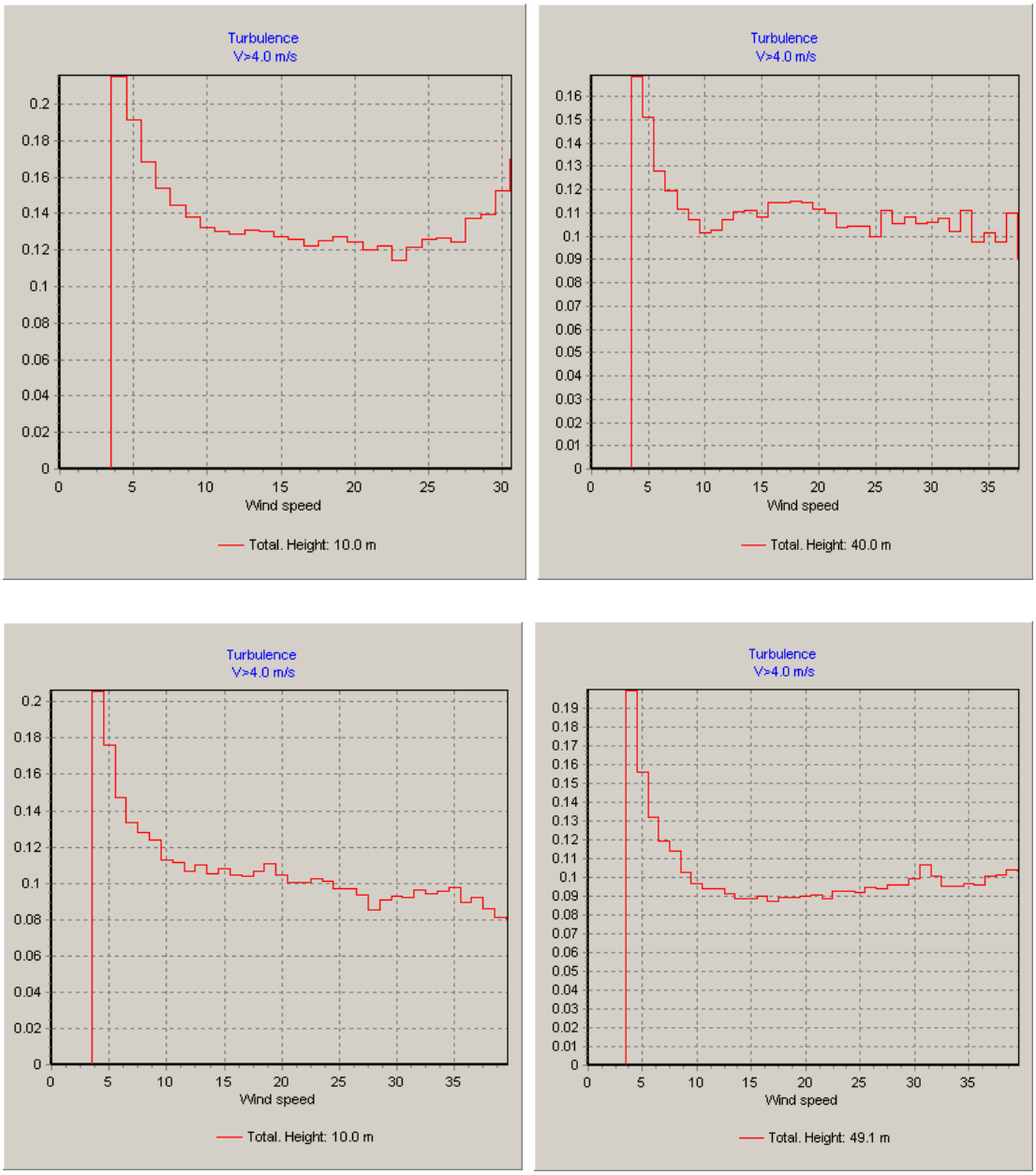

Figure 4-3 Turbulence intensity measured for PAN3, PAN5, PAN4 & M1 masts respectively

In the following Table 4-1 various integrated results are given for for each one of the time series:

MAST NAME	A-parameter [m/s]	Wind Speed [m/s]	k-parameter
PAN3	8.8	7.8	1.69
PAN5	8.8	7.9	1.6
PAN4	11.1	10.0	1.51
M1	11.3	10.1	1.66

Table 4-1 Parameters of Weibull fitted distribution and frequency of mean wind speed for 12 months measurements where gathered

4.2 Comparison of turbulence models, including energy analysis

The wind turbulence induces major effects on the wind farm's operation and the annual energy production. In typical wind farm calculations, the turbulence intensity (TI) is a key parameter characterizing wind turbulence. TI is defined by the turbulent kinetic energy (KE) and the wind speeds UCRT and VCRT in East-West North-South directions, respectively in Equation 4-1

$$\mathrm{TI} = \frac{\sqrt{\frac{2}{3}\mathrm{KE}}}{\sqrt{\mathrm{UCRT}^2 + \mathrm{VCRT}^2 \text{ x } 100}} \qquad \textbf{(4-1)}$$

Simulations over a complex terrain have been performed with three turbulence models to obtain results for the wind speed, shear and turbulence with height. Although there are no field measurements available for comparing the simulation results, our aim is to assess the uncertainty in the numerical predictions arising from using different turbulence models (VanLuvanee et al, 2009).

The models used in the present simulations are: the k-ε (Equation 4-2), (see also Sec. *2.1.4*), the k-epsilon with YAP correction (henceforth labeled as YAP), and the RNG k-epsilon (henceforth labeled as RNG). The YAP correction takes into account the variations of the turbulence length scale from its local equilibrium level and then the correction is added in the form of a source term below to the right hand side of Equation 2-15

$$\mathcal{V}_t = C_\mu \frac{k^2}{\varepsilon} \left(\frac{\mathrm{k}^{1.5}}{\varepsilon \mathrm{l_e}} - 1\right)\left(\frac{\mathrm{k}^{1.5}}{\in \mathrm{l_e}}\right)^2 \qquad \textbf{(4-2)}$$

The effects of the correction are expected in non-equilibrium flows as well as in flows featuring separation.

The RNG version of the k-ε model is obtained by applying the Renormalized Group Theory (RNG) to obtain the coefficients of the model (Pironneau et al, 1994). RNG is a mathematical technique that is used to overcome deficiencies of the k-ε model by providing a sound mathematical and physical derivation of the k-ε model, including mathematically derived constant coefficients to replace empirical ones. The most important refinements are presented further down:

- The RNG model has an additional term in its **ε** equation that improves the accuracy for rapidly strained flows.
- The effect of swirl on turbulence is included in the RNG model, enhancing accuracy for swirling flows.
- While the standard **k-ε** model is a high-Reynolds-number model, the RNG theory provides an analytically-derived differential formula for effective viscosity that accounts for low-Reynolds-number effects. Effective use of this feature does, however, depend on an appropriate treatment of the near-wall region.

The coefficients of the k-ε with the Yap correction are the same as the coefficients of the original k-ε model. The coefficients of the original k-ε and RNG k-ε are described as following:

k-ε constants:

Cμ=0.09, σk=1.0, σε=1.3, C1ε=1.44 and C2ε=1.92

RNG constants:

Cμ=0.0845, σk=0.7194, σε=0.7194, C1ε=1.4 , C2ε=1.68, ηo=4.38 and β=0.012

All the models have been initialized with a log profile from the ground up to 500m height and speed of 10 m/s on the edge and above the boundary layer. In addition, the surface roughness is assumed to be 0.1m comparing the results obtained from both software (WindPro & WindSim) with the experimental. The comparison of turbulence models was performed in the framework of WindSim.

The comparison of the results using the three different turbulence models has been carried out for three wind turbines (WTG) **No16** , **No 17** and **No 19** in sector 30. The WTGs chosen are indicative of a wind farm layout where multiple wakes are experienced. The terrain where WTG No 17 is located drops away steeply, therefore, we expect the turbulence intensity to be significant. WTGs No 16 and No 19 are located 145m and 645m downstream of No 17, respectively.

Turbulence Intensity

The results for the turbulence intensity are presented for WTGs **No16** to **No 19** in Figures 4-4 to 4-6, respectively. The main outcomes arising from the simulations are summarized below:

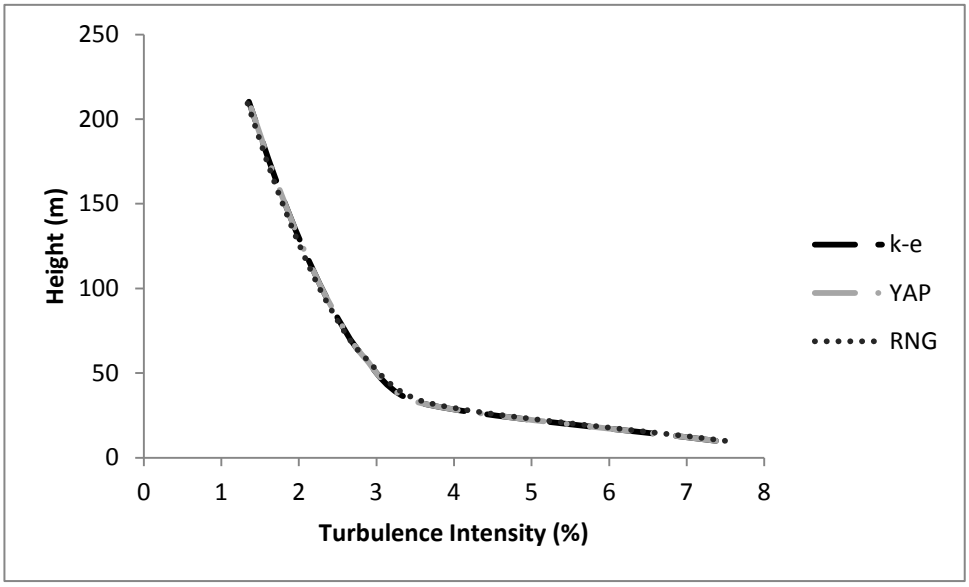

Figure 4-4 Turbulence intensity predictions against height for WTG No16 using three k-ε variants

- The calculations show that there are small differences between the results obtained from different turbulence models. We note the following:

  (i) the turbulence models used here are not significantly different in

terms of the governing equations and modelling principles regarding the source terms.

- (ii) Low Reynolds number effects are not expected to be captured due to the coarseness of the grid in the near ground region. Thus, the Yap correction does not result in any (significant) changes in the results.
- (iii)The RNG model is expected to be more responsive to streamline curvature and higher strain rates than the standard model but for the present terrain both parameters do not take such large values, which will result in the RNG model giving significantly different results compared to the k-epsilon. The turbulence intensity increases as the height decreases for the all turbulence models.

The turbulence intensity at lower height is slightly higher for WTG No17 compared to WTGs 16 and 19 WTG. This is probably due to the position of No 17, but in any case the differences with respect to the TI are small. The RNG predictions for WTG No 19 show slightly lower turbulence intensity towards the far field compared to the Yap and k-ε results. This effect can be possibly attributed to the RNG's properties, particularly in relation to more consistent mathematically derived constants. This effect can be possibly attributed to the RNG properties, particularly in relation to more consistent mathematically derived constants and the model's response to streamline curvature.

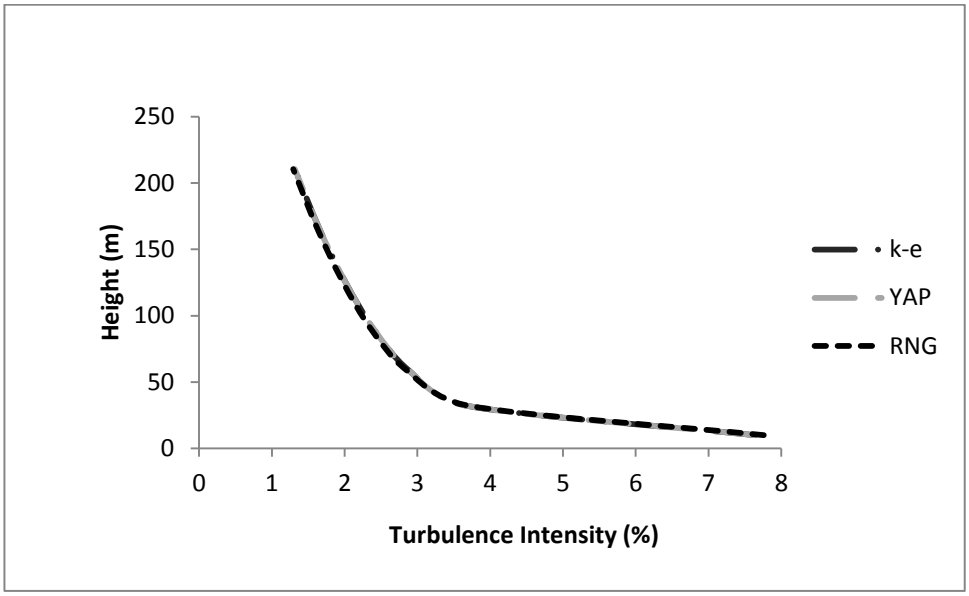

Figure 4-5 Turbulence intensity predictions against height for WTG No 17 using three k-ε variants

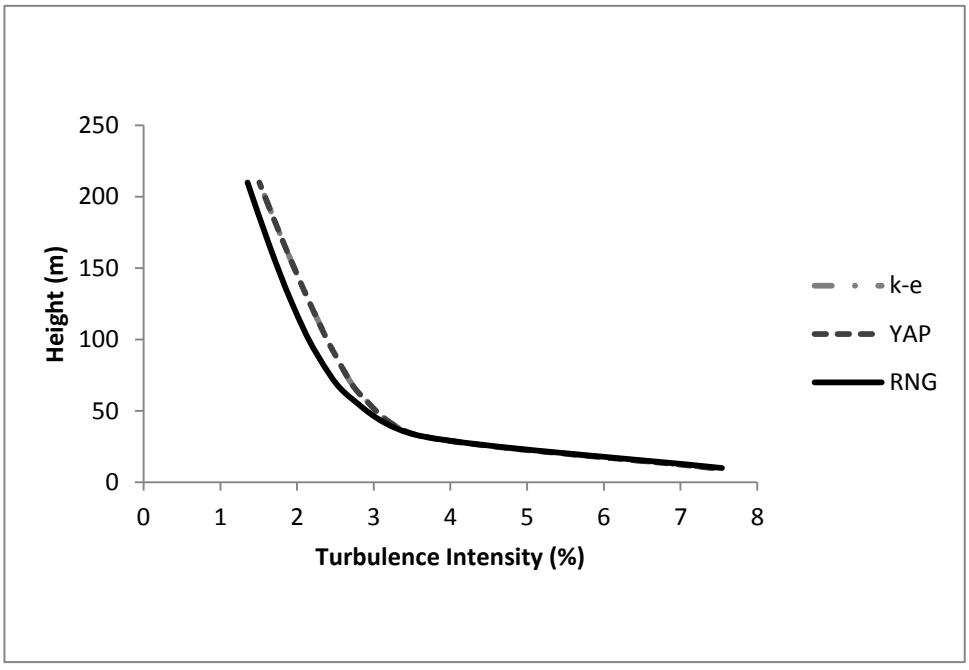

Figure 4-6 Turbulence intensity predictions against height for WTG No 19 using three k-ε variants

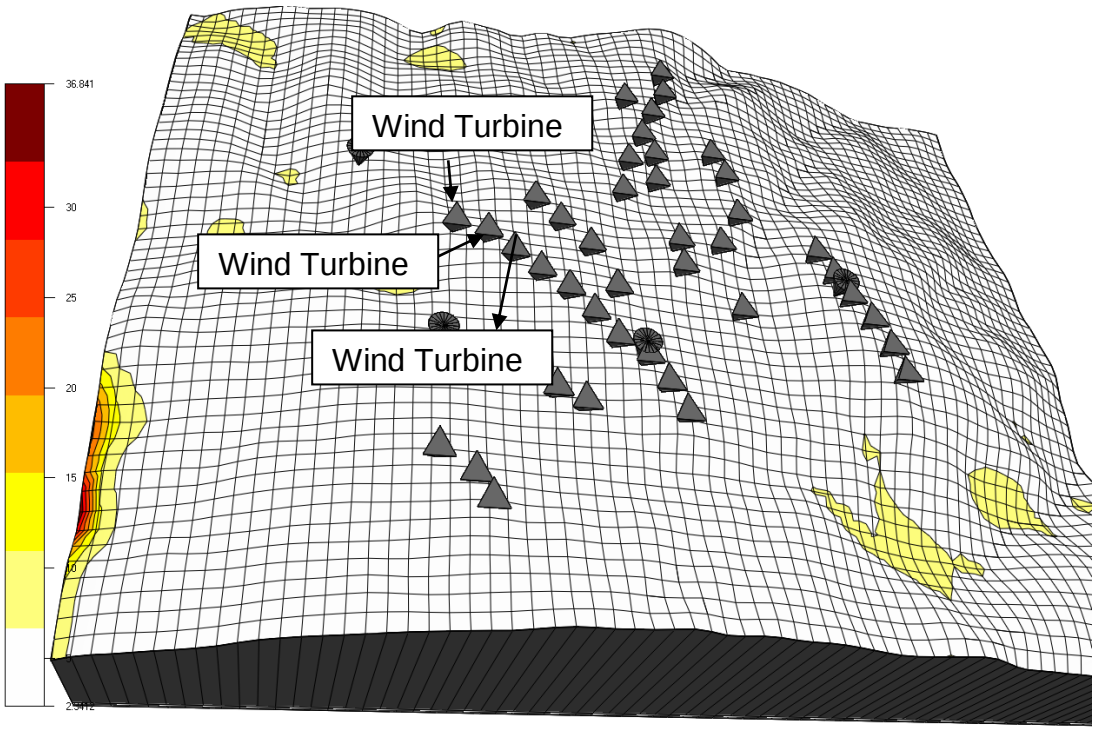

Figure 4-7 Turbulence Intensity (TI) from NNW at 65m height, the figure's legend shows TI's percentage

Wind speed variation

The results for the wind speed variation are presented for WTGs **No16** to **No 19** in Figures 4-8 to 4-10, respectively. The results show that all models predict similar flow patterns and wind speeds. Note that the results have been plotted starting from the first grid node above the ground. Due to the coarseness of the grid near the ground, the near-wall turbulence effects cannot be captured. This is not unusual in environmental applications where we have to deal with large domains. Moreover, the results very close to the ground are of less interest compared to the mid height results that have an effect on the wind turbines performance.

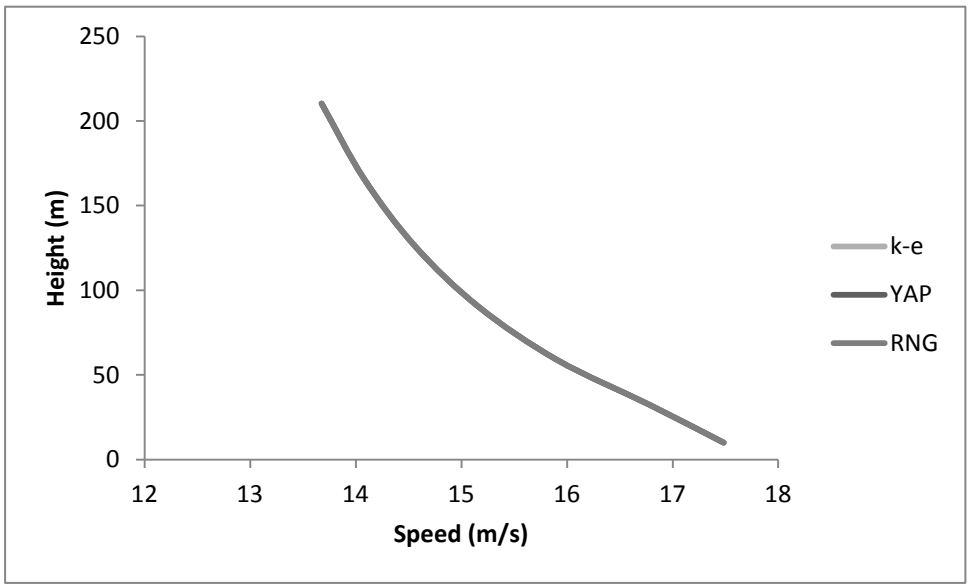

Figure 4-8 Wind speed predictions against height for WTG No16 using three k-ε variants

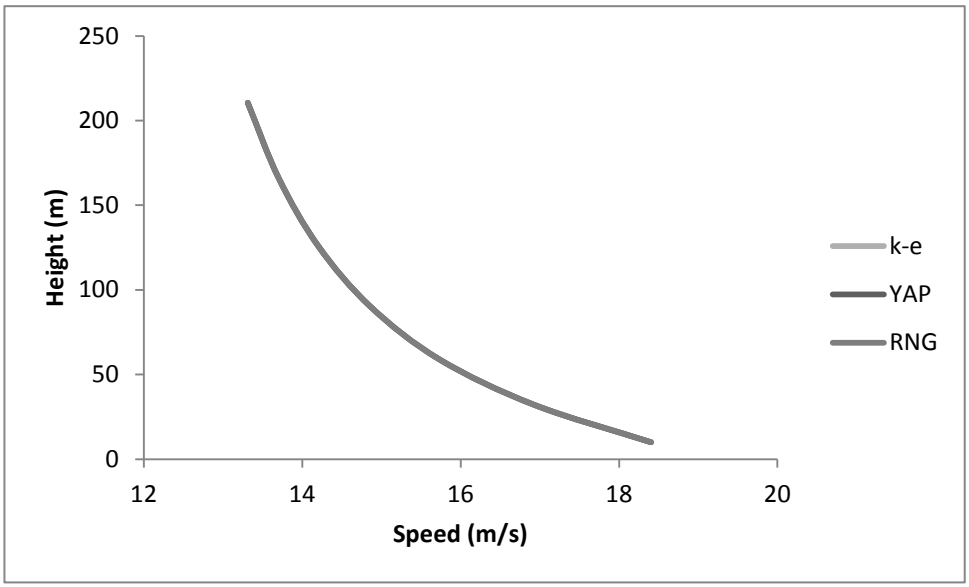

Figure 4-9 Wind speed predictions against height for WTG No 17 using three k-ε variants

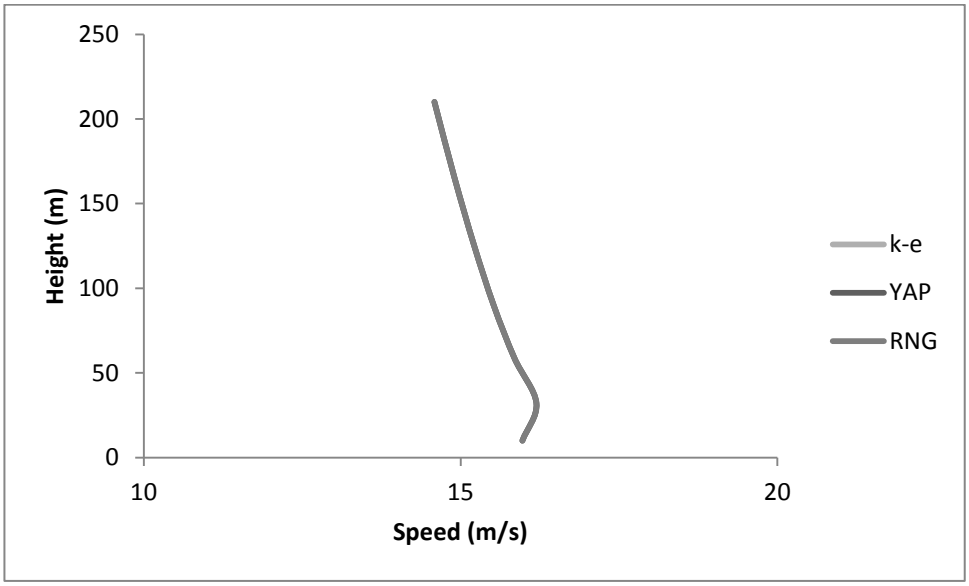

Figure 4-10 Wind speed predictions against height for WTG No 19 using three k-ε variants

Shear variation

The results for the shear variation are presented for WTGs **N16** to **No19** in Figures 4-11 to 4-13, respectively. The wind shear gradually increases towards the far field.

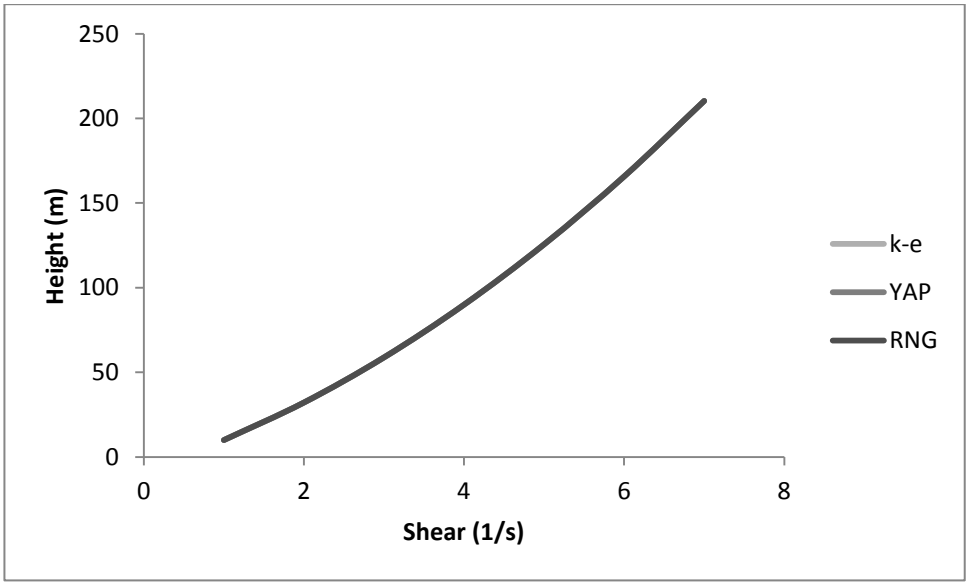

Figure 4-11 Predictions of wind shear against height for WTG No16 using three k-ε variants

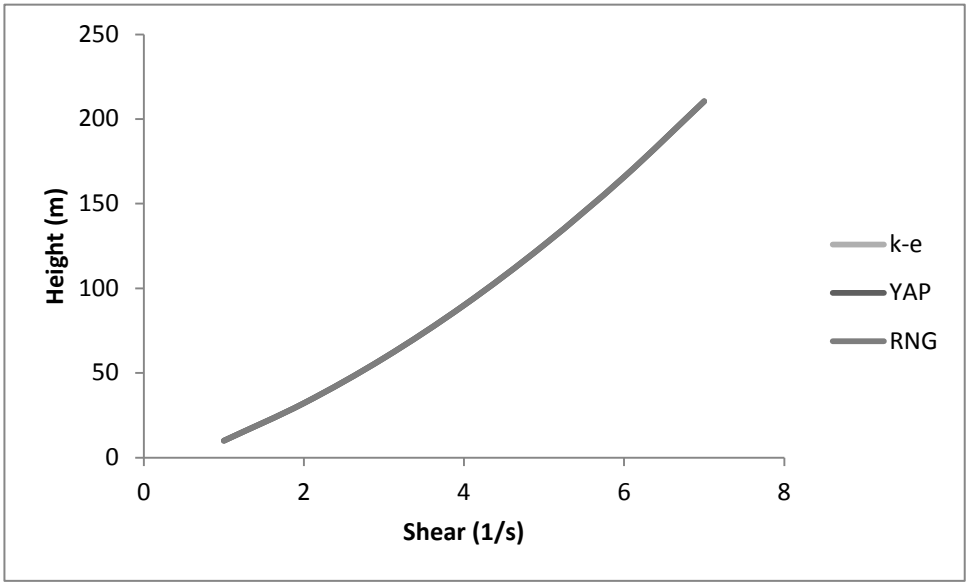

Figure 4-12 Predictions of wind shear against height for WTG No17 using three k-ε variants

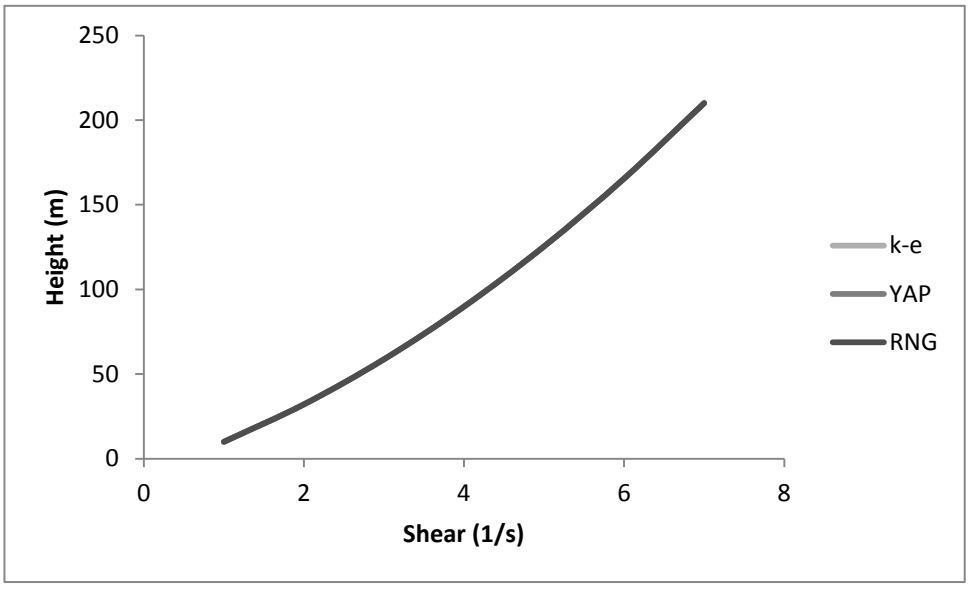

Figure 4-13 Predictions of wind shear against height for WTG No19 using three k-ε variants

Overall comparison of results for different WTGs and annual energy production

An overall assessment of the three k-ε variants and WTGs positions can be made through the plots of Figure 4-14, where the TIs for different WTGs are compared.

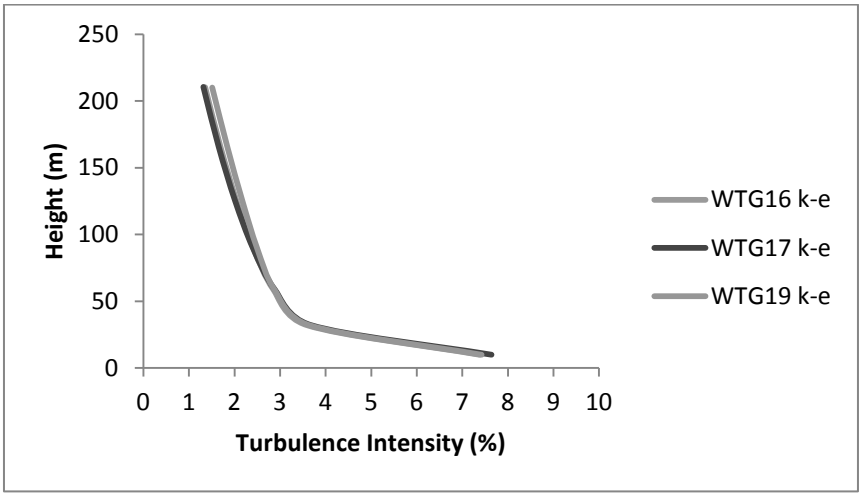

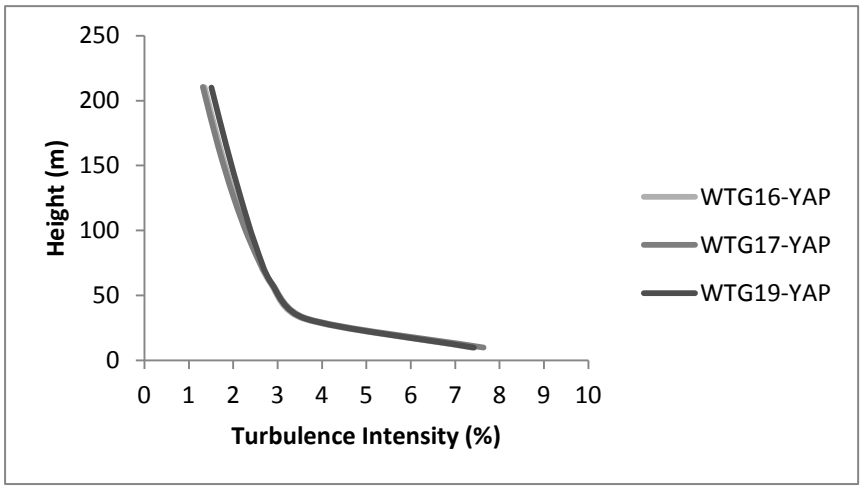

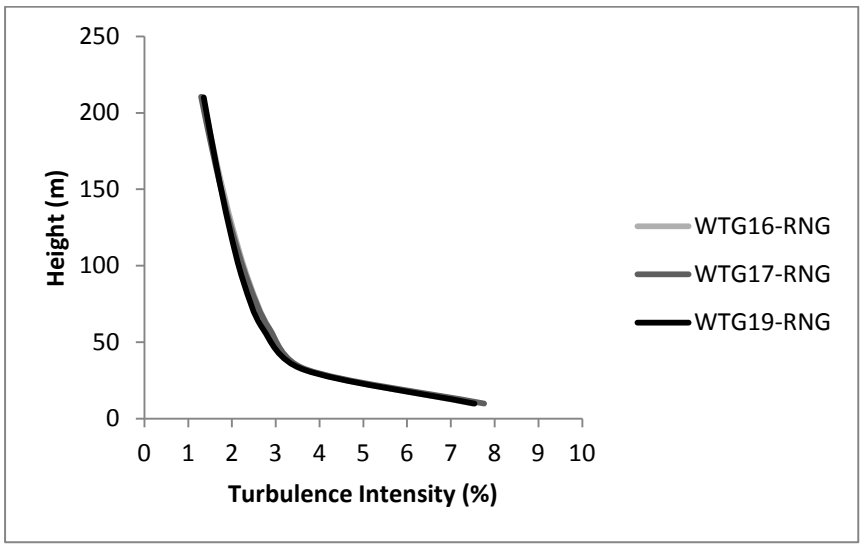

Figure 4-14 Comparison of TIs for different WTGs using the three turbulence model variants

The main conclusions are summarized below:

- The TI seems to increase for WTG No19 between 70m to 210m height compared to the other two WTGs. It seems to decrease at WTG19 slightly between 40m to 125m compared to the other two WTGs.
- The RNG's effects on TI for WTG17 are possibly due to the location of this turbine in relation to WTG16 and 19. WTG 17 This turbine is located in a region of steep terrain descent. Overall the results do not seem to be affected by the variant of the k-∈ turbulence model employed.
- The absolute values of the TI results for the three turbulence model are presented in Table 4-2

Height	TI calculated by k-ε	TI calculated by YAP	TI calculated by RNG
(m)	(%)	(%)	(%)
9.951	7.43	7.43	7.54
32.095	3.63	3.64	3.64
58.72	2.83	2.88	2.71
89.827	2.5	2.49	2.26
125.415	2.17	2.17	1.94
165.485	1.85	1.84	1.64
210.037	1.51	1.51	1.35

Table 4-2 Turbulence models results with respect to turbulence intensity

The results also make sense with respect to their physical interpretation. Since the TI is higher near the ground in the proximity of the wind turbines and gradually decreases towards the far field.

The calculation of the annual energy production was also performed at grid resolution of 217,080 cells using the three turbulence models and the results are presented in Table 4-3 Moreover, the AEP results for each WTG and for the three models are shown in Figure 4-15 where the difference with respect to the results of the AEP between the application of k-ε and Yap correction amounts to 0.003% and with RNG amounts to 0.04%.

The results show very good agreement between the three models.

Turbulence model	AEP (GWh)
k-∈	121.6475
YAP	121.6509
RNG	121.6917

Table 4-3 AEP results as obtained from the three k-ε variants,

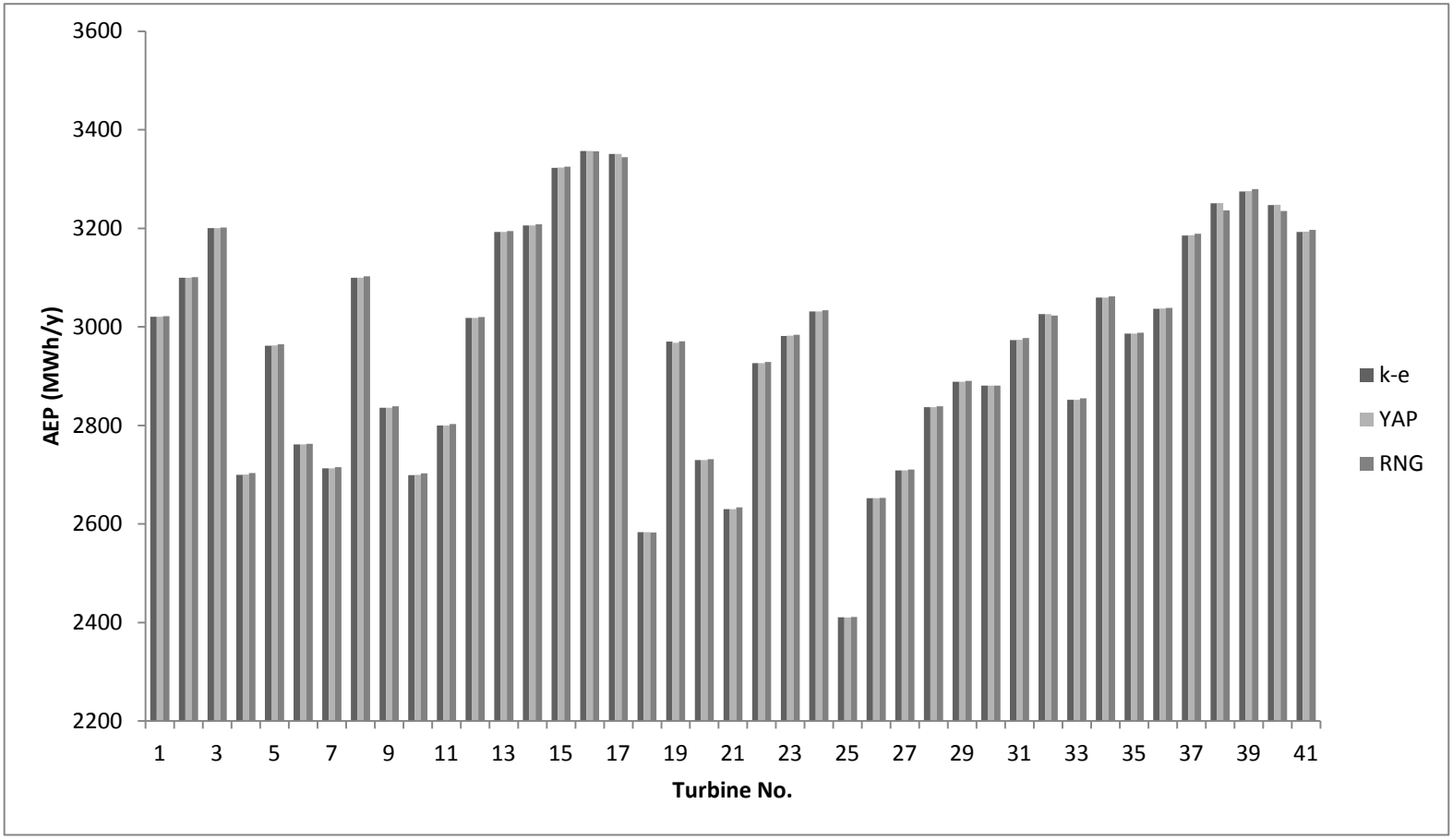

Figure 4-15 Comparison of Annual Energy Production (AEP) for the various WTGs and for the three turbulence model

4.3 Effects of surface roughness

The annual energy production (AEP) in a wind farm is influenced by the boundary layer profile over the terrain. In turn, the boundary layer profile depends on the surface roughness. Therefore, the effects of surface roughness on AEP should be carefully examined when a wind is to be designed.

The roughness of a terrain can be described by the so-called roughness length z_o which is the height above ground level where the wind speed is theoretical zero. The roughness length describes the amount of friction which produced at the ground of a surface which causes wind delay (Walmsley et al, 1981) at the lower level described as shear at section 1.1.1, Equation. 1-4

Three different roughness lengths have been considered corresponding to different types of surfaces as shown in Table 4-4

Type of surface	Roughness length (m)
Open farmland-Only smooth hills	0.03
Farmland with some buildings & crossing hedges of 8m height and about 800m apart	0.10
Villages, small towns, very close farmland with many or heigh hedges, forests	0.40

Table 4-4 Selection of roughness length

The Atmospheric Boundary Layer (ABL) is also influenced by the roughness of the ground. In practice, as the roughness of the terrain increases (Crasto , 2007), the higher ABL is selected as also shown in Figure 4-16

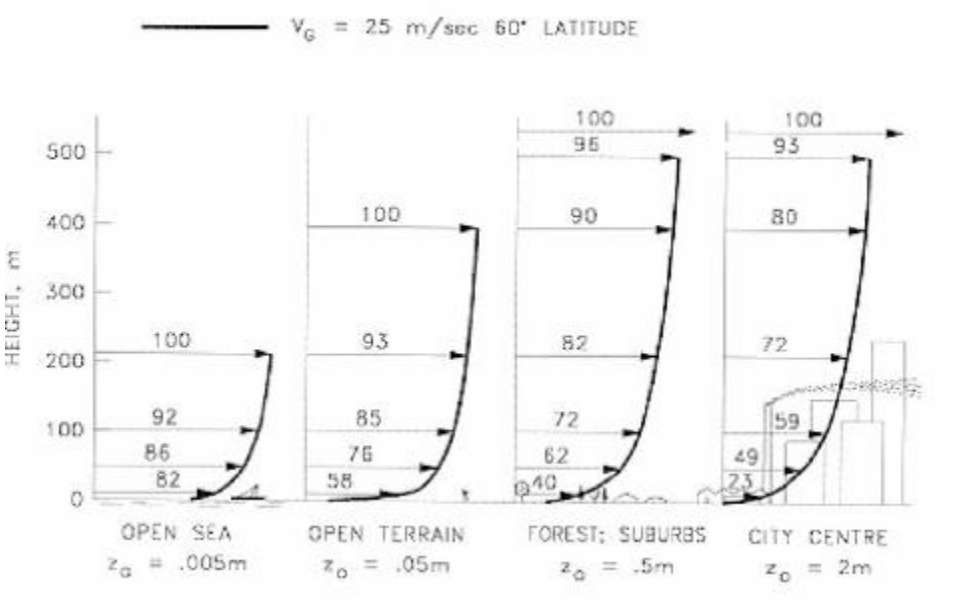

Figure 4-16 Height of ABL according to roughness length
Source: http://mae.ucdavis.edu

The following heights values (Table 4-5) of ABL have been selected for the three roughness cases considered in this study.

Atmospheric Boundary Layer Height (m)	Roughness Length (m)
380	0.03
440	0.1
480	0.4

Table 4-5 ABL used for different roughness lengths

The simulations using various roughness lengths were performed for a grid size of 217.018 cells. Below are shown details about the horizontal resolution.

	x	y	z	total
Grid spacing(m)	75.0	75.0	Variable	-
Number of cells	67	54	60	217080

Table 4-6 Horizontal resolution of the WindSim model

The vertical resolution is estimated based on the highest and lowest point in the calculation area. The grid extends 9000.0 (m) above the point in the terrain with the highest elevation. The grid is refined towards the ground. The left and right columns display a schematic view of the distribution at the position with maximum and minimum elevation respectively. The nodes, where results from the simulations are available, are situated in the cell centers indicated by dots as seen in the table 4-7below.

	1	2	3	4	5	6	7	8	9	10
z-dist,max (m)	9.8	31.6	57.9	88.6	123.7	163.2	207.1	255.5	308.2	365.4
z-dist,min (m)	10.9	35.2	64.3	98.4	137.4	181.3	230.1	283.9	342.5	406.1

Table 4-7 Vertical resolution of the WindSim model

To achieve convergence, the terrain has been smoothed throughout given a smoothing limiting value of 0.01, which means that areas with second order derivative higher than 0.01, are set equal to 0.01 and therefore are smoothed. The simulations performed by WindPro, which is a linear flow model, cannot adequately model the flow.

The AEP results obtained from WindPro and WindSim are shown in Fig. 4-17. The roughness length was set as 0.03m.

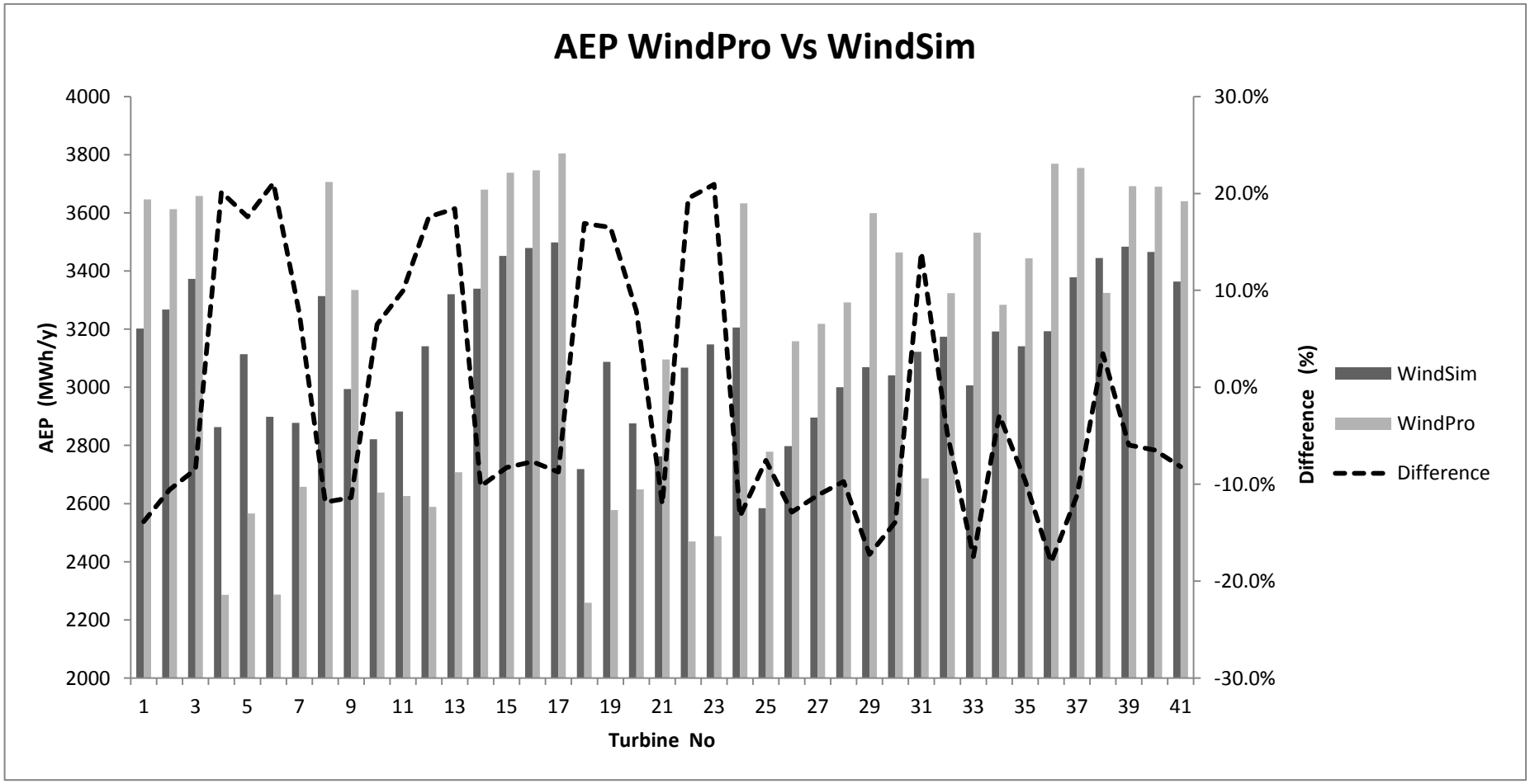

Figure 4-17 Comparison of Annual Energy Production results between WindPro and WindSim

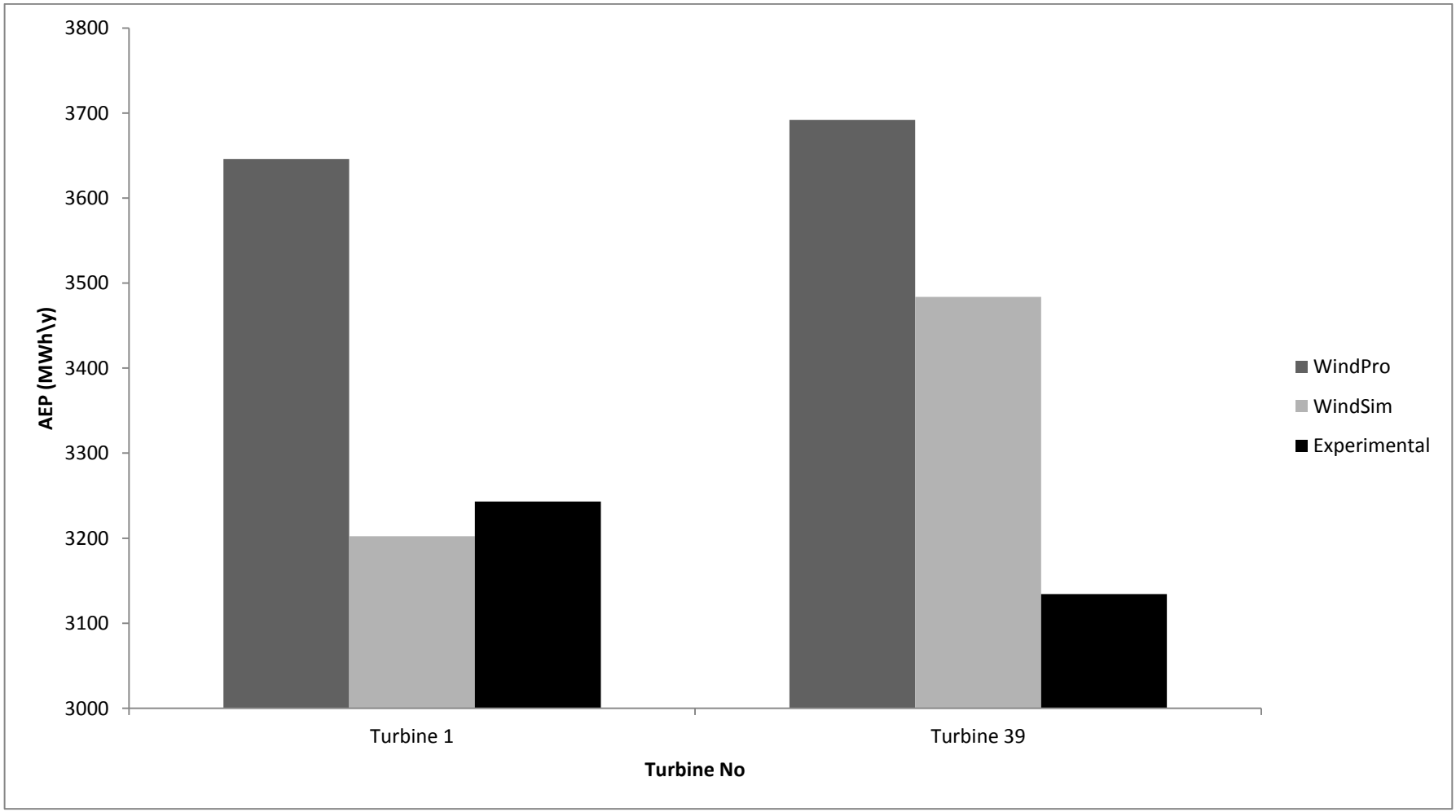

Figure 4-18 Comparison of Annual Energy Production results between WindPro, WindSim and experimental

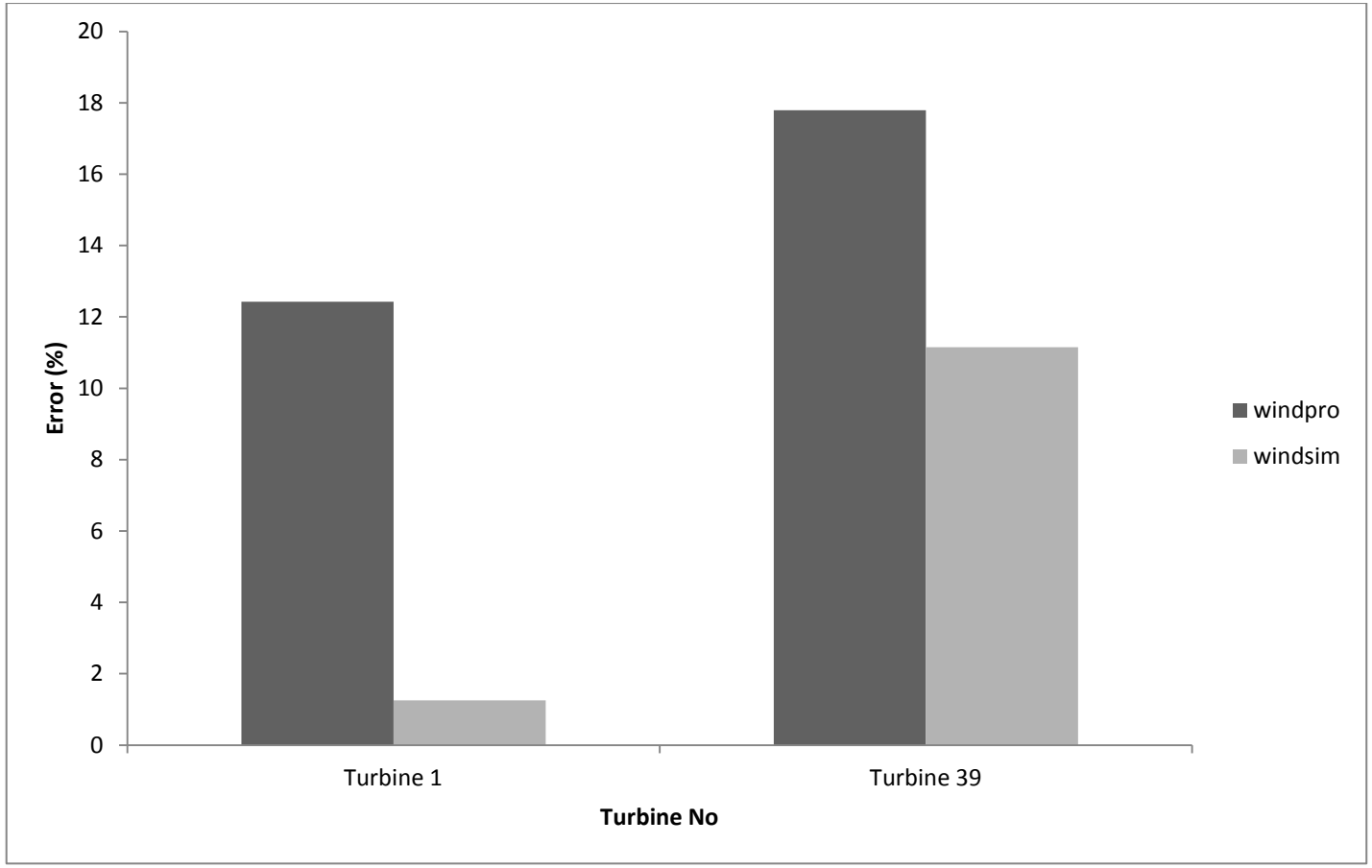

Figure 4-19 Presentation of error between WindPro, WindSim performance

The results of Figure 4-17 should be considered by bearing in mind that the linear model WindPro is recommended for terrains with steepness less than 0.3m (roughness length). Therefore, the turbulence produced by a steeper area cannot be accurately estimated since it does not lie within the recommended operational envelope. Consequently, WindPro is expected to over/under-predict AEP. This indicates that the difference between the results obtained from WindPro and WindSim with respect to the park energy production amounts to 1.55% (Figure 4-18) and the error between the experimental results and WindPro (Figure 4-19), e.g., for Wind turbine No 1 is 12.42% while using WindSim is 1.25%. For Wind turbine No 39 the corresponding errors are 17.85% and 11.15% for the WindPro and WindSim, respectively. The error is greater for Wind turbine No 39 than Wind turbine No1 because No 39 is located in a steeper part of the terrain, where the computational inaccuracies due to the grid and flow complexity are higher.

The AEP results for different surface roughness using both WindSim and WindPro are shown in Figs 4-20 and 4-21. The energy production calculated by WindSim against roughness length is increased when increasing the roughness length (Figure 4.20). Using WindPro, the annual energy production seems to slightly change with respect to different roughness lengths (Figure 4-21), however, WindPro shows a different trend in the AEP variations.

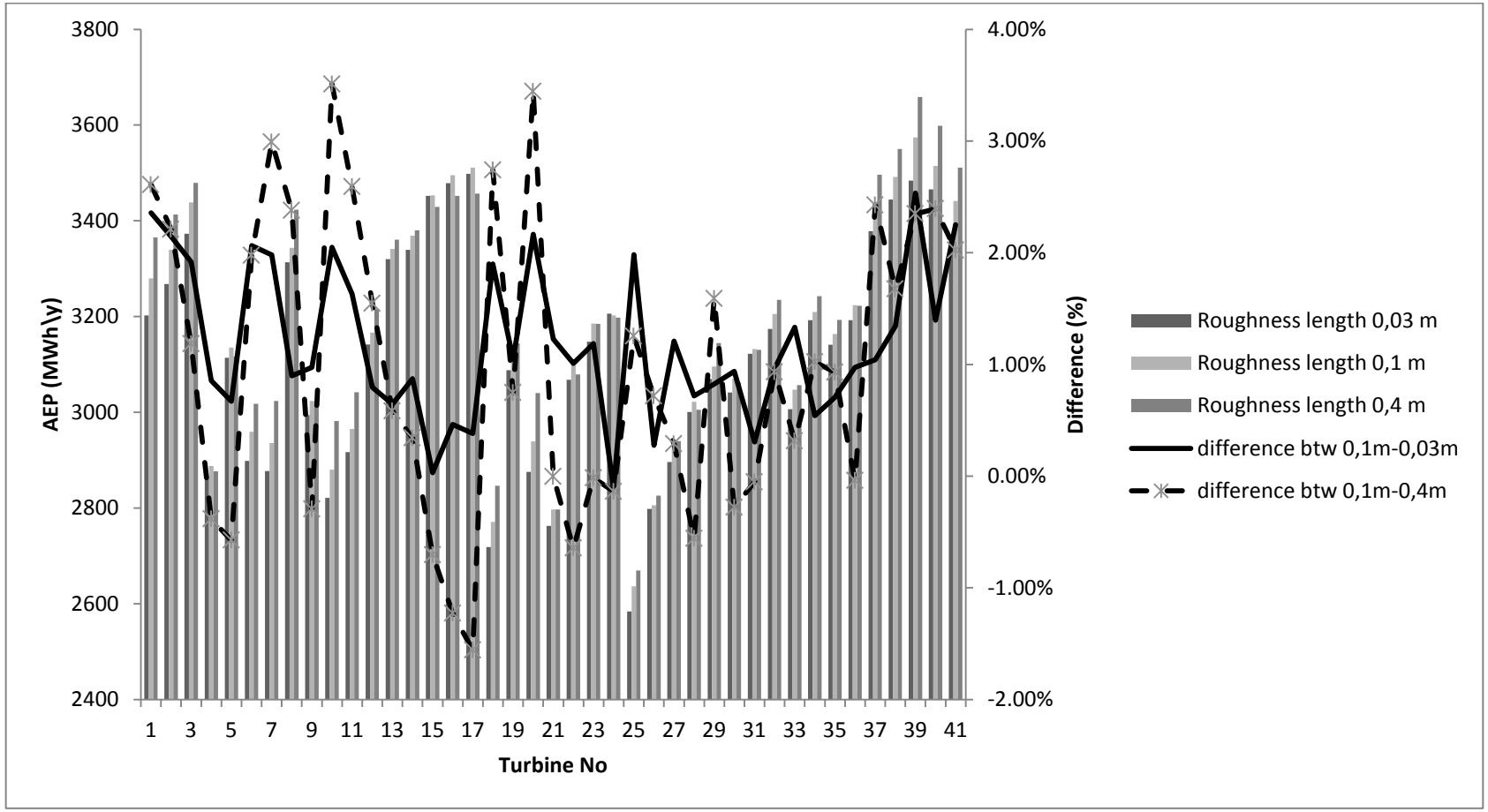

Figure 4-20 Energy production against roughness length calculated by WindSim

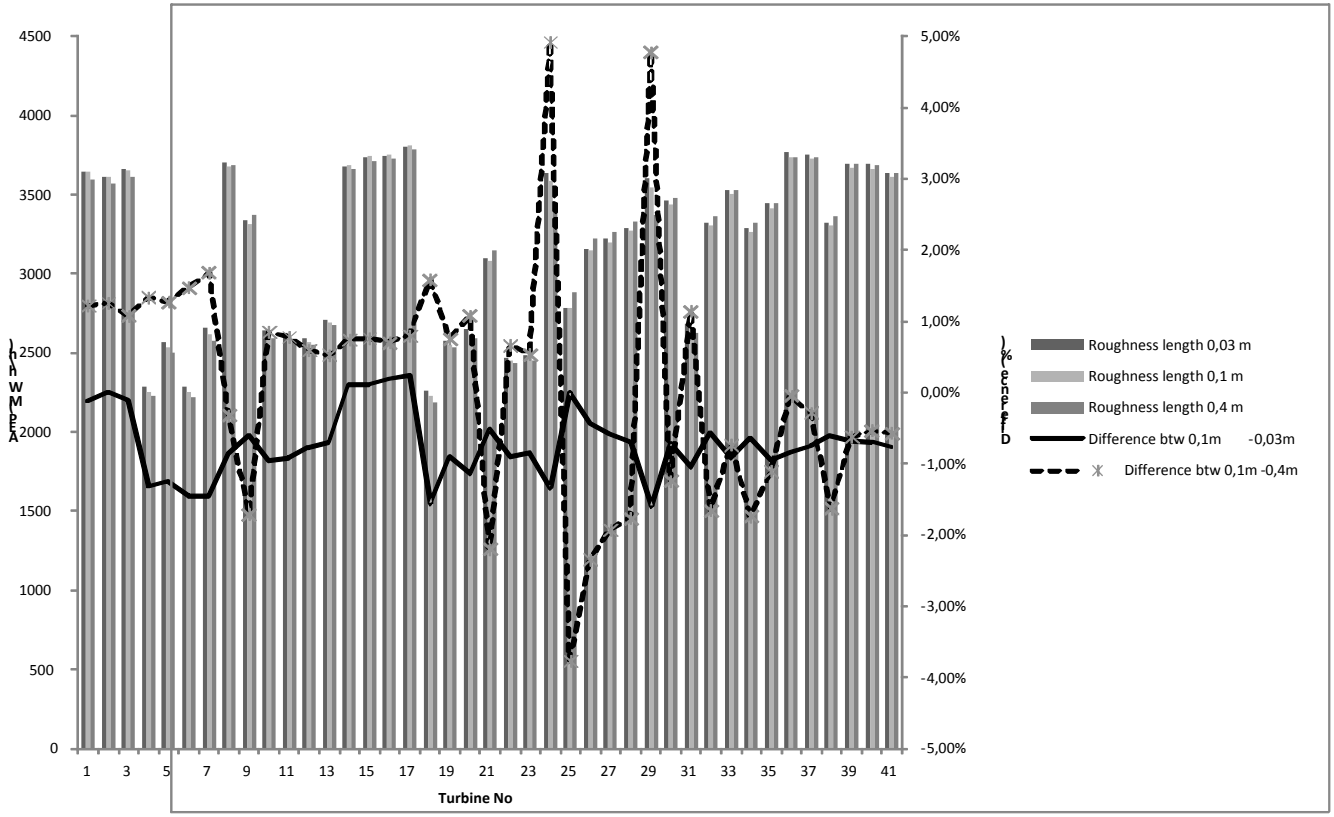

Figure 4-21 Energy production against roughness length calculated by WindPro

Experience dictates that turbulence increases when the flow passes over a steep hill. Therefore, wind turbines micro sitting has major effects on the results obtained from the area of examination related to wind turbines efficiency in accordance to the roughness length respectively.

In this study the measurements obtained for a turbulent flow over a steep hill, where wind turbines are placed very close over a step producing flow separation from the hill (Klemp, 1979). The velocity profile is examined at the separation and reattachment points and, in particular, within the reverse flow region on the lee side of the hill. This phenomenon is noticed in the area where wind turbine No17 is placed and the wind comes from N, NNW, NWW and SSE, E and EEN which are representative sectors 0 and 30, as shown in Figure 4.22. When the shape of a hill is steep enough to provoke adverse pressure gradient, then flow separation may occur. Having regions where the flow is strongly retarded, the convective effects remove vorticity from the boundary at a lower rate than the feeding rate of vorticity from the upstream flow. Therefore, for the velocity outside the boundary layer to decrease downstream, the vorticity generated at the wall must have the opposite sense of rotation (negative vorticity) (Loureiro, 2008). Provided the generation of negative vorticity at the wall is sufficiently large to overcome the effects of diffusion of positive vorticity towards the wall, a reverse flow region develops over the wall. For turbulent flow, the rates of diffusion increase. Increasing the rate of turbulent diffusion by surface roughness is a manner of delaying or even preventing separation.

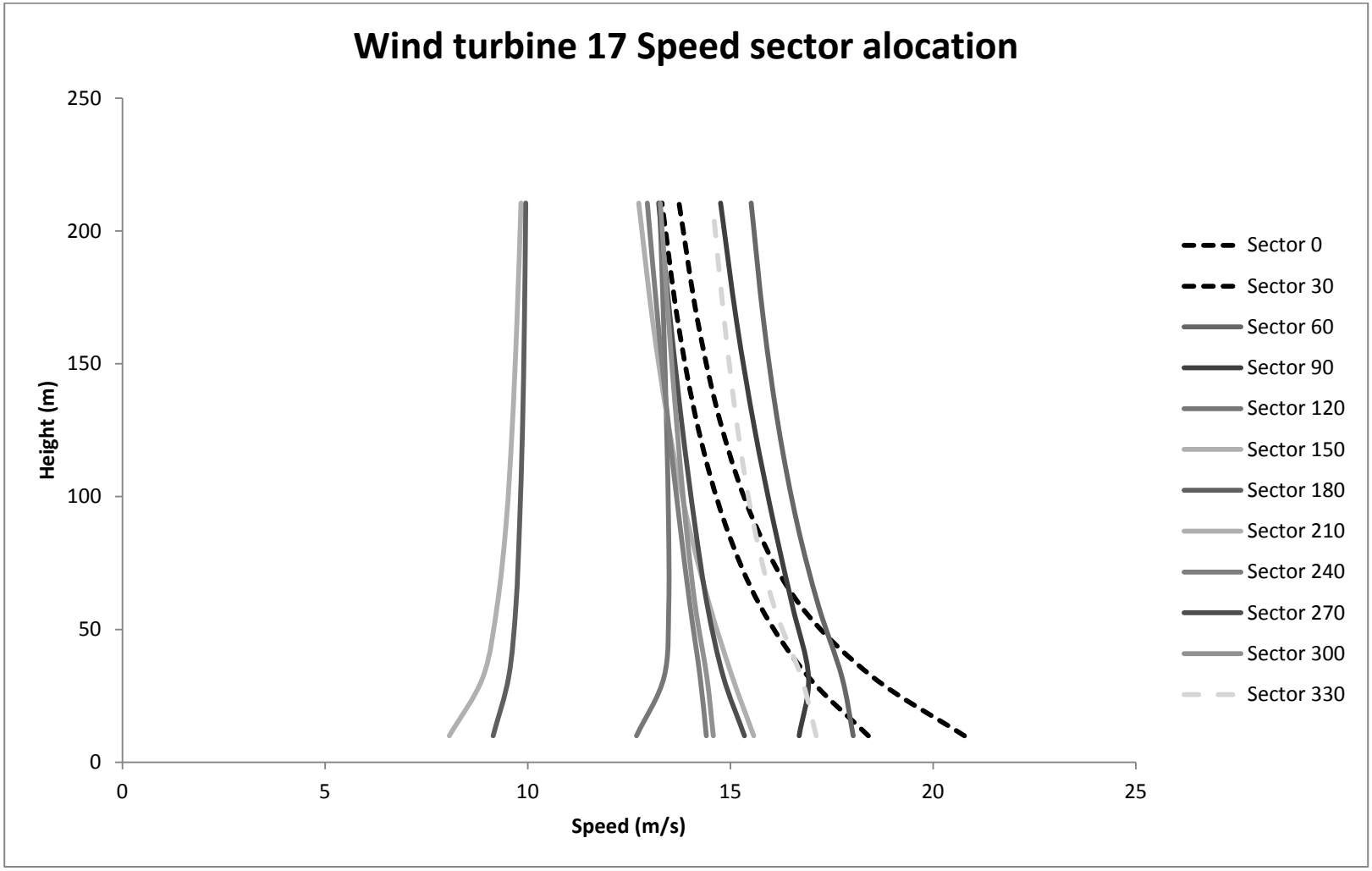

/

Figure 4-22 Wind speed profiles in 12 sectors with reference to wind turbine No17

The roughness effects with have been studied for three different WTGs**16, 17** and **19.** The above wind turbines are placed the one behind the other, starting with 17 located close to the edge of the hill; close to the step WTG 19 is installed in the centre of the wind farm.

The results of Figure 4-23 show that the wind speed decreases for a rougher terrain. Furthermore, the wind speed increases in the areas where the terrain is steeper. As expected, the results also show that the roughness has an effect on the wind speeds near the ground and its effects diminish towards the far field.

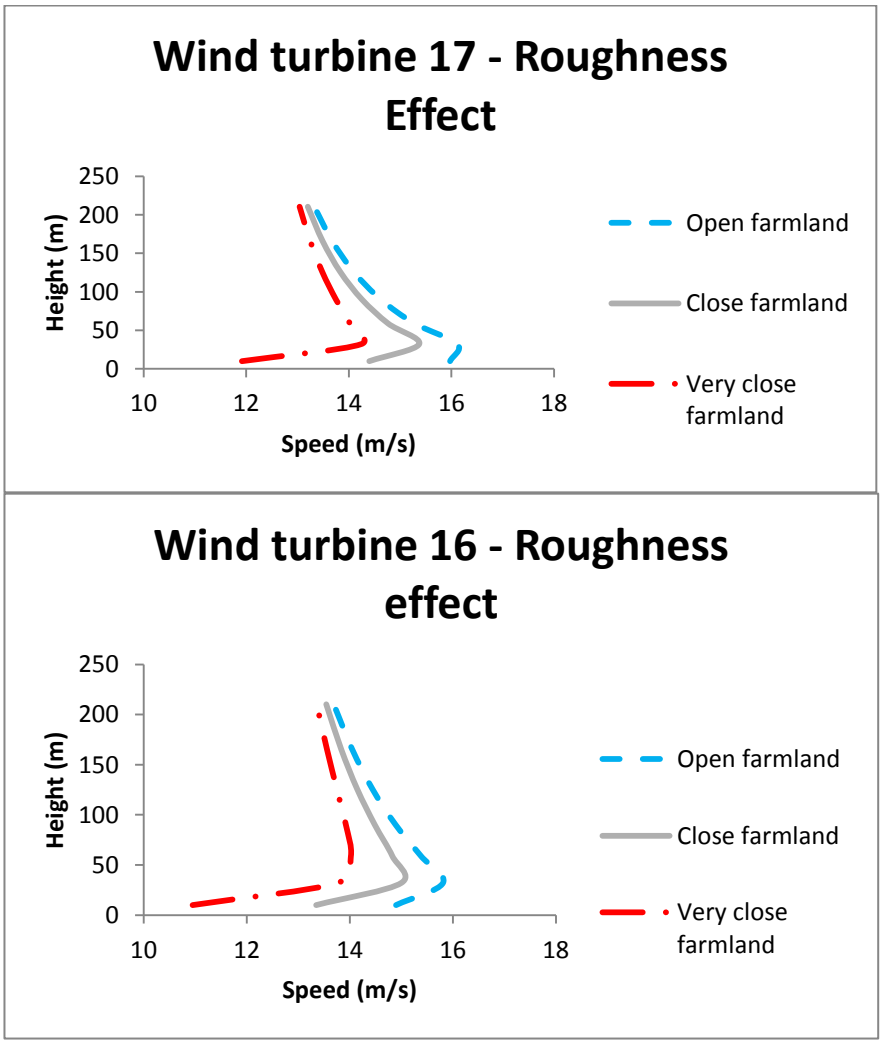

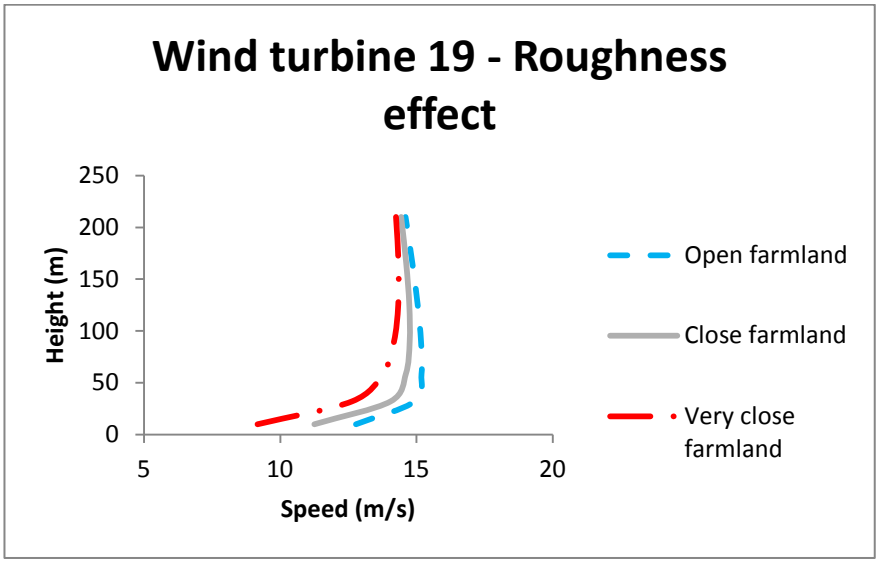

Figure 4-23 Roughness effect against wind turbine position

4.4 Wake effects on different terrains

For the development of a wind farm, the turbulence intensity due to wind turbines should be taken into account in the stability and the load calculation for the rotor's proper operation (Crasto et al, 2008). The wakes behind a wind turbine is an issue of intensive research (Pastorrel, 1991)since they are characterized by increased turbulence levels, which are the reason of load increase and energy decrease. Understanding of wake losses is also important for installing the wind turbines as close as possible in order to exploit the largest part of the land, which is available for the wind farm development. This is particularly the case for a complex terrain where the space is limited compared to a smooth area (Frandsen et al, 2008).

For the simulation of wakes behind wind turbines, many models have been developed (Nielsen, 2003). Calculations in this study have been carried out using the Jensen model (Sørensen et al, 2008) in WindPro and Jensen and Larsen model in WindSim (see for further details section 2.1.2) (Sorensen et al, 2006), (Zigras & Moennich, 2011).

Following the simulations obtained using WindPro, the calculation of wake losses for individual wind turbines is carried out. In contrast, the total wake losses of the whole wind farm are carried out using WindSim.

Wind turbines in Panachaiko have been installed in three rows. However, some wind turbines are placed randomly according to the terrain orography. The space between the rows is 3.5 times the rotor diameter in order to provide the appropriate space between wind turbines, thus achieving the optimum efficiency of wind turbines (see Figure 4-24) The surface roughness selected for the comparison of wake models between the two software has been selected as 0.03 (roughness length), which is most common and appropriate roughness length for the construction of a wind farm.

The scope of this study is to examine the effect of wake on wind turbine operation with respect to the efficiency of wind farm. The set up of simulations for both software is based on standard parameters due to limitations of changing parameters on WindPro version 2.4. As regards the Jensen model, the decay constant was chosen as 0.075 and no internal roughness selected (Sten Frandsen, 2010).

The total energy production without wake effect compared to the energy production with wake existence is shown in Figure 4-25. As expected, the energy production calculated in WindPro with Jensen model considering the wake effect is decreased 6.15% compared to the case with no wake effects; this is due to the absence of wake turbulence on the rotor of wind turbine (Thomas Hahm, 2010). The error between the experimental results and calculations with WindPro shown in Figure 4-26, taking into account the wake effect, is 12.06% as regards the wind turbine No 1 and 9.91% regarding the wind turbine No 39. The effect of wake was examined also using WindSim in conjunction with the Jensen and Larsen wake models (Figure 4.27). Comparing the above mentioned wake models, the differences in the results for the above wake models is 1.51%, which is considered to be small.

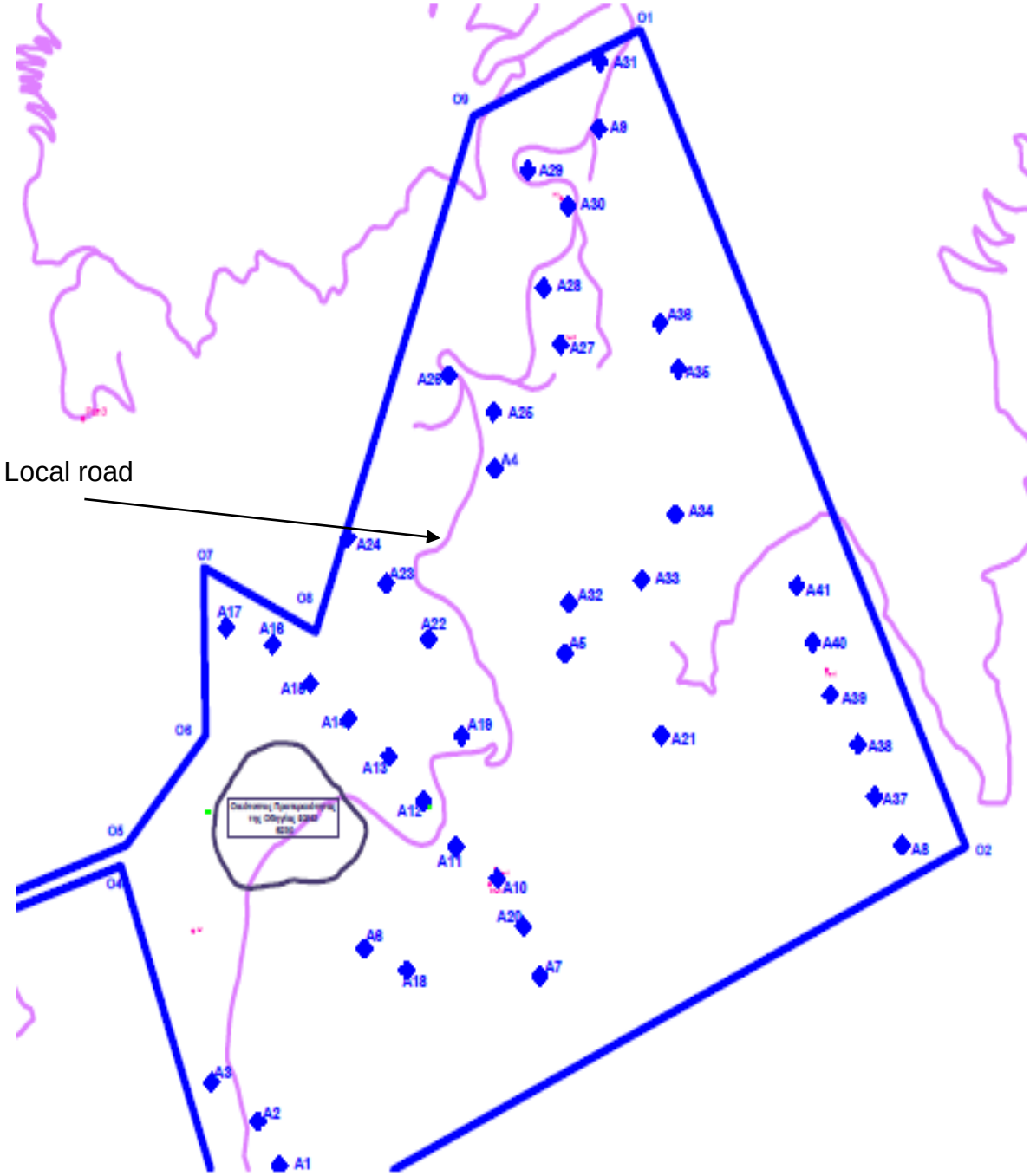

Figure 4-24 Panachaiko wind farm micro sitting

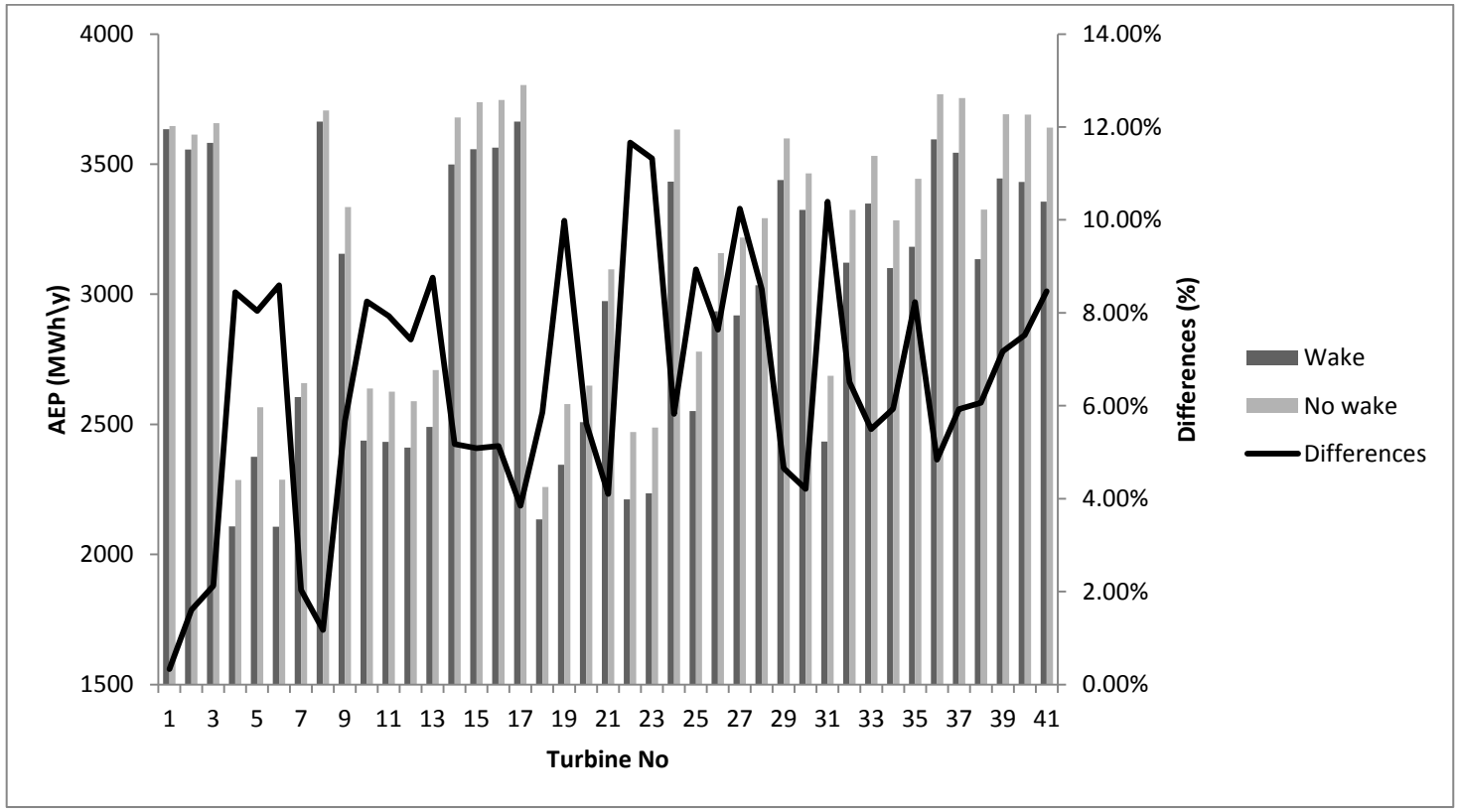

Figure 4-25 Calculated Energy Production with WindPro

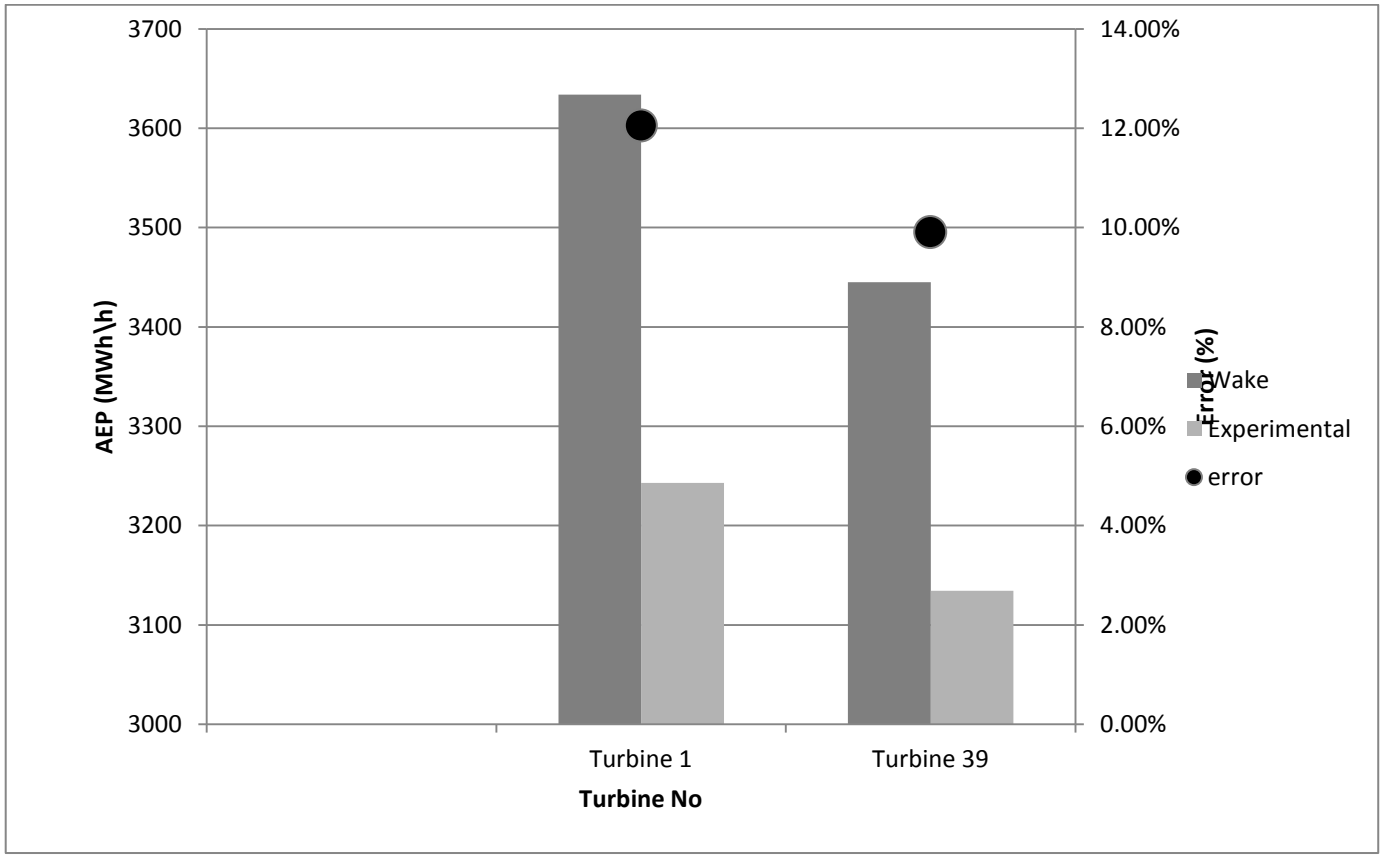

Figure 4-26 Presentation of error between experimental results and wake effect in WindPro

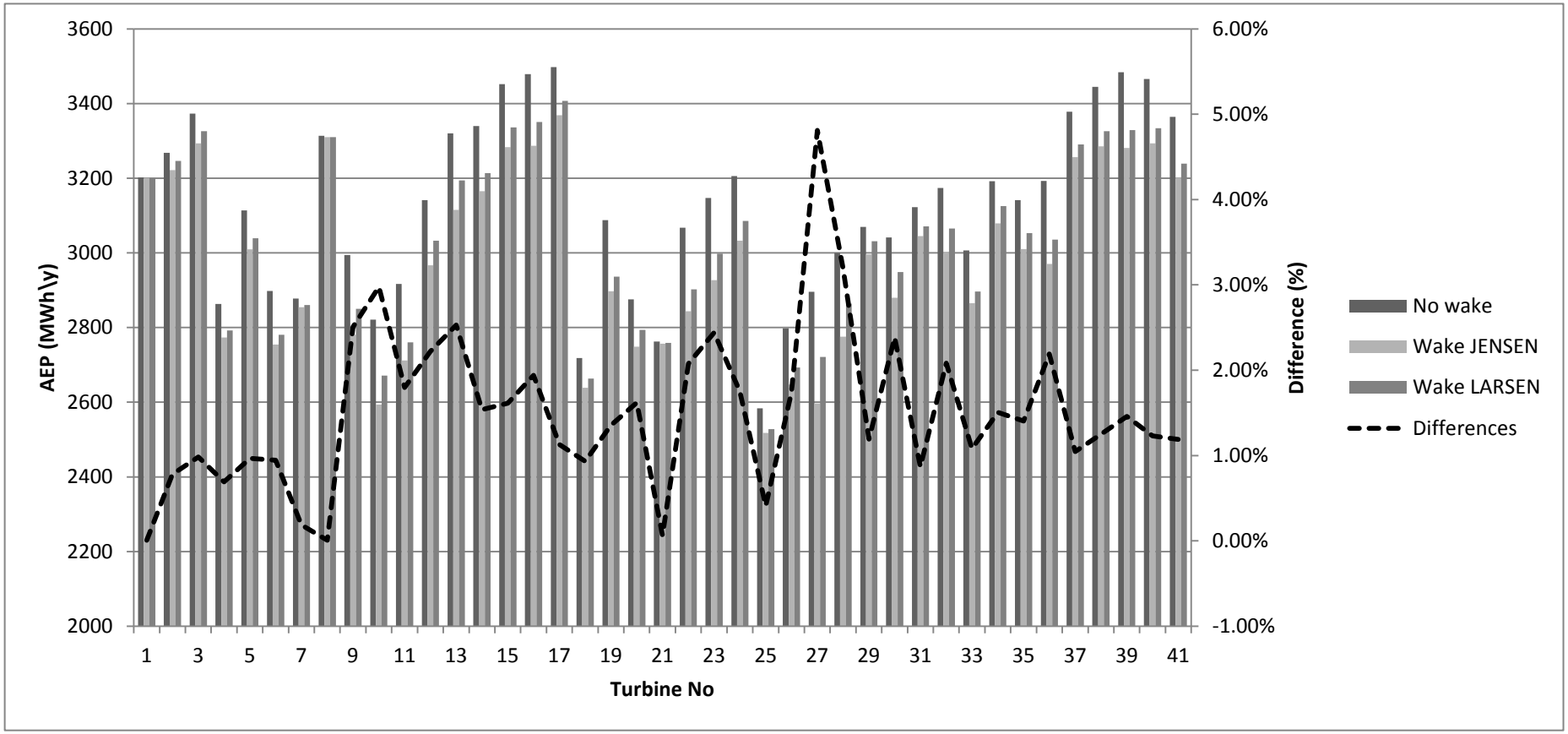

Figure 4-27 Calculated Energy Production with WindSim

The results of energy production following the implementation of the Jensen model in WindPro and WindSim, as well as the Larsen model in WindSim are shown in Figure 4-28.

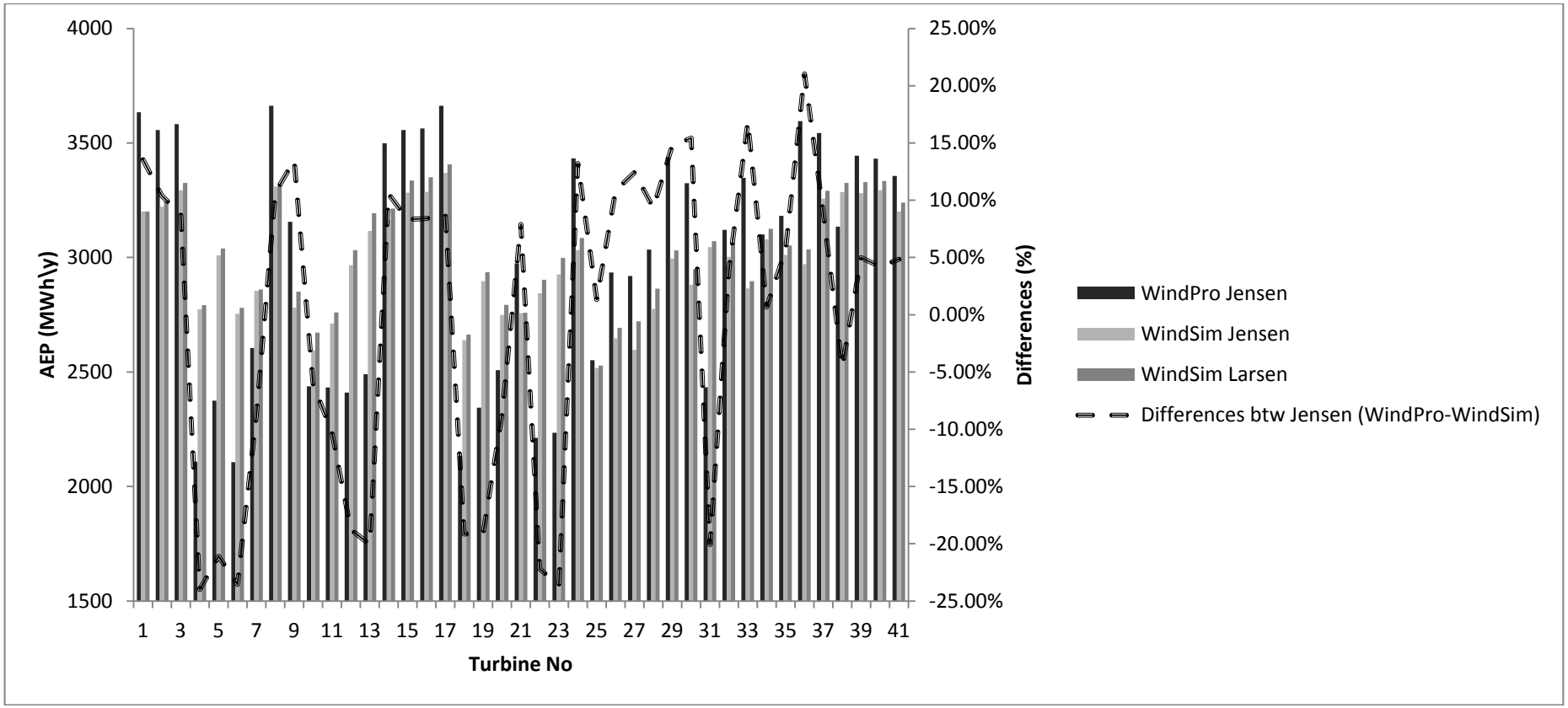

Figure 4-28 Calculated Energy Production with wake effect by the implementation of Jensen & Larsen model

The results obtained using the Jensen model in conjunction with different software did not show any significant differences; higher energy production is predicted by WindPro (0.27% higher).
However, the results of WindSim using the Jensen and Larsen model are more optimistic calculating the AEP in most cases slightly decreased compared to WindPro, having very good agreement between them, show that higher energy production is predicted by Larsen model (1.47% higher) owed to different modelling assumptions. Specifically, The Jensen model is a simple wake kinematic model with respect to the initial velocity deficit and wake decay constant. The main modelling assumption is that the wake behind the wind turbine has a starting diameter equal to the rotor diameter, which is linearly expanding as a function of the downwind distance. The Larsen model is expected to be more accurate because it is based on the Prandtl's rotational symmetric turbulent boundary layer equations, which are an asymptotic version of Navier-Stokes equations for large Reynolds numbers.

The wake effect was also examined with respect to different roughness lengths

- 0.03m
- 0.1m
- 0.4m

The results are presented in Tables 4-8 and 4-9 as well as in Figures 4-29, 4-30 and 4-31.

Roughness Length (m)	AEP Without wake (MWh)	AEP Jensen (MWh)	AEP Larsen (MWh)
0.03	128.0905	122.2356	124.06
0.1	129.6154	124.4775	125.9633
0.4	130.8776	126.3928	127.8983

Table 4-8 AEP calculated by WindSim with respect to wake effect according to the application of roughness length

Roughness Length (m)	AEP Without wake (MWh)	AEP Jensen (MWh)
0.03	130.106,5	122.569,90
0.1	129.224,3	121.806,70
0.4	129.057,7	121.908,20

Table 4-9 AEP calculated by WindPro with respect to wake effect according to the application of roughness length

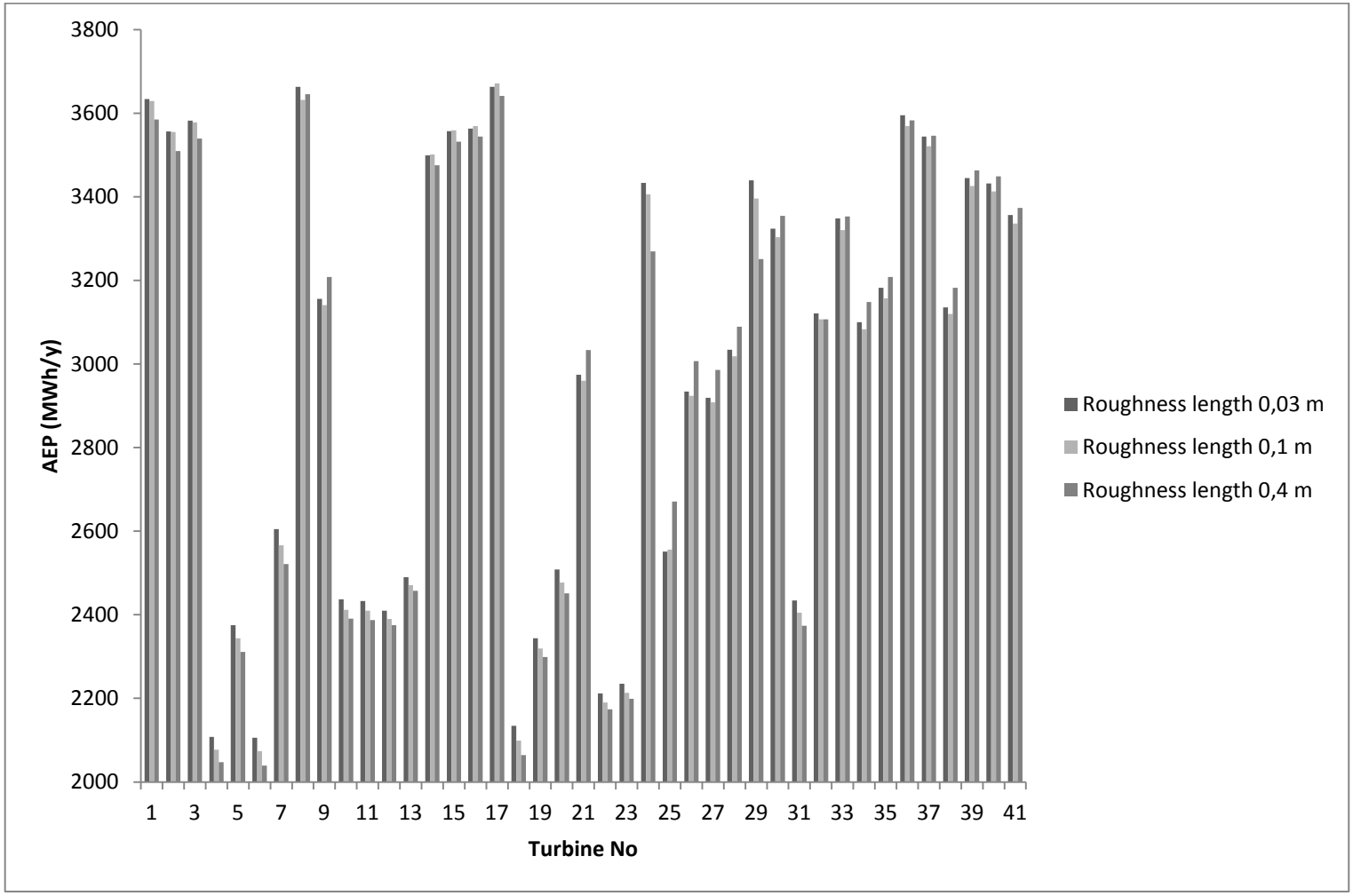

Figure 4-29 WindPro wake effect Vs Roughness length by the application of Jensen mode

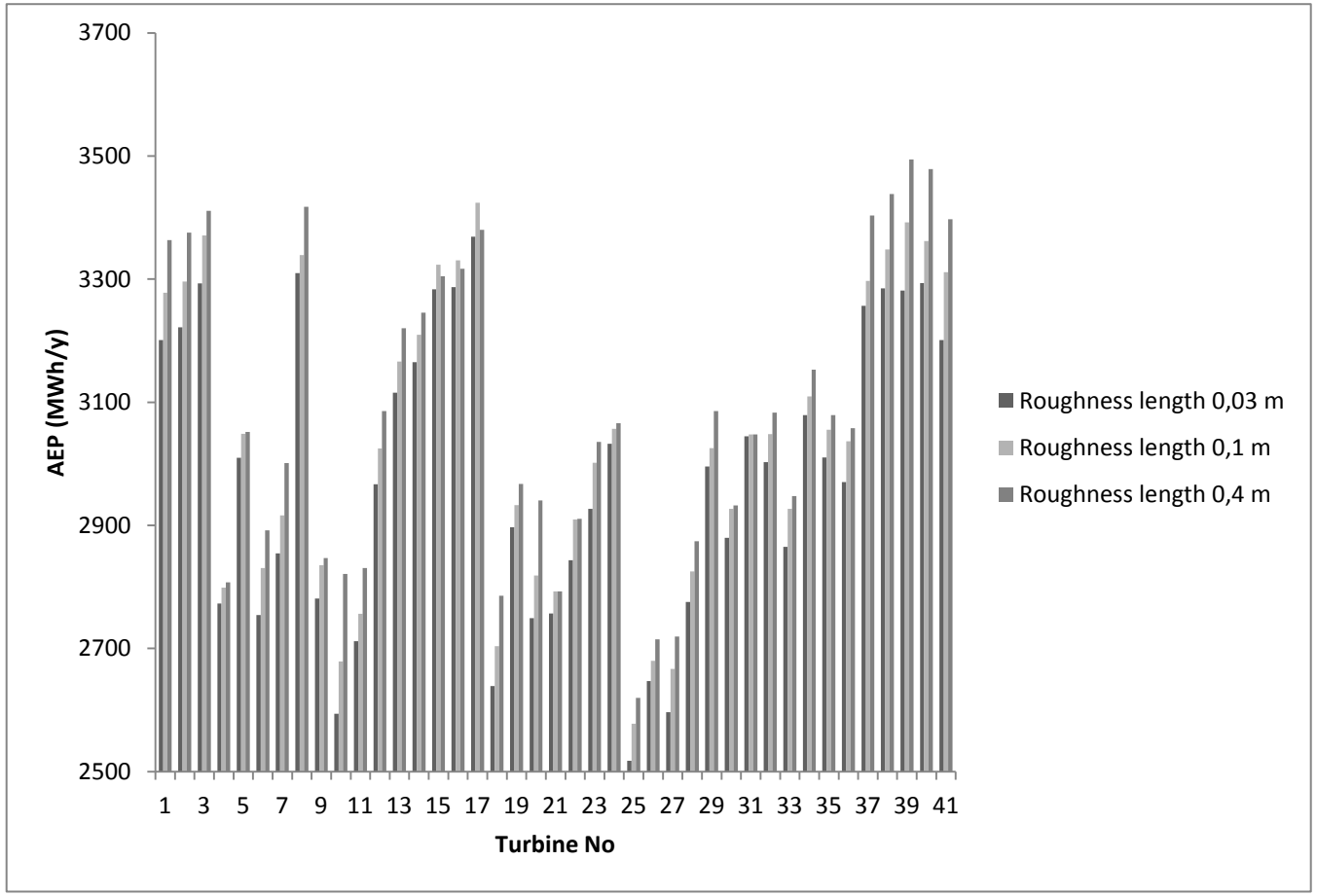

Figure 4-30 WindSim wake effect Vs Roughness length by the application of Jensen model

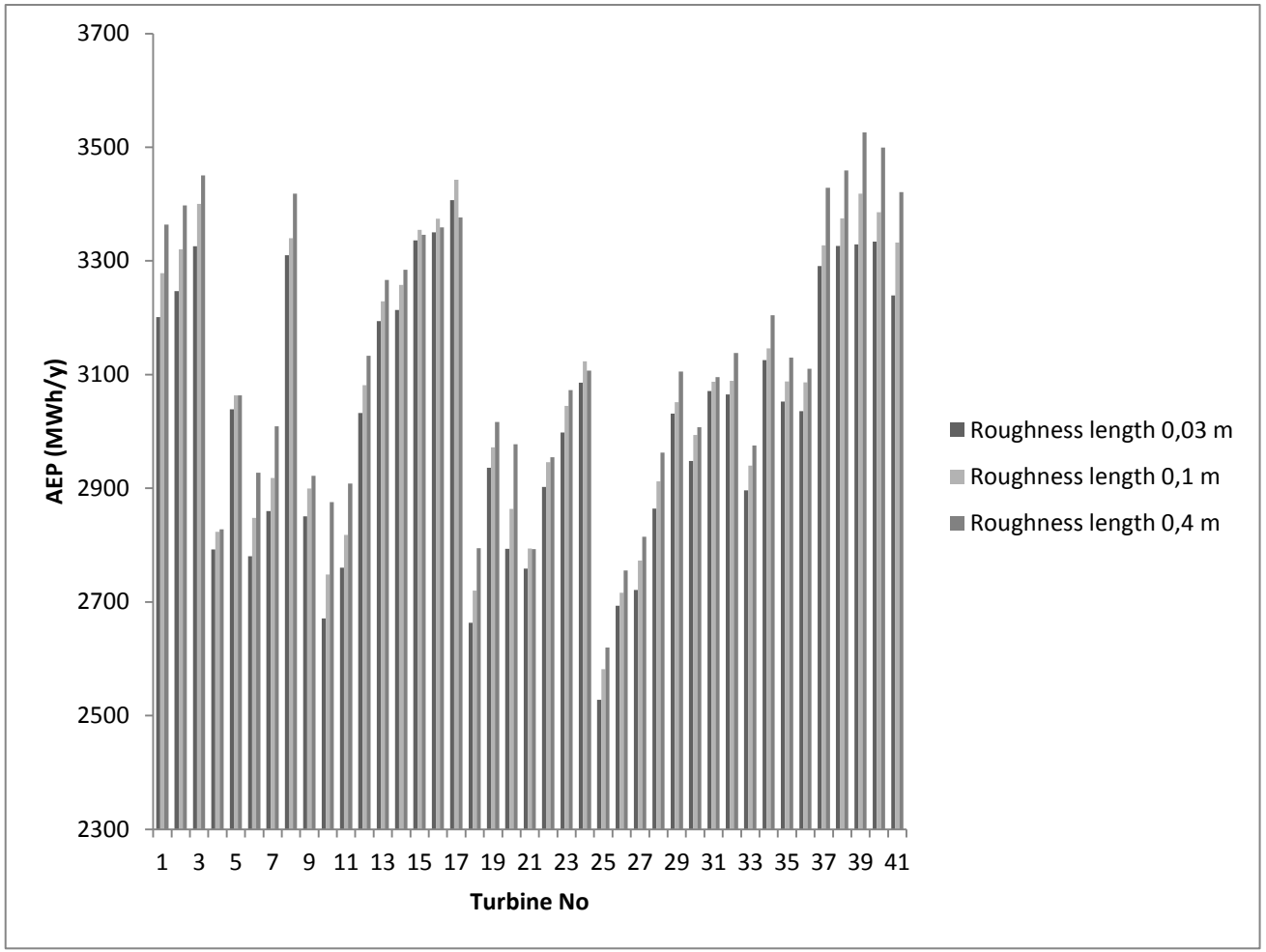

Figure 4-31 WindSim wake effect Vs Roughness length by the application of Larsen model

Following the results obtained from the simulations with WindSim, the energy production increases when increasing the roughness length. However in WindPro the energy production increases when the roughness decreases and this is due to the fact that the model is linear, thus less accurate than the non-linear CFD model. The average park efficiency is displayed in Table 4-10 showing small differences between the three models employed.

Normal wake model	Wind farm efficiency (%)	wake loss (%)
N.O. Jensen applied by WindPro	94,20	5,8
N.O. Jensen applied by WinSim	95,43	4,57
Larsen applyied by WinSim	96,85	3,15

Table 4-10 Wind farm efficiency with respect to different wake models

A validation of the AEP calculated for wind turbines No 1 and No 39 against the available experimental data (see sec. 2.2.4) for the two sets of values is shown in Figure 4-32. The differences with respect to the AEP of wind turbine No 1 are ineligible, when using WindSim, but quite significant when using WindPro (at the level of 12.06%). The differences are increasing for wind turbine No39 where the discrepancy between the experimental data and the simulations using the Jensen and Larsen models in WindSim are 6.21% and 4.68%, respectively. Using the Jensen wake model in WindPro the discrepancy is 9.91%.

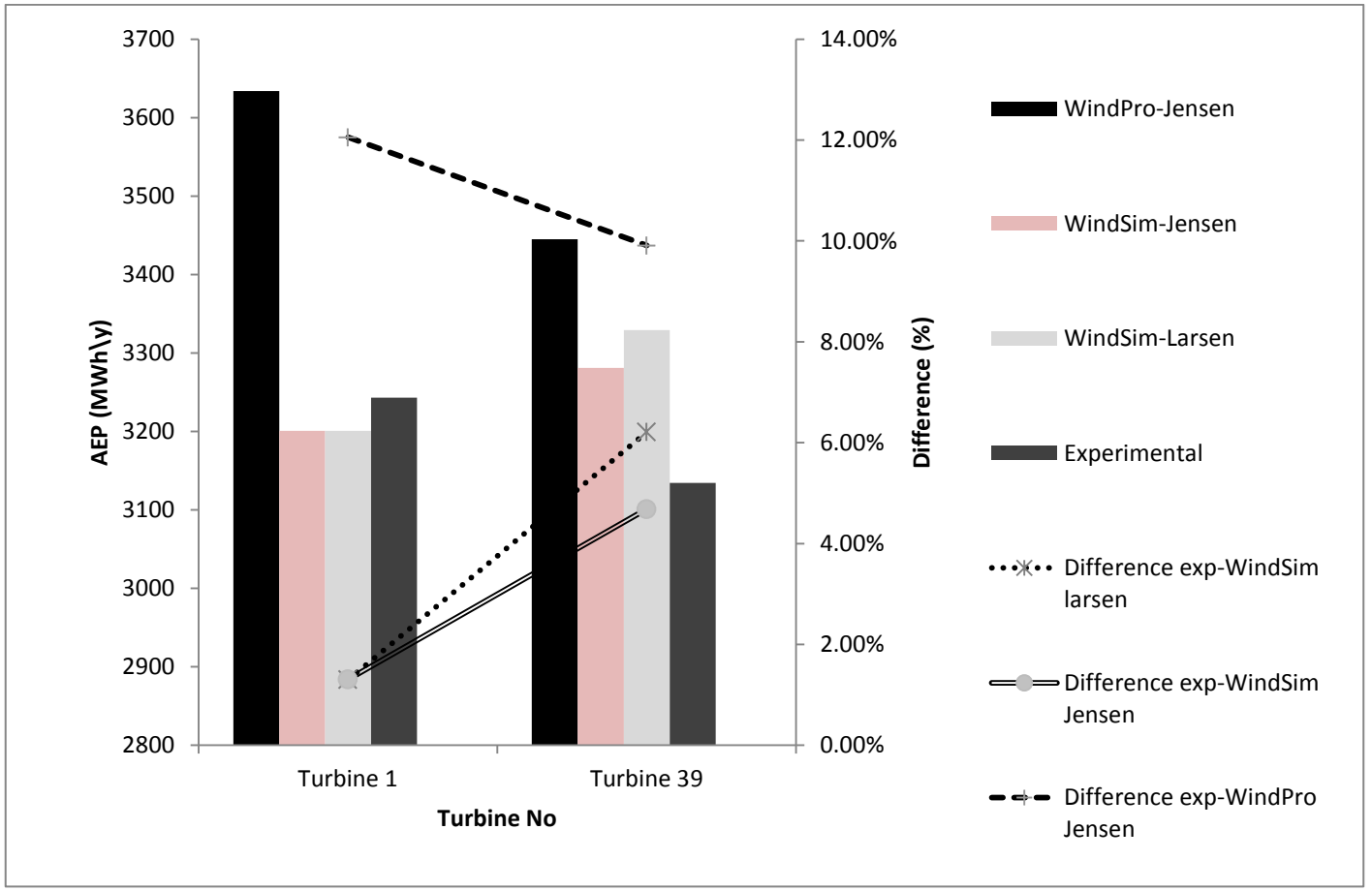

Figure 4-32 Energy production calculated with wake effect by the implementation of Jensen & Larsen model against experimental data

5 CONCLUSIONS AND FUTURE WORK

A computational investigation of a complex wind farm was carried out using the state-of-the-art of engineering CFD software aiming to assess the annual energy production and examine the influence of a range of parameters on the results. Based on the results of this study, as well as the experience accumulating through the literature, a number of conclusions can be drawn:

- The efficiency of the wind farm as expected is strongly linked with the terrain and the wind flow dynamics of the area. As the terrain becomes more complex the prediction uncertainties increase and detailed studies have to be embraced.
- Installation of wind turbines should be avoided in steep areas of the terrain, which may lead to mild or severe flow separation depending on the slope.
- The RANS modelling approach based on the WindSim engineering software requires longer computational times than the linearised WindPro models that require roughly from 2h to 15h depending on the examined case complexity. The CFD modelling should be preferred in complex terrain since it can accommodate turbulent effects through the utilization of more advanced numerical and turbulence models.
- The WindSim assumes a stratified atmosphere, which does not always represent real conditions. However, when a mast is available for a restricted area then the results could be representative. Additionally, CFD computations are carried out based on the assumption of steady state turbulent field which is not representative of a real scenario.
- WindPro accuracy drops as the terrains complexity is increased and as turbulence is introduced.
- Complex terrain simulations exhibit slow and very oscillatory convergence in some cases. This is due to the two reasons: (i) the computational mesh

is highly anisotropic and non-uniform due to the complexity of the terrain, thus making the convergence more difficult; (ii) for highly complex terrain finer grids than the one used here may be required.

- The three turbulence model variants did not show significant differences in the numerical results range from 0.003% between k-ϵ and Yap correction and 0.04% between k-ϵ and RNG. In case having uniform and finer grid then it was expected the difference between turbulence to be increased. Although the grid near the ground is coarse and the near-wall turbulence effects cannot be captured, the turbulence intensity is higher near the ground in the proximity of the wind turbines and gradually decreases towards the far field.
- WindPro shows a different trend in the AEP variations compared to WindSim as regards the energy production calculations amounts to 1.55% and the error between the experimental results range from 12.42% to 17.85% while WindSim range from 1.25% to 11.15% corresponding to wind turbine No1 and No39 respectively. WindPro is expected to over/under-predict AEP due to its deficiency to estimate accurately the turbulence produced over steep areas. The energy production calculated by WindSim is increased as the roughness length increases range from 1.18% going from open farm land to close farm land and increase 0.97% going from close farm land to very close farm land due to the increase of turbulence when the flow passes over a steep hill. Therefore, wind turbines micro sitting has major effects on the results obtained from the area of examination.
- The results also show that the roughness has an effect on the wind speeds near the ground and its effects diminish towards the far field.
- The wind speed decreases for a rougher terrain, whereas increases in the areas where the terrain is steeper.
- Following the results obtained using the Jensen model compared with different software the differences were minor, show that higher energy production is predicted by WindPro (0.27% higher).

Furthermore according the calculations performed for the estimation of

AEP comparing the results of WindSim using the Jensen and Larsen model show that higher energy production is predicted by Larsen model (1.47% higher). This is due to the more physical accurate properties embedded in Larsen's model.

- A significant advantage of CFD based software over WAsP one is the direct computation of turbulent quantities that provides better insights regarding turbulent areas that should be excluded for power exploitation.
- The main disadvantage of the CFD based software compared the WAsP ones is the use additional constants and parameterization assumptions that increase the uncertainty level of simulation procedure.

There are a few recommendations that can be offered regarding future research directions:

1) Simulations on much finer grids should be carried out to examine the effects of the grid resolution on the results. Simulation of finer flow scales may show to what extent features such as flow separation and turbulence may affect the annual energy production.
2) The flow field should be examined in more detail aiming to identify the optimized locations for the turbines that have to be taken into account as the wind farm goes through an upgrade phase.
3) The uncertainties related to varying temperature and how can affect the energy production of the wind farm should be also examined in the future
4) More complex simulation approaches, though currently not available in the framework of the commercial software, should be examined. Such models include large eddy simulations on coarse and fine grids (Sagaut, 2005), (Grinstein et al, 2007)
5) Higher-order methods should be investigated as well. Currently, the Phoenics CFD code supports methods of second-order of accuracy (Drikakis & Rider, 2005).

6) Finally, the implementation of unstructured grids for capturing better than structured grids the geographical features of a complex terrain, should be considered (Thompson et al, 1999).

The assessment of wind farms resource will continue to be a topic of significant interest; therefore investment of time and resources into research with respect to the state of the art numerical methods and models is both desirable and necessary.

6 REFERENCES

Anderson, David J. (1995). *Computation Fluid Dynamics:The basics with applications.*

Arne Wessel, J. P. (2006). *Verification of a new model to calculate turbulence intensity inside a wind farm*.

Beat Schaffner, Arne Reidar Gravdahl (2003). *Wind Modeling in Mountains: Intercomparison and Validation of Models.* Switzerland.

Carsten Albrecht, M. K. *Three-Dimensional wind field calculation above orographic complex terrain in Southern Europe.*

Crasto, G. (2007). *Numerical Simulations of the Atmospheric Boundery Layer .*

Cabezon d., A Iniesta, E.Ferrer, I.Marti (2005). *Comparing linear and non linear wind flow models.* Spain.

David R. VanLuvanee, Rogers T., Randall G., Williamson A. and Miller T. (2009). *Comparison of WAsP, CFD, NWP and analytical methods for estimating site wide wind speeds.*

Demetrios Zigras, D. K. (2011). *Farm Efficiencies in Large Wind Farms.*

Drikakis D. and Rider, W., (2005). High-Resolution Methods for Incompressible Flows.

Berge E., Gravdahl A. R., Schelling J., Tallhaug L., (2010) Ove Undheim *Wind in complex terrain. A comparison of WAsP and two CFD-models.*

Eric L.Petersen, N. G. (1998). WIND ENERGY. *Wind Power Meteorology:Part II: Siting and models* , pp. 55-72.

Evaldas Birgiolas, V. K. (2004). *Investigation of wind flow turbulence and energy parameters.*

Fernando D. Bianchi, Hernαn De Battista, Ricardo J. Mantz. (2007). The Wind and Wind Turbines. Castellani F., Vignaroli A., Gravdahl A. (2011). *Wind Simulation on Complex terrain: About the dependencies of inlet flow orthogonality*. Italy.

G.Mortensen, A. J. *W., Exploring the limits of WAsP-The Wind Atlas Analysis and Application Program.* Denmark.

Crasto G., Gravdahl A.R.(2008, February 15). CFD wake modeling using a porus disc.

Watson G, Douglas N., Hal S. (2004) *Comparison of wind flow models in complex terrain.*

R.Gravdahl, Arne (1998). *Meso Scale modeling with a Reynolds Averaged Navier-Stokes Solver. 31th IEA Experts Meeting.* Denmark.

Grinstein, F.F., Margolin, L.G. & Rider, W.J., (2007). I*mplicit Large Eddy Simulation: Computing Turbulent Fluid Dynamics*. Cambridge University Press .

Miller H., Rene (1978). *Aerodynamics of Horizonatl Axis Wind Turbines.*

http://en.wikipedia.org/ Retrieved from Wind energy software.

http://www.brighton-webs.co.uk/

http://www.risoe.dtu.dk/. (n.d.).

http://www.therenewableenergycentre.co.uk/. (n.d.).

Troen I., (1990). *A high resolution spectral model for flow in complex terrain.*

Prospathopoulos J.M., Politis E.S., Chaviaropoulos P.K.,(2008). *Modelling Wind Turbine Wakes in Complex Terrain.*

Mann J., Astrup P., Kristensen L., Rathmenn O., Madsen P.H. & Heathfield D., (2000). *WAsP Engineering DK.* Denmark.

Tu J., Yeoh G.H. , Liu C.(2008). *Computational Fluid Dymnamics:a practical approach.*

Thompson J.F., Soni B. K., Weatherill N. P. (1999). *Handbook of grid generation.* CRC press .

John L. Walmsley, Salmon J.R.,.Taylor P.A (1981). *On the application of a model of Boundery-Layer flow over low hills to real terrain.*

Klemp, D. K. (1979). The effects of terrain shape on nonlinear Hydrostatic waves. *Journal of fluid mechanics-Cambridge University Press* , 241-261.

Larcen, Gunner C. (1998). *A simple Wake calculation procedure.* Denmark.

Liseikin, Vladimir D. (2009). *Grid Generation Methods.*

Loureiro, J. (2008). *The effect of roughness on separating flow over two-dimensional hills*.

Nielsen M., Larsen G .C, Hansen K .S. (2007). *Simulation of inhomogeneous, non-stationary and non-Gaussian turbulent winds.* Journal of Physics .

Afzal, N. (2001). *Power law and log law velocity profiles in fully developed turbulent pipe flow: equivalent relations at large Reynolds numbers .*

Mortensen N. G., Bowen A.J., Antoniou I., (2004). *Improving WAsP Predictions in (too) Complex terrain.*

Nielsen, P. (2003). *Comparing WindPRO and Windfarmer wake loss calculation.*

Nilsson, Karl J. (2010). *Estimation of wind energy production in relation to orographic complexity.*

Rathmann O, Mortensen N., Landberg L., and Bowen A.,(1996). *Assesing the accuracy of WAsP in non-simple terrain*. University of Exeter,UK.

Ott, Berg J., Soren (2008). *A new linearized flow model for complex terrain.*

Pastorrel, MasseB. and Henri (1991). *Stress Calculation for the Sandia 34-Meter Wind Turbine Using the Local Circulation Method and Turbulent Wind.*

Frohboese P., Schmuck C.(2010). Thrusts Coefficients used for estimation of wake effects for fatigue load calculations. *European Wind Energy Conference.* Poland.

Petersen. (1991). *Wind power meteorology. Part II: siting and models.*

Petersen, Ib Troen and Eric Lundtang (1989). *European Wind Atlas.*

Petersen N. G., Mortensen N., (1997). *Influence of topographical input data on the accuracy of wind flow modeling in complex terrain.*

Phoenics Encyclopedia. (n.d.). Retrieved from CONVERGENCE MONITORING AND CONTROL.

Pinard, J. (1999). *Computer Models for Wind Flow over Mesoscale Mountainous.*

Pinard, J. (1999). *Computer Models for Wind Flow over Mesoscale Mountainous Terrain applied to the Yukon.*

Pironneau, Mohammadi B. and Olivie (1994). *Analysis of the K-Epsilon Turbulence Model (Wiley-Masson Series Research in Applied Mathematics) by.*

Gravdahl, A. R. (2007). On the sensitivity of Numerical Wind Field Modeling. *WINDPOWER .* Los Angeles,

Schepers J.G., van der Pijl S.P. , Rathmann O. and Frandsen S.T., Cabezon D., Politis E.and Prospathopoulos J., Rados K., Hansen K., Schlez W., Phillips J., Neubert A. (2007). Flow and wakes in complex terrain and offshore:Model development and verification in Up Wind.

Cattin R., Schaffner B., Dr. Kunz S.(2004). *Validation of CFD Wind Resource Modeling in Highly Complex Terrain.*

Sagaut, P. (2005). Large-eddy simulation for incompressible ows - An introduction (third edition). *Springer-Verlag, Scientific Computation series* .

Frandsen S.T., Jorgensen H.E., Barthelmie R., Rathmann O., Badger J, Hansen K., Ott S., Rethore, Soren P.E. Larsen E.,Jensen L.E. (2010). *WAKE DECAY CONSTANT FOR THE INFINITE WIND TURBINE ARRAY.*

Frandsen S., Nielsen M.(2008). *The making of a second-generation wind farm efficiency model complex.*

Hahm T., Wuβow S., (2010). *Turbulence Wakes in Wind Farm Configuration.*

Sørensen T., Thøgersen M.L., Nielsen P.(2008). *Adapting and calibration of existing wake models.*

Sorensen T., Nielsen P., Thogenrsen M.L. (2006). *Racalibrating Wind Turbine Wake Model Parameters-Validating the Wake Model Performance for large Offshore Wind Farma.*

Burton T., Sharpe D. , Jenkins N. , Bossanyi E. (2001). *WIND ENERGY HANDBOOK.*

Troen and Petersen E. L. (1989). *The stability model.*

Wallbank, Tristan. (2008). *WindSim Validation Study.*

WINDPRO SOFTWARE . (n.d.). *Modules Description* .

http://www.reuk.co.uk/Wind-Speed-Distribution-Weibull

http://www.windsim.com

http://www.geosolutions.gr

http://www.google earth.com

http://www.Gamesa/technical description.com